Sizing, Dynamic Modelling and Control of a Solar Water Pumping System for Irrigation

by

© Shatadru Bipasha Biswas

A thesis submitted to the

School of Graduate Studies

in partial fulfillment of the requirements for the degree of

Master of Engineering (Electrical)

Faculty of Engineering and applied science

Memorial university of Newfoundland

October 2018

St. john's Newfoundland and Labrador Canada

ABSTRACT

This thesis describes the sizing, dynamic modelling, and control of an automatic solar irrigation pumping system with energy storage for extraction of groundwater for irrigation utilizing an alternative source of energy. The system design is based on site data of an existing project in Bangladesh. Sizing estimation, sensitivity analysis, and optimization are done in HOMER. MATLAB simulation is performed for all alternative types of energy storage systems to study the dynamic behaviors of system components. A water level sensor observes the tank water level and a programmed sensor module measures the temperature, humidity, soil moisture level and send the information to ESP32 microcontroller. Based on the information and boundary conditions, the microcontroller decides either to start or to stop the pump motor and sends results to the web server so that the user can see that. The user can operate the irrigation system far from the field by a simple click on a cellphone. This research also provides a comparative study among all alternative systems as well as the conventional diesel engine system from the economic point of view to give an optimal solution of an automated solar irrigation pumping system with energy storage.

ACKNOWLEDGEMENT

I would like to thank Dr. Tariq Iqbal for his consisting inspiration and encouragement in doing research in electrical engineering. Without his supervision, guidance, patience, immense knowledge, insightful comments, and encouragement, I would not be able to finish this thesis.

I am grateful to the Memorial University of Newfoundland for giving me the opportunity to pursue my Master of Engineering degree.

I would like to thank the Natural Sciences and Engineering Research Council of Canada (NSERC) and Memorial University of Newfoundland School of Graduate Studies (MUNSGS) for providing funding for my research.

I would like to thank Sherpa Power Engineering Limited of Bangladesh for providing the necessary site data for this research purpose.

I would like to thank my father, mother, brother, husband and extended family members for their consistent support. Finally, I want to dedicate this thesis to my parents.

Contents

APPENDICES

LIST OF TABLES

LIST OF FIGURES

LIST OF ABBREVIATIONS

PV	Photovoltaic
DC	Direct Current
AC	Alternating Current
PWM	Pulse Width Modulation
MPPT	Maximum Power Point Tacker
OLPC	Openable Low Pressure Compensating
I	Current
V	Voltage
I/O	Input/Output
P & O	Perturb & Observe
TCP	Transmission Control Protocol
IP	Internet Protocol
GPS	Global Positioning System
CPU	Central Processing Unit
SMS	Short Message Service
GSM	Global System for Mobile communication
UART	Universal Asynchronous Receiver/Transmitter
GPRS	General Packet Radio Service
PLC	Programmable Logic Circuit
HOMER	Hybrid Optimization and Multiple Energy Resources

NPC	Net Present Cost
COE	Cost of Energy

LIST OF SYMBOLS

m	Mass
V	Output voltage
I	Output Current
R_{sh}	Shunt resistance
R_s	Series resistance
I_D	Diode saturation current
I_l	Light-generated current
a	Diode ideality factor
K	Boltzmann constant
q	Electron charge
N_{cell}	Number of cells connected in series in a module
I_d	Diode current
V_d	Diode voltage
T	Cell temperature
ω	Rotor speed
T_e	Electromagnetic torque
P	Power
Q	Water discharge rate
ρ	Water density
h	Total dynamic head of the liquid

g	Gravity

CHAPTER 1

INTRODUCTION

1.1 Motivation

Bangladesh is an agriculture-based, densely populated developing country and its 35 percent of GDP comes from agriculture sector [1]. Around 59 percent of cultivable land needs irrigation because monsoon-based cultivation cannot meet the challenges as described by Khan et al. [2]. Irrigation is needed to produce rice; the main crop of Bangladesh, during the dry season (January to May). Above 85 percent of the cultivable land needs underground water irrigation system, rest is under surface water irrigation system [3]. Generally, electric power (where available) and diesel engine (in off-grid areas) are used for irrigation. Moreover, only 53 percent population has access to electricity [2]. There are 1.71 million pumps in Bangladesh; 83% diesel operated and 17% electrically operated [3]. Bangladesh has to import billions of liters of diesel to run these pumps. Bangladesh is blessed with enormous solar resources because of geographical location (Figure.1.1). It is situated between 20.30°-26.38°N and 88.04°-92.44°E, with an average solar radiation of 4.0 to 6.5 $kWh/m^2/day$ and in bright sunshine 6.0 to 9.0 $KWh/m^2/day$ [4]. In this situation, solar irrigation pumps may be an alternative for irrigation in the off-grid areas.

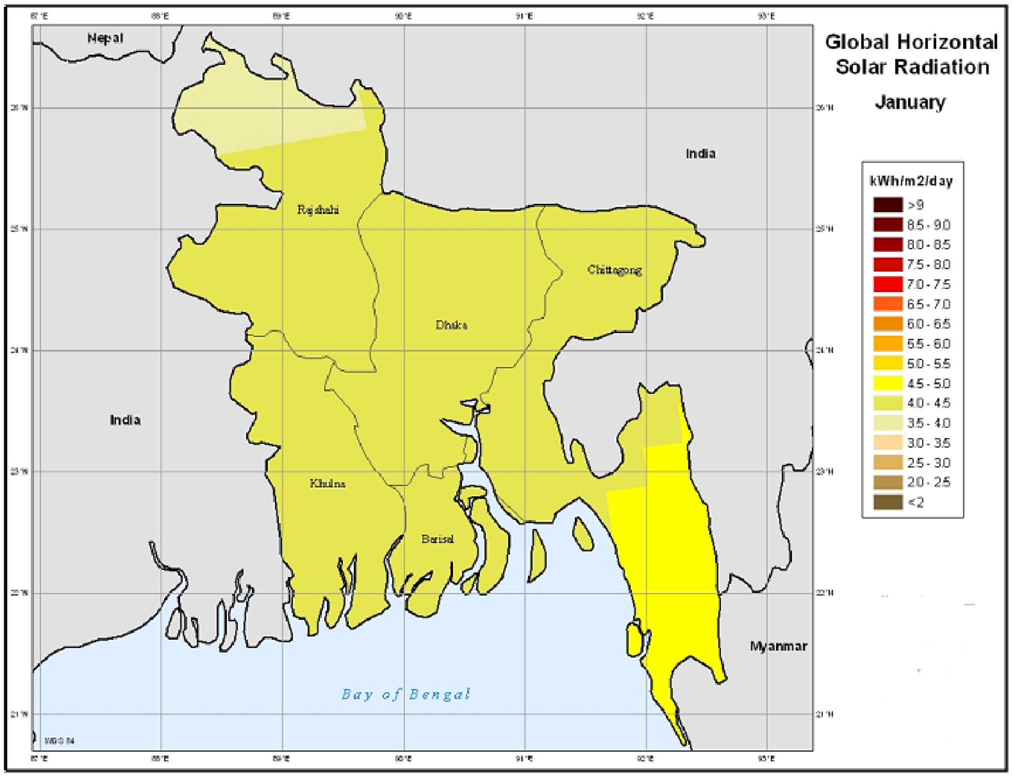

Figure.1.1: Global horizontal solar radiation

Hossain et al. [5] stated that, according to the baseline survey, there were only 150 solar pumps existed in Bangladesh in 2010. Among them, 65% pumps were used for supplying drinking water and only 35% used for irrigation purpose. The authors also stated that in Bangladesh, the small-scale solar pumping system is available which ranges from 300 Wp to 1190 Wp and the discharge capacity was 2000 to 80,000 L/d. Moreover, photovoltaic (PV) pumping system requires high capital cost, water storage for cloudy weather and, skilled personnel [6].

According to Arrouf and Ghabrour [7], the technology of solar cell is growing fast. Golpal et al. [8] stated that solar PV water pumping systems are the most widely used renewable energy source water pumping system for irrigation and domestic use. Some advantages of solar PV system include unattended operation, low maintenance, easy installation and long life [6].

The main objective of this thesis is to find out an optimal solution for an automated alternative source water pumping system to meet the irrigation challenges faced during the dry season. Most of the farmers in developing countries are marginal farmers. They only possess small pieces of lands for cultivation. It is not possible for them to afford costly irrigation systems in off-grid areas. This research work tries to find out a cost-effective automated solar irrigation pumping system where the user does not have to be present in the field to control the operating time of motor-pump.

1.2 Study Approach

The Government of Bangladesh is promoting alternative sources of energy to meet the energy deficiency. Many governmental and non-governmental organizations are encouraging people to use renewable sources of energy. Bangladesh government is giving subsidies for alternative energy projects [9]. Even the bank loan interest rate is lower (9%-10%) for this kind of projects [10]. A lot of organizations are coming forward to finance large renewable energy projects. A suitable site for solar water pumping system was selected for investigation. Grameen Shakti is one of the non-governmental organizations which has installed a large Solar Irrigation Pumping System (SIPS) to irrigate a considerable land area in Bangladesh [11]. Sherpa Power Engineering Limited provides the technical support. The project name is Grameen Shakti -Gorol or GS-Gorol project which is situated in Gorol (Kamlartari), Kaligonj, Lalmonirhat, Bangladesh (26^0 N, 89.28^0 E).

1.3 Simulation Method

A solar irrigation pumping system is modeled in HOMER according to the selected site data. The components are selected carefully for the HOMER inputs. The present costs of all elements are collected from different websites. HOMER optimization result provides only the feasible solution of the battery-based system. The battery equivalent tank size is also calculated to build a battery-less alternative system. Sensitivity analysis is done with 10% variation in load and irradiance. To find out the cost-effective solution, an economic comparison is done among the alternatives.

Dynamic modeling of all the alternative systems are done in MATLAB Simulink to observe the dynamic behavior of system components. The responses of each system are compared to find out the feasible solution. The total amount of water discharge is also calculated from the output response for each model.

A microcontroller unit is programmed in such a way that it takes the decision to run the motor or stop the motor after getting the information about field conditions. The field condition includes soil moisture level, temperature, humidity and tank water level. The user can also control the motor operation far from the field just by clicking on a mobile phone.

1.4 Summary

Although a rich body of research has been conducted on sizing and designing of a solar water pumping system for irrigation, a comparison of energy storage methods and detail dynamic modeling of solar irrigation pumping system is missing. This research attempts to give a feasible solution for a low cost automated solar irrigation system.

A detailed background of previous work and the importance of the current research is explained in Chapter 2. In Chapter 3, HOMER optimization provides the most feasible solution. Dynamic modeling of the system is provided in Chapter 4. Chapter 5 shows the economic comparisons, sensitivity analysis, and optimization. The instrumentation and control strategy of the system is provided in Chapter 6. Finally, in Chapter 7, a detailed summary of the work with significant results is presented. A potential future work is also suggested at the end of this chapter.

CHAPTER 2

LITERATURE REVIEW

This chapter provides literature review related to solar water pumping systems. Literature review is divided into four sections. The first section provides literature review on sizing and modeling of solar water pumping systems. The second section basically discusses literature review on dynamic modeling and simulation of solar PV pumping system. The third section discusses the literature review on control of automated solar water pumping system. The final section provides literature review on economic analysis of solar irrigation pumping system.

2.1 Sizing and Modelling of Solar PV Pumping System

Anis and Nour [12] attempted to find out an optimum design of a photovoltaic pumping system. The authors discussed and compared three different alternatives: (i) directly coupled direct current DC motor pump set, (ii) battery buffered system where the battery is connected across the array and feed the dc motor, and (iii) switching mode where the system becomes direct coupled when the battery is fully charged. The authors considered four main parameters for the same location to design the system, i.e., DC motor pump set, PV size, battery size and tank size. The authors calculated array factor, battery storage factor, tank storage factor and pump installation cost parameters for above alternatives. Cost analysis of each component also done from the economic point of view. To obtain the optimum design, the analysis was done for both fixed array and fixed storage factors. The authors suggested that the designer must choose one of following alternatives: either to increase the water tank size or to increase both array and battery storage sizes simultaneously. The authors stated that the former choice is the most economical.

Argaw [13] designed a PV pumping system with an interfacing pulse width modulated DC to alternating current (AC) inverter. The author stated that PV arrays can be configured from the V-I characteristic of a single cell and required rated power for the motor/pump. The author was motivated by pulse width modulation (PWM) technique because it minimizes voltage harmonics, loss in the motor, torque pulsation, and acoustic noise. Load matching factor was also analyzed to find out the optimum solution. Load matching factor is defined by the ratio of the energy acquired by the motor/pump subsystem to the maximum PV array power produced in one day period. It improves with higher irradiance. A satisfactory load matching factor can be achieved by selecting proper PV array size and motor/pump subsystem. The author concluded that the utilisability of PV array depends on the seasonal variation of solar irradiance, the array size and the load characteristics.

Loxsom and Veroj [14] developed an algorithm to estimate the monthly water discharge of a batteryless PV water pumping system. Starting of the pump depends upon the available insolation level. The available insolation should be greater than the threshold value. At higher insolation level, the pumping rate increases at a smaller rate than at intermediate level with the increase of insolation. This algorithm reduces the amount of computation which was required for hourly simulation. The proposed algorithm is based on this insolation threshold and nonlinear relationship between the pumping rate and insolation. This algorithm reduces the amount of computation which was required for hourly simulation. The algorithm could estimate the annual performance of a PV pumping system within 2% - 4% of the result.

Katan et al. [15] analyzed the performance of a solar water pumping system. The system includes PV array, permanent magnet DC motor, and a helical rotor pump. The operation was analyzed in PSPICE software. The overall cell efficiency decreases with the increase of temperature and the rate of power decrease is about 0.5% per ^{o}C. The authors concluded that the performance could be increased by using maximum power point tacking (MPPT) and Sun tracker as the static system supplies only 64% of the total energy a tracking system can supply. The authors stated that the helical rotor is suitable for large heads, efficient and less sensitive, it has higher starting torque and poor performance for small heads. The field test result implies that the motor speed decreases as head increases.

Hoque [16] designed a photovoltaic water pumping system for a farm in Bangladesh. The author estimated the system for 1.8 hectors of irrigated land, 260 numbers of cattle and 3000 numbers of poultry. The paper shows that the water requirement is the highest in the month of April. The author concluded that for consecutive three season's irrigations, the unit cost of water is cheaper in case of PV water pumping system comparing with diesel engine system.

Pande et al. [17] proposed a PV water pumping model to ensure uniform irrigation in arid regions in India using drippers and manual tracking. The system consists of PV array, dc-motor pump set, microfilters and openable low pressure compensating (OLPC) drippers. The authors first considered water requirement and then calculated the total energy needed to run the drip irrigation. Water requirement depends on the various stages of crop cultivation and evaporation rate of the soil. The authors considered the volume of water to be pumped, the pressure required, head loss, delivery lines, and efficiencies of subcomponent while deciding the total PV energy requirement. The tilt angle was decided to change once a month. Variation of irradiance causes a change in pressure. Drippers are needed to be compensated in order to provide uniform water discharge. To solve this problem, the authors compared three different types of dripper: low pressure compensating, openable low pressure compensating, and threaded type. The experiment decided that the openable low pressure compensating dripper gave the most feasible solution. There are some disadvantages of this system was noted by the authors i.e. clogging of drippers, PV output affected by dust, chocking of microfilters by algae and the carbon brushes of the DC motor need to be replaced.

Cuadros et al. [18] proposed an elaborate computer program which was based on Cropwat version 7 for MS-DOS to design a PV installation for irrigation which consists of three stages i.e. irrigation requirement, hydraulic analysis and PV power requirement. Their aim was to introduce a design procedure that considers the above criteria before any PV pumping installation. If the soil's water content is less than the transpiration, the crops are needed to be irrigated. The major water loss occurs by evaporation which basically depends on meteorological factors and soil characteristics. Summation of transpiration and evaporation is called evapotranspiration. Evapotranspiration of any crop depends on reference evapotranspiration, type of crop and growth coefficient of the crop. While doing hydraulic analysis, the authors considered the energy losses due to the friction of the water in the irrigation system. There are losses in the photovoltaic generator, AC/DC converter, losses in the pump. The fraction of the daytime when solar irradiance is greater than the threshold value also needs to be calculated. The authors suggested that these losses are needed to be considered while estimation the total energy required from the photovoltaic panel.

Generally, the sizing of PV water pumping system is done on the basis of hydraulic energy demand and available solar energy. Zvonimir and Margeta [19] developed a mathematical model to acquire an optimal PV system by considering not only water demand or irradiance but also including natural process i.e. climate, hydrology, boreholes, pumping system, irrigation, agriculture and power supply. Climate determines the moisture, solar irradiance and water requirement for irrigation. Climate inputs are needed to be treated especially throughout the entire period as those are stochastic parameters. Land and geological features decide water storage capacity of the soil. PV pumping system consists of PV generator, nominal electric power, motor-pump unit, and inverter. The authors put an importance on the need for compatibility between discharge capacity of the borehole and pumped water. The authors also adopted the cost-effective trickle irrigation method with the efficiency of 85%. Soil moisture determines the system condition and water requirement. It is a result of the natural process i.e. precipitation and evapotranspiration. If the moisture from natural processes is inadequate, irrigation is needed. This mathematical model was established after verification and it described the system very well. This paper proves that the electrical power of PV generator obtained by the proposed model is relatively smaller than that obtained by the usual method.

Forero et al. [20] introduced a system for monitoring solar PV plants that supply power to AC and DC loads. The system is based on virtual instrumentation. The monitoring system includes three units: (i) analog input unit, (ii) interface unit, and (iii) unit for current (I) - voltage (V) measurement. Analog input unit consists of field point (FP) modules and data acquisition card. Former is used to measure the low sampling rate signals and the latter is used to capture signals at high rates. Data acquisition card also analyzes the harmonics of the AC signal generated by the DC/AC inverter. Interface unit communicates between the host computer and the input/output (I/O) modules. The process control, acquisition, processing, storing and reporting of all data is attained through a virtual instrument. The information is stored in computer hard disk in a universal format for further processing with Lab VIEW. The monitoring system shows that the short circuit current increases with the increasing irradiance and the open circuit voltage decreases when the irradiance decreases.

Odeh et al. [21] studied the influence of pumping head, irradiance and PV size on the performance of PV water pumping system. The authors developed a Transient System Simulation Tool (TRNSYS) based model and conducted the experiment on an AC centrifugal PV water pumping system. The effect of a certain parameter on the whole system is easier to study in TRNSYS. The authors compared the model result with both laboratory result and field data and found that the annual predicted flow rate approximately matched the laboratory and field data. Subsystem efficiency was calculated from pumping head and insolation. The authors found that only average efficiency is required to find out the optimum pumping head. In other words, optimum pumping head can give the highest average system efficiency which is mainly influenced by PV and sub-system efficiency. Economic analysis reveals that the oversizing PV array slightly increases the water unit cost whereas the under-sizing sharply increases water unit cost. The authors suggested that PV system sizing should be done on average daily, monthly or yearly basis, not on instantaneous basis.

Hamidat and Benyoucef [22] proposed a mathematical model to find out the best choice of motor, pump, and the inverter as the sizing of the PV pumping system is the most significant stage. The authors proposed mathematical models to calculate the water flow. First model can find out the total water flow for a fixed total head. The second one is more general applicable for any total head of pumping. The testing was done for two different pumping systems. First one consists of three-phase DC/AC inverter, submersible AC motor and multistage centrifugal pump. The second option includes DC/DC controller, submersible DC brushless motor, and a positive displacement pump. The authors applied the proposed mathematical models to observe the PV pumping system efficiency and found that DC engine with a positive displacement pump is more efficient and discharge more water than AC engine with a centrifugal pump for a wide range of total dynamic head.

Meah, et al. [23] found that solar PV pumping system is a cost-effective application in developed countries whereas in developing countries, it is facing some challenges, especially in operation and maintenance. The authors noticed that the capital cost is not only the constraint for solar PV application; some other technical and socio-environmental challenges are associated with it. Cell efficiency, availability of spare parts, skilled technicians, operation costs and maintenance costs ate technical challenges. On the other hand, socio-environmental challenges include health, ownership, theft/vandalism, community, and educational problem. The authors gave some suggestion to overcome these problems. Capital costs can be reduced by using local skills, local materials, and local financial resources. Involvement of everyone in the community with an equal right would minimize the theft or vandalism problem. Operation and maintenance costs can be managed by raising little money according to the ability of the people. If the local people are being trained and the local shops can provide the spare parts, operation and maintenance issues can be resolved. The authors also suggested simple system design, clean water conservation and workshops to overcome the socio-environmental challenges.

Bakelli et al. [24] attempted to find out a feasible solution for solar PV pumping system with water tank storage. The authors followed two optimization criteria: reliability and economic evaluation. Reliability analysis and economic evaluation were performed using the loss of power supply probability (LPSP) concept and the life-cycle cost (LCC) accordingly. The configuration of PV water pumping system which satisfies the system reliability requirements can be obtained from LPSP concept. On the other hand, the optimum configuration can be identified from lowest LCC. The authors considered a case study in Algeria and suggested am optimum solution based on LPSP and LCC concepts.

Mokaddem et al. 2011 [25] carried out an experimental study to investigate the performance of a low-cost direct-current PV system. The system consists of PV array, permanent magnet (PM) DC. motor coupled with a single impeller centrifugal pump and identical water storage tank. The authors tested the system for two different static heads and recorded all relevant operational parameters for four months. Fixed operating point for steady state operation was decided from the I-V characteristics of motor-pump set and PV array I-V characteristics. The authors also obtained the PV array characteristics for different irradiance level and the head versus flow rate characteristics. Long-term performance of directly coupled pump was also predicted. The authors assumed that there is no transmission loss between the motor and pump. Additionally, the adopted three conditions were verified during testing. The conditions were: motor and pump torque remain equal, the voltage across motor armatures is equal to the voltage supplied by the PV array, and motor armature current is same as the current delivered by the PV array. The authors observed that the motor has a greater impact on motor-pump overall efficiency than the pump. From the observations, the authors found that the system is suitable for low delivery flow rate application

2.2 Dynamic Modelling and Simulation of Solar PV Pumping System

Gad [26] proposed a MATLAB simulation program to predict the performance of a direct coupled solar photovoltaic water pumping system in Egypt. Solar irradiance data, PV array with intermittent tracking and the pump models are used in this program. The proposed system consists of PV array, pump controller, and submersible pump. When PV output current reaches the suitable operational level, the pump starts running and it stops working when the current is lower. That means the current is directly proportional to the level of solar irradiance. The controller also switches off the pump when the water level in the well goes down to avoid the pump dry operation condition. The pump stops working when the tank is full. A MATLAB program is developed to find out the most feasible solution for performance prediction. The experiment was done for three different tilt positions all over the years. The south-facing PV array with different tilt angles yields the same result. The predicted values of PV array efficiency ranges from 13.86% (winter) to 13.91% (summer) which is larger than the specified efficiency (13%) by tender.

Akihiro Oi et al. [27] designed a small standalone direct coupled solar photovoltaic pumping system incorporated with MPPT. They developed a transferable MPPT model which could be implemented easily in a microcontroller. The system included positive displacement pump along with brushed permanent magnet DC motor to deliver water. They admitted the problem that the solar water pumping system without MPPT could not utilize the irradiance fairly in the morning. They also noticed that the produced power is low current-high voltage type at the maximum power point (MPP) which is totally opposite to the requirement of pump-motor set. To solve this problem, they thought about linear current booster (LCB) which could convert power into high current-low voltage power as required. To locate MPP by tracking algorithm as it was changing dynamically, they followed both perturb & observe (P & O) and incremental conductance methods. They compared the results between the two methods in both sunny and cloudy day and found incremental conductance method is more efficient. They modeled the system in MATLAB Simulink with modified parameters and found that their operating point was close to MPP.

Then the simulated result was compared with DC water pumping system without MPPT. They concluded that the MPPT improved the efficiency of the system significantly. The system is suitable for small-scale operation only. The pump type used is a low volume pump and brushed of the DC motor need to be replaced repeatedly.

Malla et al. [28] designed a stand-alone PV water pumping system without battery storage and simulated the system in MATLAB/Simulink. The system consists of perturb and observe algorithm based MPPT for improving efficiency. The authors described the control strategy to regulate the water discharge for a single induction motor as well as a multi induction motor. The speed control of the induction motor was based on vector control and the authors found satisfactory results for both single and multi-motor type system.

2.3 Control of Automated Solar Irrigation Pumping System

Yunseop et al. [29] designed a controlled irrigation system using distributed wireless sensor network for semi-arid and arid regions. The system consists of : (i) in-field sensing station, (ii) base station, and (iii) irrigation control station. In-field sensing station monitors the field conditions and the nearby weather station monitors micrometeorological information of the field. In-field sensing station and weather station have three important parts: data logging, wireless data communication, and power management. Field data are logged by the data logger and the data logger is programmed for reading, scanning, data storing and downloading. Water content reflectometers and temperature probe are used to measures soil moisture content and soil temperature. A humidity probe and a pyranometer measure relative humidity and solar radiation. Power management is done for both standby mode and active mode. Wireless data communication between in-field sensing station and the base station is done through a Bluetooth module. The base station processes the data received from in-field sensing station through a decision-making program and sends the commands to the irrigation control station. The Bluetooth receiver of the base station receives data from sensing stations and sends them to the base computer via transmission control protocol (TCP) or internet protocol (IP) Ethernet. A user-friendly software allows the user to read the global positioning system (GPS) data from the control station and sensor data from sensor station. It also helps to send control signals to the irrigation control unit for individual sprinkler operation. After receiving the control signal the irrigation control station updates and sends georeferenced locations to the base station for real-time monitoring and control. Based on the sprinkler location (GPS mounted on sprinkler head), the base station sends back the control signal to the irrigation control unit to apply a specific amount of water by the individual sprinkler.

Dursun and Ozden 2011 [30] described a low-cost wireless controlled drip irrigation system for dwarf cherry orchard located in Anatolia, Turkey. Their target was to design a solar-powered automatic feedback controller and a wireless acquisition station to control drip irrigation. The irrigation system consisted of two solar-powered pumps; one carried water from lake to tank and another used to irrigate the orchard. Their proposed system was included three portable units; sensor unit, base station unit and valve unit. All the units had RF (Radio Frequency) module, antenna, solar panels, and microcontroller chip. A pre-calibrated soil moisture sensor measured the dielectric constant of the soil to find the soil moisture content using a capacitance technique. Then the analog data, produced by the sensor, converted into digital data by PIC (Programmable Integrated Circuit) and sent to base station unit. The base station unit was the master device which controlled the valves after analyzing the sensors data communicated with other units. The output of the valve unit controlled the valve after getting signal from base station unit. Their proposed circuit includes various types of equipment i.e. a wireless module, antenna, PIC, Electronic components, battery valve, solar panel, sensor and PCB (Printed Circuit Board) which makes the circuit quite complicated. Troubleshooting would also be difficult for the user in remote locations.

Prisilla [31] proposed an intelligent control system based on artificial neural network (ANN) for effective use of water during irrigation in India. Their proposed system could give an optimal solution for various time delays and system parameters whereas most of the existing controllers are on/off type. They proceeded with the closed loop controllers as those could receive feedback from different types of sensors. The proposed control system was consisting of four stages. At first stage, system parameters, i.e., humidity, soil moisture level, temperature, radiation and wind speed were collected and passed to the next stage. The actual soil moisture level/content was calculated in the second stage using the system parameter. The authors followed Penman-Monteith equation to find out the evapotranspiration model. The third stage was for determining the required soil moisture for proper growth of the plants. At the final stage, the ANN controller made decision dynamically by comparing the required soil moisture with actual soil moisture. During the rainy season, water might stage in the field and cause a flash flood. The ANN controller was able to control the valves to drain the excess water and saved it for later use.

Uddin et al. 2012 [32] proposed an automated solar irrigation system for large paddy field. The sensors measure the water level and send the data to the user's cell phone through dual tone multi-frequency (DTMF) signaling. If the water level reaches the minimum value, the microcontroller sends the command to start the motor. The pump remains to switch on until the water level reaches the secured level. If the water level goes down to mid-level, the sensors send a signal to the microcontroller and the microcontroller sends a message to the user. Then the user sends a message back to the microcontroller through the DTMF decoder. Each message has the assigned code depending upon the action taken; start up or shut down the motor. The authors designed the system in this way that the user can also control the pump just by pressing any key of the mobile phone. However, the microcontroller sends the signal to switch on the pump if the water level reaches the minimum level even without getting the code from the user. A small PV cell with a 6V battery supply the necessary energy needed to run the control circuit here. This proposed system needs three different sensors: (i) mid sensor, (ii) low sensor, and (iii) high sensor to control the whole irrigation system. This system is suitable for the specific type of cultivation where standing water is needed, but not appropriate for dryland farming.

Li [33] designed an intelligent irrigation system in the arid region based on ZigBee wireless communication technology. The system structure included management center station, first control station, soil moisture monitoring points, automatic weather station and micro-irrigation central processing unit CPU control points. The main function of the decision-making system had four parts; information management, decision making, production management and reasoning. The user can check the stored data by browsing a specified page in webserver.

Pavithra and Srinath [34] proposed a controlled drip irrigation system using android phone application. They proposed a centralized unit which could able to interact with the irrigation system. The user also able to communicate with the centralized unit. Those were done through receiving short message service (SMS) by global system for mobile communication (GSM). The GSM was connected with the microcontroller through universal asynchronous receiver/transmitter (UART). When the moisture content of the soil became low, it gave a signal to the microcontroller. Then the microcontroller sent a signal to the user mobile which is already kept in auto answering mode. The user could give the signal back to the microcontroller to open the valve for irrigation purpose by simply pressing the button on the calling function. When the soil moisture level reached the required value, it sent the signal again and the user could switch off the valve in the same way. When the user sent an activation command, the system could check all the field conditions and gave a detailed feedback message. Temperature, soil moisture level and water level in the tank were included in the field condition. Depending on the soil moisture condition, the subscriber had to decide whether to start the motor or not.

Harishankar [35] proposed an automatic irrigation system in which a simple valve mechanism controls the irrigation. Soil moisture sensor detects the moisture content of the soil. Depending on the soil moisture value, the valve is controlled using an intelligent algorithm and regulates the water flow in the field. The irrigation system consists of two modules; solar pumping module and automatic irrigation module. Solar pumping module includes solar panel, converter, battery and water pump. The control circuit charges the battery and from the battery, the converter provides enough power to run a submersible pump. Then the water pumped into the overhead tank. Automatic irrigation module includes a storage tank, a moisture sensor, and actuators. Soil moisture sensor electronically controls the outlet valve of the tank. Depending upon the moisture sensor result, a control signal is given to the stepper motor. The stepper motor controls the cross-sectional area of the valve to be opened for water flow. When the soil moisture content reaches the required value, the valve is fully closed, and the controller is put into sleep mode. On the other hand, if the soil becomes dry, the controller comes out of sleep mode and start irrigating.

Hussain [36] proposed a smart irrigation system based on wireless sensor networks and general packet radio service (GPRS) technology. The irrigation system includes three different units; a wireless sensor unit, a wireless information unit, and watering module. Several wireless sensor units are used in the field to set up a distributed network. The wireless information unit consists of GPRS module, the master controller, and web application. All sensors data are receiving, identified and analyzed here in this unit. The microcontroller unit operates the electromagnetic relays to control the pumps for irrigation purpose.

2.4 Economic Analysis of Solar Irrigation Pumping System

Pande et al. [17] designed a solar irrigation pumping system for pomegranate cultivation in the arid region. The area needs to be irrigated was around 5 hectors. The authors concluded that the benefit-cost radio comes around 2.6 for a discount rate of 10% and the pay-back period comes to around 6 years. The authors concluded that, if the PV price goes down, solar irrigation would be a boon to the farmers of the arid region.

Kim [29] estimated that the total cost of Bluetooth wireless module for the in-field wireless sensing network is approximately $1000.

Mahir [30] concluded that the total cost of electronics used in automated solar irrigation system was around $530. The authors selected all low-cost materials as the system component so that it can be used for all commercial application.

Harishankar [35] concluded that though the initial investment is higher in case of solar water pumping system, it can be earned back within two and half years. If the excess energy is sold to the national grid, it will add to the revenue of the farmers.

Hossain, Hassan, Mottalib, Hossain 2015 [5] addressed the main problem that in Bangladesh, panel cost was the major cost (45%) in solar irrigation system followed by installation (18%), motor (16%), pump (10%), pipes and fittings (4%). For less than five years of the operational period, diesel engine pump is more profitable. For five years or more than five years of the period, solar pump becomes more beneficial. The benefit-cost ratio of the solar pump is also higher than the diesel-operated pump. The authors suggested investing more on solar pumps because those are more profitable than diesel engine pumps.

2.5 Summery

Presented literature review shows that details of solar water pumping sizing using current software is missing in the current literature. A comparison of sizing for a battery based and water tank-based system design is also missing in the literature. The literature review also shows that designed water pumping system controller cost thousands of dollars and need an application of specific programmable logic circuit PLC. Such controllers are difficult to maintain in developing countries like Bangladesh and those need dedicated display screens and warning systems. This thesis addresses these issues. It presents detailed system sizing, a comparison of systems with battery storage and water storage, system modeling and design of an extremely low-cost controller for solar water pumping system for irrigation in poor countries.

Chapter 3

SELECTED SITE DATA ANALYSIS AND SYSTEM SIZING

3.1 Selected Site

A lot of organizations are coming forward to finance large renewable energy projects. Grameen Shakti is one of them and installed a large solar water pumping system (SIPS) to irrigate a considerable land area in Bangladesh and Sherpa Power Engineering Limited gave the technical support. The project name is Grameen Shakti -Gorol or GS-Gorol project which is situated in Gorol (Kamlartari), Kaligonj, Lalmonirhat, Bangladesh (26^0 N, 89.28^0 E). The average water discharge is 1700 cubic meter per day with a total dynamic head of 12m. According to Sherpa Power Engineering Limited, 26.775kWp solar photovoltaic panel provides enough power to run a 15kW submersible motor-pump set to lift 1700,000 liters water per day (Figure.3.1) below shows some photos of the installed system. As it is clear in figures below that system has a water tank and its main application is irrigation.

Figure.3.1 (a): Solar module, GS-Gorol (Kamlartari), Kaligonj, Lalmonirhat, Bangladesh

Figure.3.1 (b): Water tank and control room, GS-Gorol (Kamlartari), Kaligonj, Lalmonirhat, Bangladesh

3.2 Technical Specifications of GS-Gorol Project

The technical specifications of the components of GS-Gorol project are provided in Table.3.1, Table.3.2 and Table.3.3 accordingly.

Table.3.1: Technical specification of solar photovoltaic module

Mode No	JC315M-24/Abs
Peak Power P_{max} [Wp]	315Wp
Tolerance [%]	0~+5A
Max. Power Current I_{mp} [A]	8.45A
Max. Power Voltage V_{mp} [V]	37.3V
Short Circuit current I_{sc} [A]	8.88A
Open Circuit Voltage V_{oc} [V]	45.4V
Temperature co-efficient of P_{max} [% / ^{0}C]	-0.44%
Temperature co-efficient of V_{oc} [% / ^{0}C]	-0.30%
Temperature co-efficient of I_{sc} [% / ^{0}C]	0.40%
Max. system voltage [V]	1000VDC
Brand	Renesola

Table.3.2: Technical specification of solar inverter

Model	SPINV-015K-3P40
Rated Capacity	15kW
Rated Input Voltage	850VDC
Output Voltage	380VAC
Output Phase	3-Phase
Output Frequency	50Hz
Max. Efficiency	98%
Ambient Temperature	40^{0}C
Brand	Sherpa
Manufacturer	Solartech/ABB

Table.3.3: Technical specification of pump-motor set

Model	SS12P215-1-A
Motor Type	Submersible
Rated Capacity	15kW
Input Voltage	380VAC
Phase	3-ϕ
Frequency (Hz)	50Hz
Max. Speed (RPM)	2850
Max. Efficiency	80%
Power Factor at full load	0.8
Max. water Temperature	40^0C
Brand	Sherpa
Country of Origin	Shakti

3.3 Site Output Data

The GS-Gorol project runs from 7:00 a.m. to 6:00 p.m. in total eleven hours to lift 1700,000 liters of water on average per day. The Water discharge reaches peaks (351,000 liters/hour) at 12:00 p.m. while the solar irradiance is maximum (941 W/m^2). Figure.3.2. gives an overview about hourly water discharge rate of this site. The System lifts the maximum amount of water per day in the month of October (1930 m^3/day). Though solar irradiance remains highest from March to May, the system cannot yield maximum water discharge as the groundwater level goes down. June to September is the rainy season in Bangladesh and the sky remains cloudy in these months. As a result, the output is lowest at that time. After four months of rainy season, the groundwater level also increases, and the sky also remains clear in October, which implies the maximum water discharge rate in the year. Figure.3.3 shows the variation of daily water discharge rate according to months.

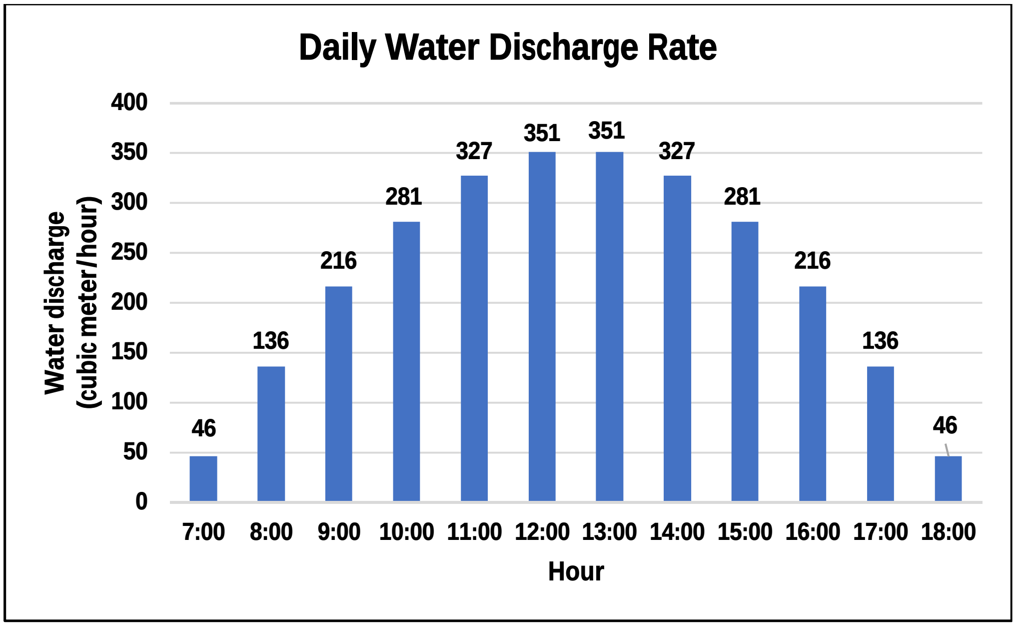

Figure.3.2: Hourly water discharge rate

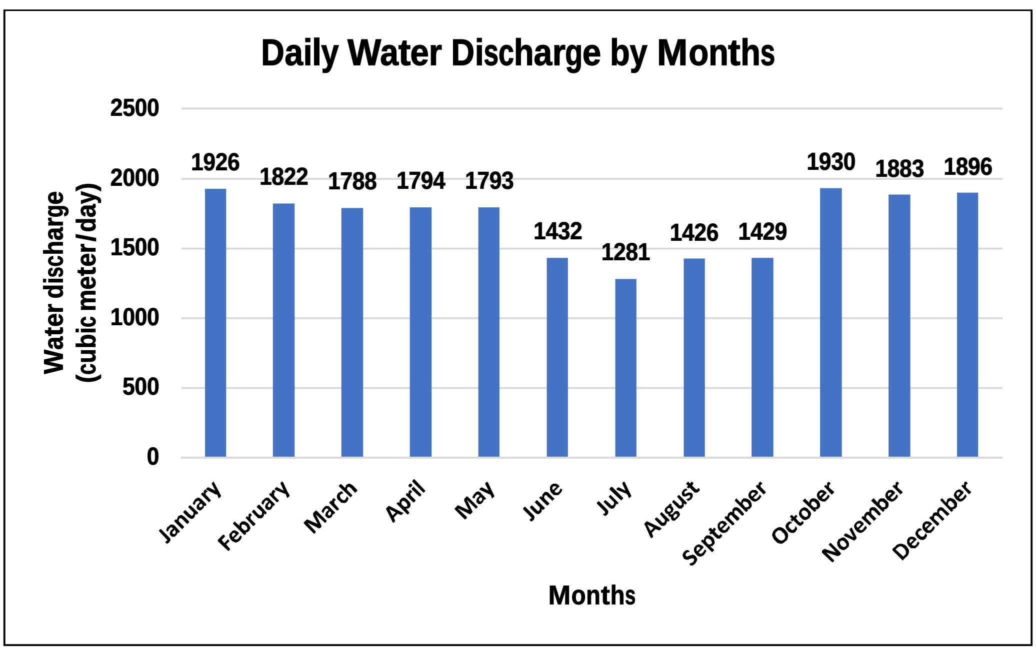

Figure.3.3: Daily water discharge rate by months

3.4 Cost Breakdown of the GS-Gorol Project

The total cost of this project is US$ 62,722.03. Solar photovoltaic panel cost is the highest among the system components. The solar pumping system includes submersible motor, motor controller, and solar inverter. Module mounting structure, boring, tube well, delivery pipe, buried pipe, control room and land development comes under the fixed costs. Cables, supply, installation, testing, commissioning, and transportation are also needed to be considered during costs breakdown. The system is a batteryless system and using a small header tank which can store 3400 liters of excess water for further use. Figure.3.4 shows the economic cost breakdown of the system.

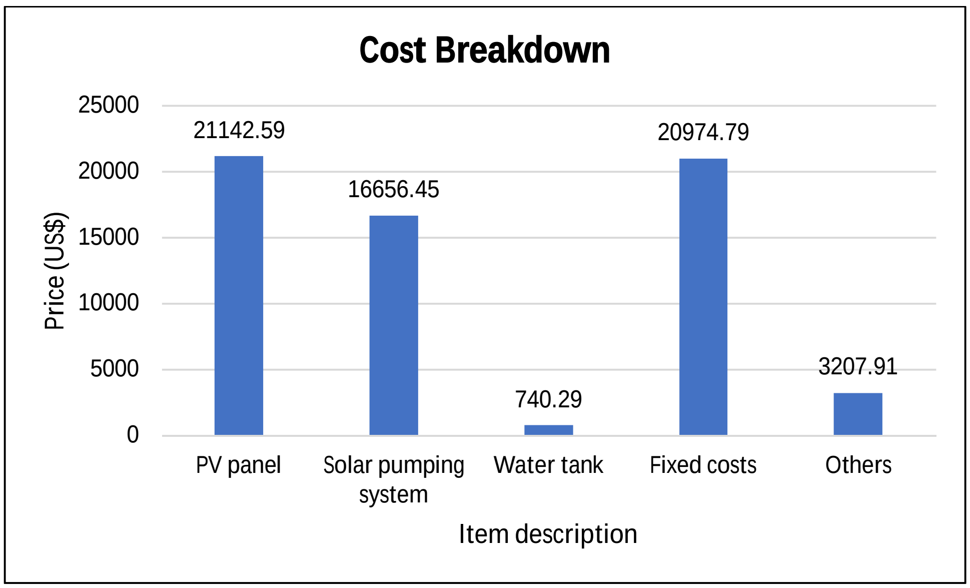

Figure.3.4: Economic cost breakdown of GS-Gorol project

3.5 Analysis of GS-Gorol Project

As per the project report of GS-Gorol project, they did not go for the battery-based system; they stored energy in a form of water storage for further use. The system irrigates the total land areas during the daytime and they stop the process during night time. The small water tank can only store a little amount of water; around 0.002% of daily total water discharge. The problem arrives when the PV modules cannot produce enough power to lift water during cloudy weather for 2-3 days. A built-in automatic ON/OFF switching system comes with the inverter which controls the system runtime with the use of a solar light sensor. The system also consists of two water level sensors; deep-well water level sensor and overhead tank water level sensor. The first one automatically switches off the system when the water level of the well goes down and the second one controls the run time of the system according to the water level in the storage tank.

This thesis will design both battery-based and battery-less solar water pumping system for irrigation in Bangladesh. Then the feasibility of the system will be discussed from the economic point of view. The system will be consisting of a solar light sensor, voltage/current sensor, and PV voltage/current sensor to ensure an uninterrupted operation. A soil moisture sensor will confirm whether the land needs irrigation or not. This research will try to achieve an optimum solution between battery based and battery-less system solar irrigation pumping system. A site in Bangladesh discussed above will be used as a reference site.

3.6 Proposed Solar Irrigation Pumping System

A solar water pumping system for irrigation in Bangladesh was assessed and sizing was done using HOMER (Hybrid Optimization and Multiple Energy Resources). For HOMER optimization, at first daily load data was calculated from site data. Figure.3.5 gives a sample daily load distribution of the selected site. More flow rate was used around noon time to best utilize the solar irradiance that day.

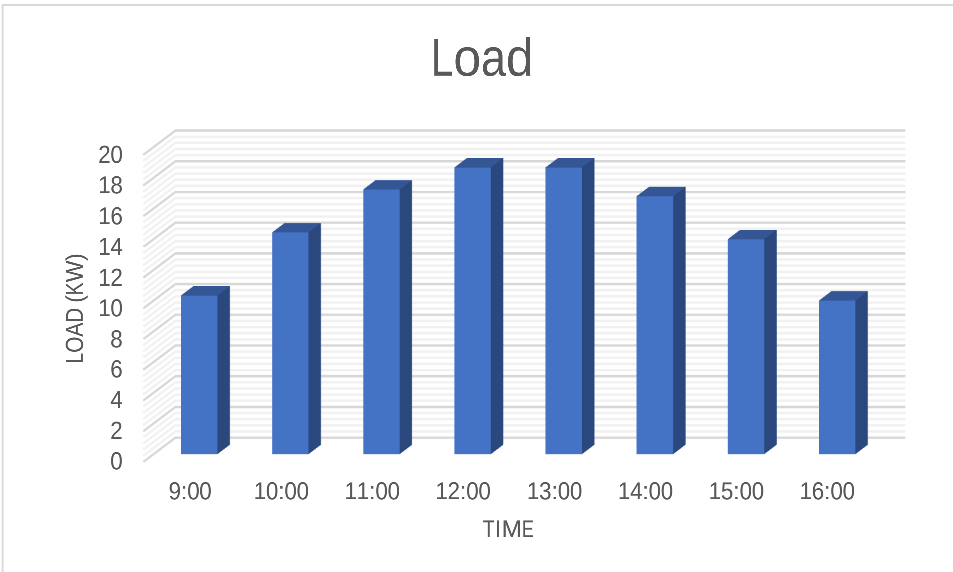

Figure.3.5 Daily load distribution

3.7 Solar GHI Data

The geographical location of the selected site is same as GS-Gorol project discussed above. The longitude and latitude of the site is 26^0 North and 89^0 28' East accordingly. The hourly and monthly geographical horizontal irradiance (GHI) data are shown in Figure.3.6 (a) and Figure.3.6 (b) respectively.

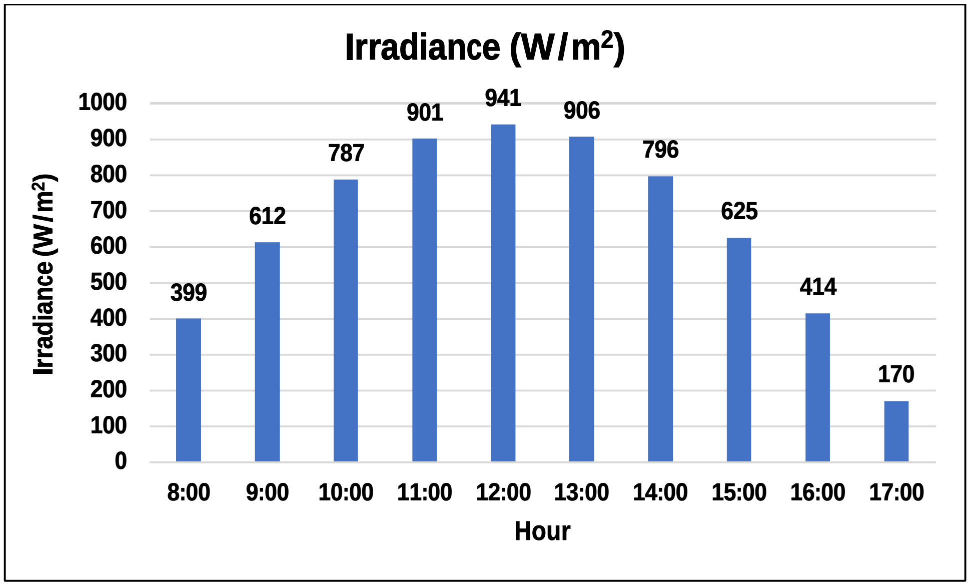

Figure.3.6 (a): Hourly GHI data

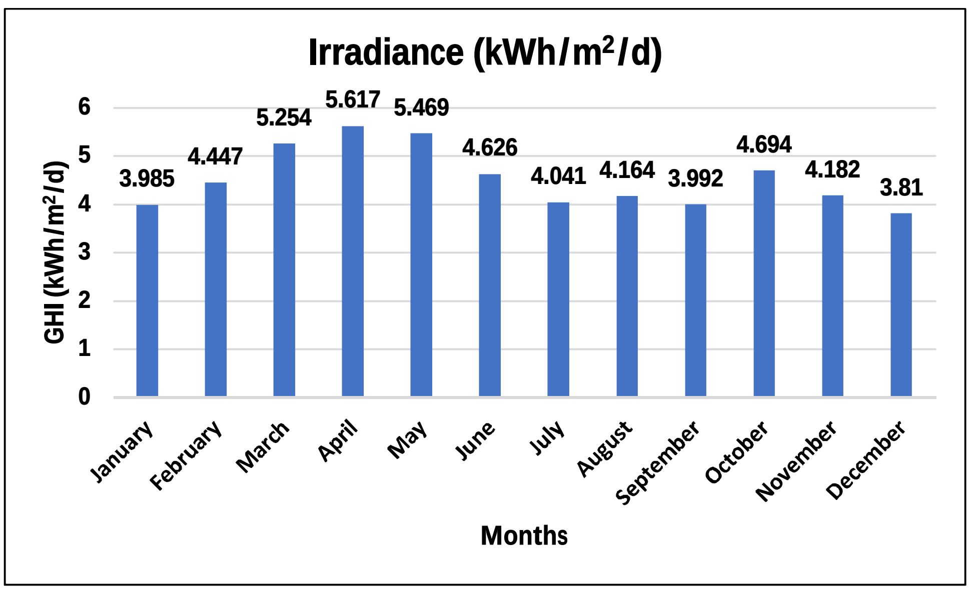

Figure.3.6 (b): Daily GHI data

3.8 Technical Specifications of the Components

The selected solar photovoltaic panel for the system was from Crystalline PV module, CHSM6612P Series. The technical specification of the PV module is described in Table.3.4.

Table.3.4: Technical specification of solar PV module

Mode No	CHSM6612P
Peak Power P_{max} [Wp]	310Wp
Max. Power Current I_{mpp} [A] at STC	8.68A
Max. Power Voltage V_{mpp} [V] at STC	35.80V
Short Circuit current I_{sc} [A] at STC	8.99A
Open Circuit Voltage V_{oc} [V] at STC	45.42V
Temperature co-efficient of P_{max} [% / ^{0}K]	-0.408%
Temperature co-efficient of V_{oc} [% / ^{0}K]	-0.311%
Temperature co-efficient of I_{sc} [% / ^{0}K]	0.050%
Max. system voltage [V]	1000VDC
Nominal Operating Cell Temperature	46±2 ^{0}C
Efficiency at STC [%]	16
Brand	ASTRONERGY

A bus voltage of 48V was selected since we plan to analyze and compare battery storage and water storage options. As the selected PV module is 72 cell module, we are using two number of modules per string.

Battery storage was used to store the excess energy. As the selected bus voltage was 48V and battery nominal bus voltage was 12V, four number of batteries used per string. The technical specification is described in Table.3.5.

Table.3.5: Technical specification of battery storage

Mode No	6FM200D
Nominal Capacity [Ah]	200
Max. Capacity [Ah]	193
Nominal Voltage [V]	12
Round Trip Efficiency [%]	80
Min. State of Charge [%]	40
Max. Charge current [A]	60
Cycles to failure at 50% depth of discharge	650
Lifetime Throughout [kWh]	917
Brand	Vision Battery

The solar inverter was used to convert the DC power into AC power. Technical specification of the selected solar inverter is shown in the following Table.3.6.

Table.3.6: Technical specification of solar inverter

Model	GS8048A
Rated Capacity	8kW
Rated Input Voltage	48VDC
Output Voltage	240VAC
Output Phase	3-Phase
Type	Pure Sine Wave
Output Frequency	50Hz/60Hz (selectable)
Max. Efficiency	95%
Brand	OutBack Power
Manufacturer	Radian series

The system was run in HOMER with 5% load sensitivity, 10% irradiance sensitivity and with a minimum renewable fraction of 100%. The minimum annual capacity shortage was decided as 10% and other constraints were set as zero. In Bangladesh, the interest rate for a bank loan for any renewable energy project is about 9 to 10%, varies from bank to bank policy. Here, for HOMER simulation, the bank interest rate was decided as 10%.

3.9 Analysis of HOMER Simulation Results

Homer simulation implies that for the selected load distribution the system components should be as follows in Table.3.7.

Table.3.7: System component

System component	Rating
PV [kW]	38.4 (310 Wp each)
Battery Storage [No]	60 (12V, 200 Ahr each)
Inverter [kW]	20.7

Total net present cost (NPC) of the system was calculated by HOMER is $156,773. The levelized cost of energy (COE) is $0.442/kWh and the total operating cost is $4,245/yr. The economic cost breakdown for twenty five years of period is shown in Table.3.8 and Figure.3.7.

Table.3.8: Economic cost breakdown

Component	Capital (US$)	Replacement (US$)	O&M (US$)	Salvage (US$)	Total ($)
PV	55,242	4,977	1,876	-2,318	59,777
Battery Storage	42,000	21,513	0	-554	62,960
Inverter	14,003	3,193	1,174	-410	17,959
Other	7,000	0	9,077	0	16,077
System	118,245	29,683	12,127	-3,282	**156,773**

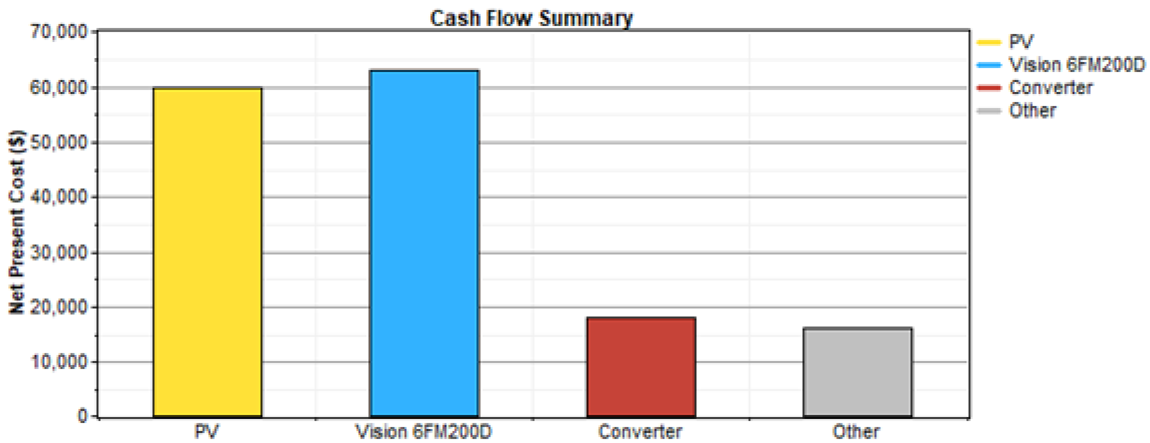

Figure.3.7: Economic cost breakdown

As June to September is the rainy season in Bangladesh, the recorded Solar Irradiance become lower in these months. So, the produced electricity would be lower in these months. The following Figure.3.8 shows the monthly average electric production of the system.

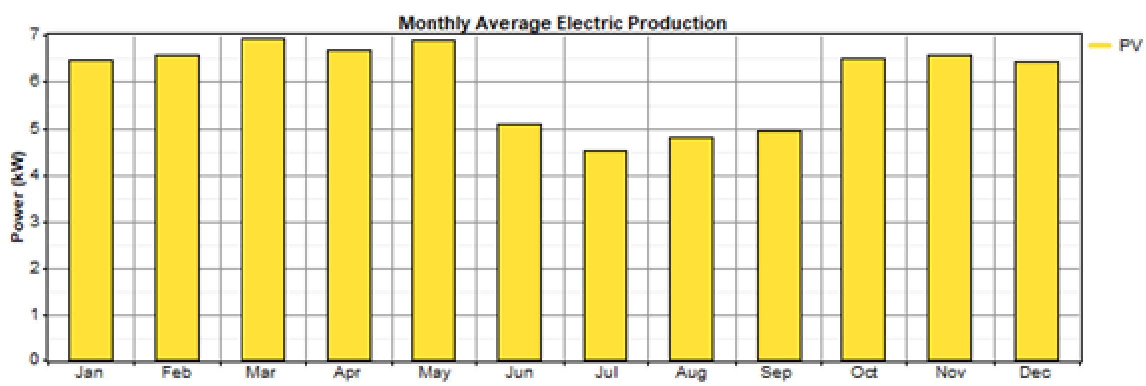

Figure.3.8: Monthly average electric production

The system can produce total 52,804 kWh energy per year and the AC primary load consumption is 100% (39,110 kWh/yr). The excess electricity is around 15.2 % (8,043 kWh/yr).

The PV output ranges from 7.2 kW to 28.8 kW mostly during the runtime. Although the rated capacity is 38.4 kW, the mean output is about 145 kWh/d with the capacity factor of 15.7 %. The following Figure.3.9 will give a clear idea about the PV output.

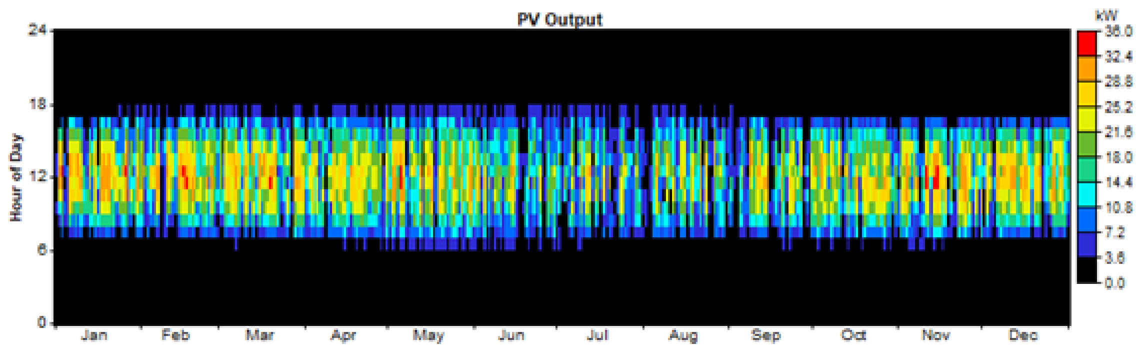

Figure.3.9: PV output

Minimum state of charge for the battery storage was decided as 40%. The frequency histogram in Figure.3.10 shows that the frequency of being 100% state of charge is around 40% and the monthly statistics in Figure.3.11 implies that the state of charge remains lower in the months from June to September.

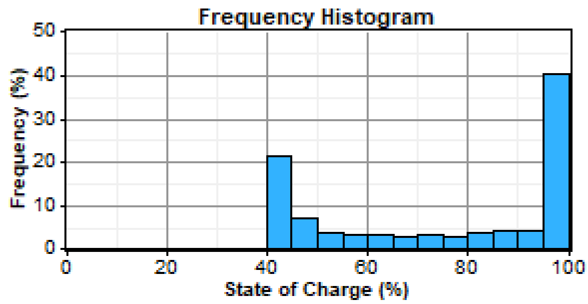

Figure.3.10: Frequency histogram

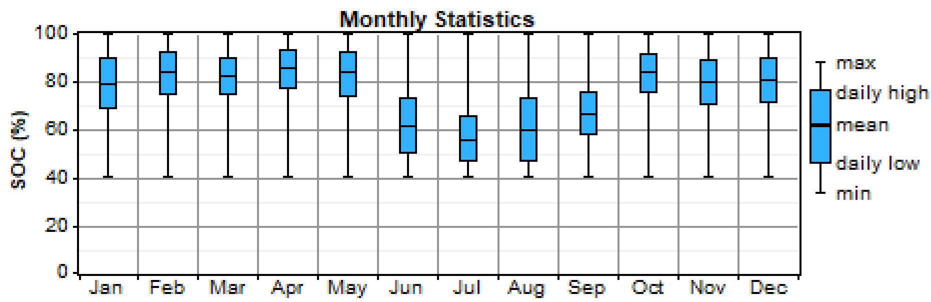

Figure.3.11: Monthly statistics

A 20.7 kW inverter was selected to convert the DC photovoltaic output into AC unit. The mean output of the inverter was 4.5 kW with a capacity factor of 21.6 %. The inverter output is shown in Figure.3.12.

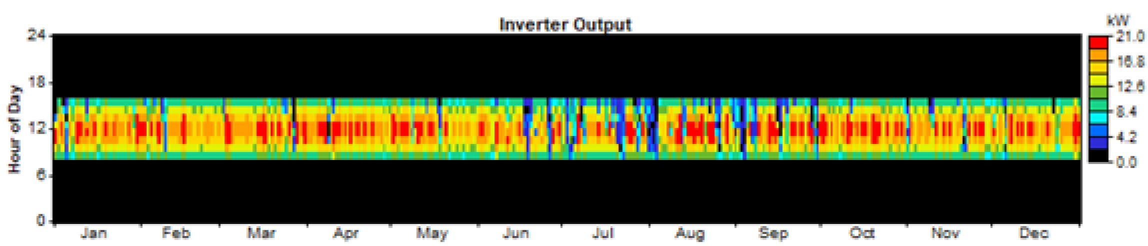

Figure.3.12: Inverter output

3.10 Water Tank Equivalent Battery Storage

The energy can be stored in two ways; either as electrical power storage in batteries or as water storage in the large water tank. The above system was simulated as a battery-based system. The simulation result implies that the 60 batteries (total of 15 strings, with 4 batteries per string) were used to store the electric energy for further use. To calculate the water tank equivalent to battery storage, following steps needed to be considered.

Battery ampere hour: 200 Ah

Bus voltage: 48 V

Number of strings: 15

Total watt-hour = $(48 \times 200 \times 15) = 144{,}000$

Calculation of Total Dynamic Head (THD):

Figur.3.13 demonstrate a water tank based solar water pumping system.

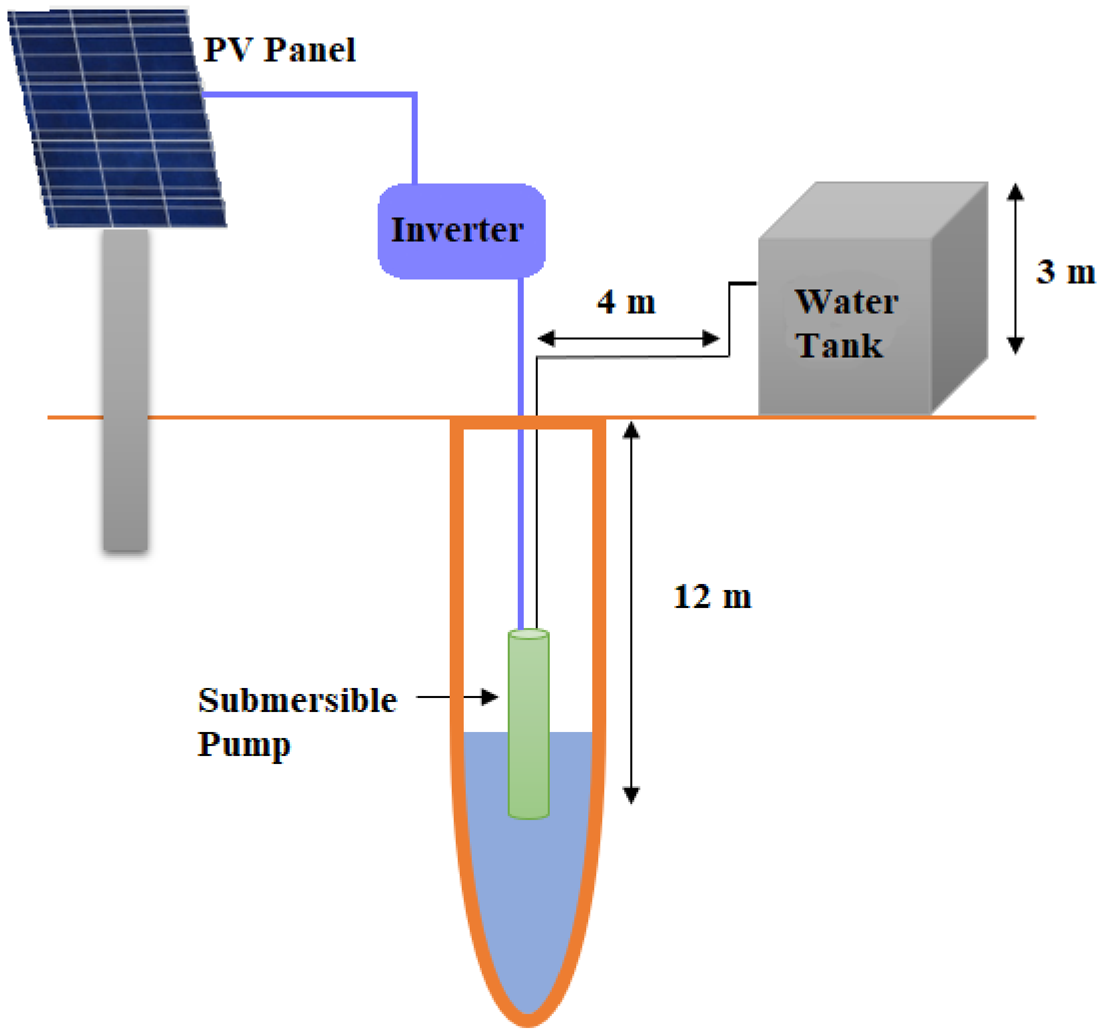

Figure.3.13: Block diagram of the water tank storage system

From Figure.3.13, Elevation Head = (12+3) m =15 m

Friction Head Loss:

The system is using 8inch diameter pipe to supply around 1700,000liter water per day. The system has three standard elbows and a gate valve. So the friction head loss for fitting will be (1.6+0.11) =1.71 m

The frictional head loss for pipe, using Hazen-Williams Formula is (0.28+0.16) m = 0.44 m

Total frictional head loss = (1.71+0.44)m= 2.15 m

We can conclude, total dynamic head = Elevation Head + Friction Head Loss

$$= 15+2.15=17.15 \text{ m}$$

The total volume of water needed to be stored in the water tank,

$$m \text{ (kg)} = (144000\times3600)/(17.15\times9.81)=3.081\times10^6 \text{ kg or } 3081 \text{ m}^3$$

To store 3.081×10^6 kg or 3081m^3 of water, we need at least 3081 cubic meters or 3100 cubic meter water tank. As The height of the tank is already decided, either we need to build a large rectangular tank (40 m×26 m×3 m). Ms. Snehal R. Metkar [34] stated that around Rs. 5,290,671 (US$. 79,911.19) is needed to construct a water tank to store 3000 m^3 water. We can calculate approximate price of the required tank size (40 m×26 m×3 m) as Rs. 5,500,935 (US$. 83,087.06) from the trend line in Figure.3.14.

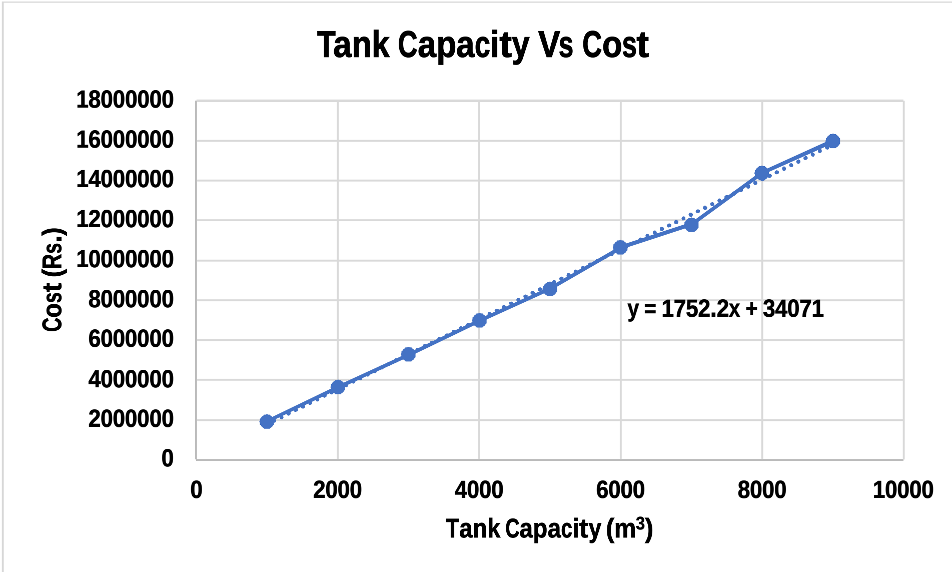

Figure3.14: Tank capacity vs. cost

The price of the land area also needs to be added total cost which varies with time and location. The land cost is assumed to be around US$ 5000 for the analysis and added with the system cost.

3.11 Summary

An established system data is studied for detail analysis of solar water pumping system for irrigation in Bangladesh. A HOMER simulink model is created based on daily load distribution and Solar GHI data. The system component is selected accordingly, and the present price is provided in US$. As the HOMER simulink model is a battery-based system, water tank equivalent battery storage is also calculated and the comparison between both is also discussed from the economic point of view. Although both systems are expensive, the battery-based system comes out as a slightly cheaper solution than the battery-less system. Building a large water tank is also inconsistent. Combination of both; battery storage and tank storage might provide an optimum solution. Dynamic simulink model of both systems will be built and be discussed in the next chapter.

CHAPTER 4

DYNAMIC MODELING AND SIMULATION IN SIMULINK

4.1 Dynamic Modeling

The name MATLAB stands for Matrix Laboratory is an effective technical computing system for handling engineering and scientific calculations [35]. Cleve Moler, the designer of MATLAB, started developing it in late 1970’s. It is a fourth-generation programming language developed and introduced by MathWorks in 1984. MATLAB is an interpreted environment. It can run both interactive sessions and batch job. The comprehensive online help system helps the user to understand in a better way.

Simulink, also introduced by MathWorks in 1984, is a graphical programming environment for modeling, simulating and analyzing multi-domain dynamic systems. The Simulink and MATLAB environments are integrated into one entity, so the simulation and analysis can be done in either environment [36]. Simulink helps to model a system in the Simulink environment and investigate the dynamic behavior of the system components. Different block diagrams can be built to represent the various parts of the whole system where the signals are used to represent the input or output relationship between the blocks. It provides a graphical editor and a block library for modeling and simulating dynamic systems [37].

HOMER optimization from the previous chapter provides the most feasible solution for the battery-based system. Water storage tank for the battery-less system was also calculated from HOMER optimization result. Above mentioned systems are designed in MATLAB Simulink environment to observe the dynamic behavior of the system components. This chapter will discuss the dynamic modeling and simulation of the above two systems. At the end of this chapter, the author will try to find out the most feasible solution combining both storage systems.

Dynamic models for solar irrigation pumping system for both; battery-based and battery-less system are built in MATLAB Simulink. Both models are simulated for same input data of irradiance and temperature. Both models are also consisting of the same solar photovoltaic array and motor pump set.

4.2 Irradiance and Temperature

The main purpose of dynamic modeling and simulation of solar irrigation pumping system simulation is to observe the response of motor speed with the variation of irradiance and temperature. The variation of irradiance and temperature from morning till night discussed in the previous chapter. As the dynamic model consists of several complicated blocks, it will take many days of computer time for one solar day simulation. To overcome this problem, it was decided to simulate the battery-less system for five seconds and battery-based system for two seconds. The irradiance and temperature data are selected in such a way that both will drop for a fraction of second due to clouds and become same as before when clouds move away. Figure.4.1 and Figure.4.2 represent the irradiance and temperature profiles for five seconds and two seconds accordingly. The following profiles also represent the variation of irradiance and temperature of one solar day.

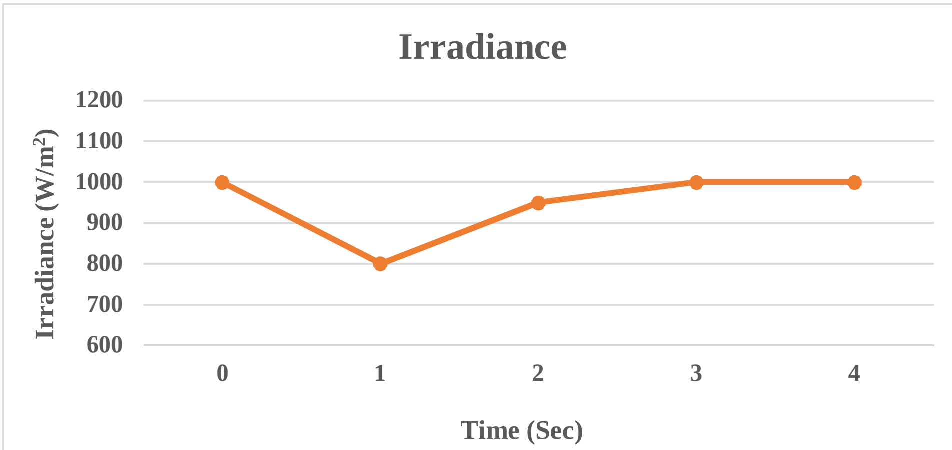

Figure.4.1 (a): Selected irradiance for the battery-less system

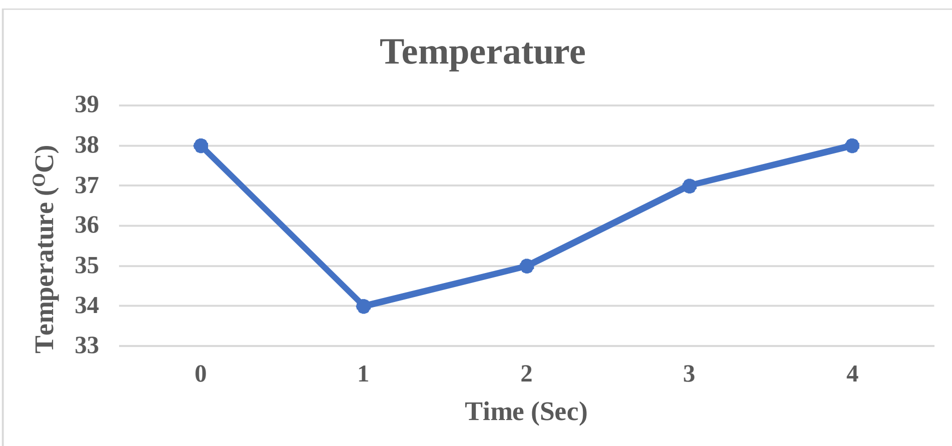

Figure.4.1 (b): Selected temperature for the battery-less system

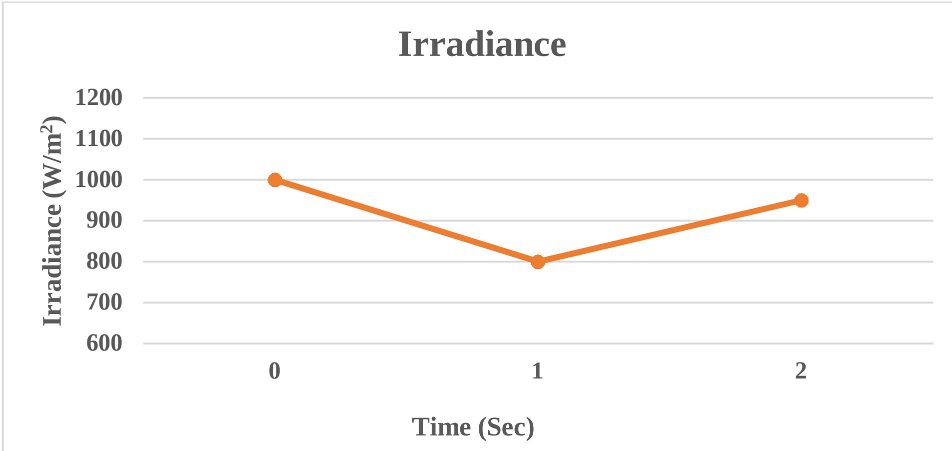

Figure.4.2 (a): Selected irradiance for the battery-based system

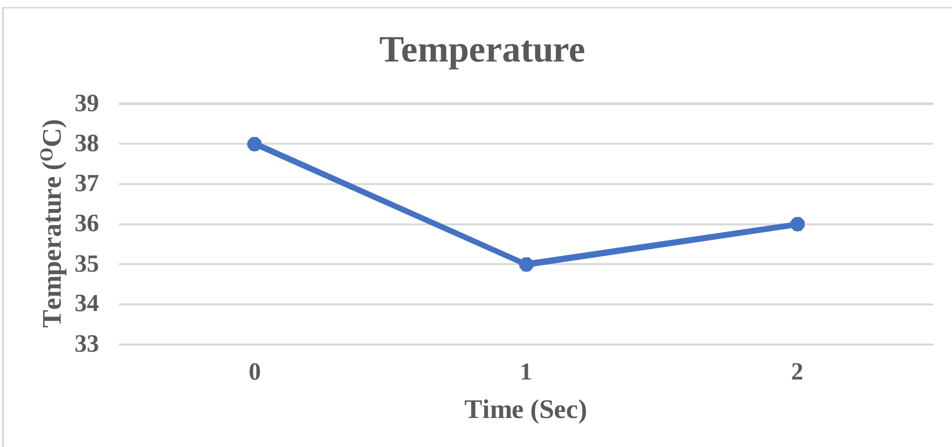

Figure.4.2 (b): Selected temperature for the battery-based system

The above-described signals of irradiance and temperature are generated in signal builder in MATLAB Simulink for providing the inputs to PV array.

4.3 Solar Photo Voltaic (PV) Array

In the MATLAB Simulink model, the selected PV module is Chint Solar (Zhejiang) CHSM6612P-310. Each module has a capacity of 310Wp. Figure.4.3 shows the PV array block in Simulink.

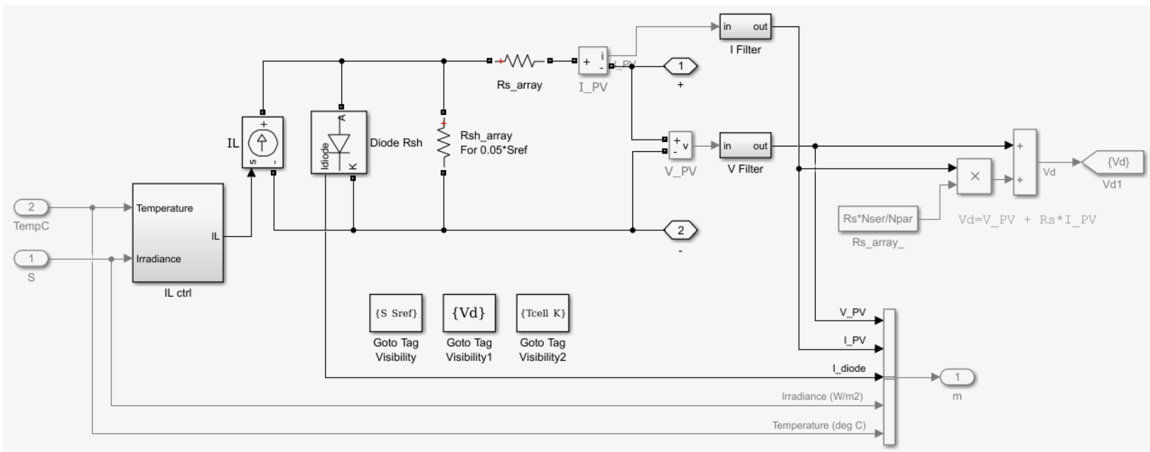

Figure.4.3. PV array block in Simulink

HOMER optimization result implied in the previous chapter that 38.4 kWp solar array is needed to provide enough energy to run the motor-pump set for extracting of the estimated amount of groundwater. The selected solar module is a 72-cell module. To provide 48 V bus voltage, it was decided to connect two number of modules in series per string. Therefore, the number of strings becomes 62.

Equivalent equation of a solar cell where V and I are output voltage and current accordingly:

$$I = I_l - I_D - \frac{(V+IR_S)}{R_{sh}} \tag{4.1}$$

Where,

Shunt resistance, R_{sh} = 85.7392 ohm

Series resistance, R_s = 0.44015 ohm

Diode saturation current, I_D = 1.8885e $^{(-09)}$ A

Light-generated current, I_l = 9.6521 A

The following equations define the diode V-I characteristics for a single module:

$$I_d = I_0 \left[exp\left(\frac{V_d}{V_T} - 1\right)\right] \tag{4.2}$$

$$V_T = \frac{KT}{q} \times a \times N_{cell} \tag{4.3}$$

Where,

Diode ideality factor, a = 1.1011

Boltzmann constant, K=1.3806×10$^{(-23)}$ J.K$^{(-1)}$

Electron charge, q = 1.6022×10$^{(-19)}$ C

Number of cells connected in series in a module, N_{cell} =72

Here in the above equations 4.2 and 4.3, I_d (A) is the diode current and V_d (V) is the diode voltage. Cell temperature, T (K) varies with time.

V-I characteristics and the power curve have been simulated in MATLAB. The MATLAB code is provided in Appendix A.

The following Figures.4.4 (a) and 4.4 (b) describe the V-I characteristics and the power curve of a single module.

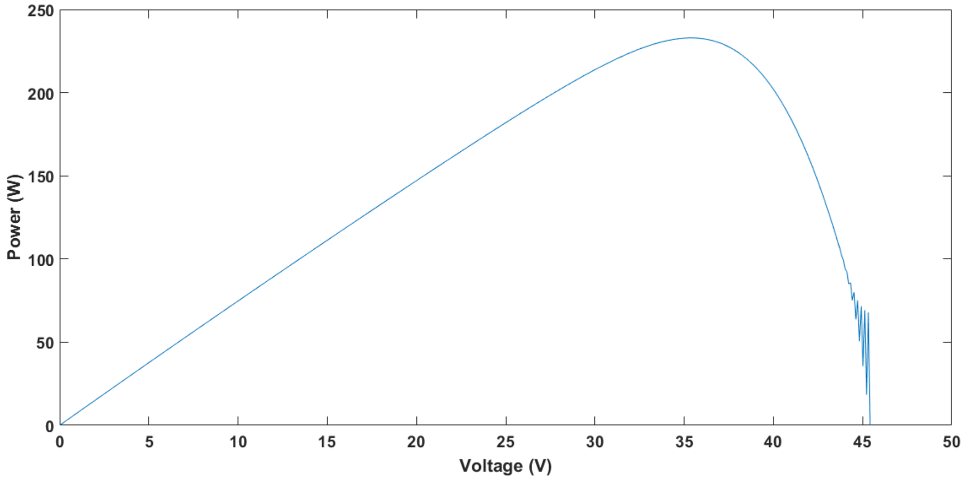

Figure.4.4 (a): V-I characteristics

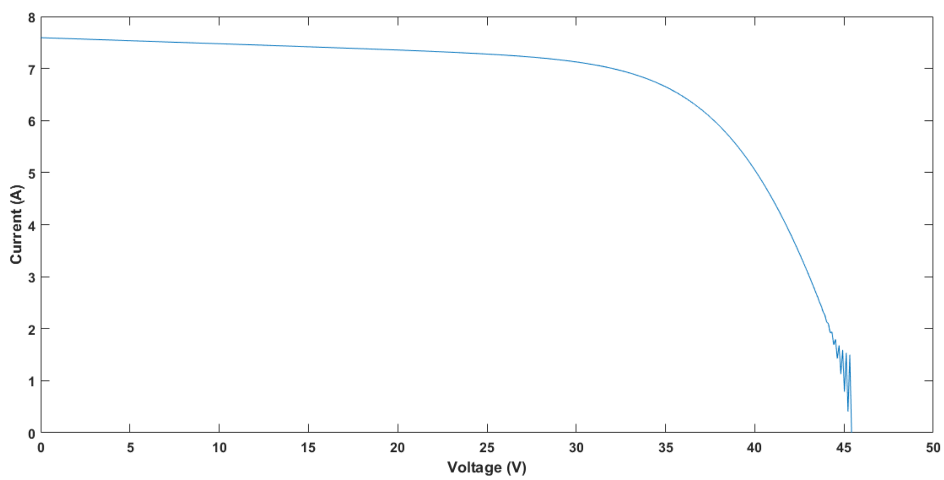

Figure.4.4 (b): Power curve

4.4 Motor Pump Set

In the dynamic modeling, a built-in Asynchronous Machine is used as a motor. The motor is squirrel cage induction motor type which is 20 HP, 460 V, 60 Hz. The nominal power is 1.492×10^4 VA and the mechanical power is 1.492×10^6 W. The nominal speed of the rotor is 1760 RPM. The rotor is selected as a reference frame and the value of mechanical torque input is 8 N.m. Figure.4.5 shows the asynchronous machine block in detail.

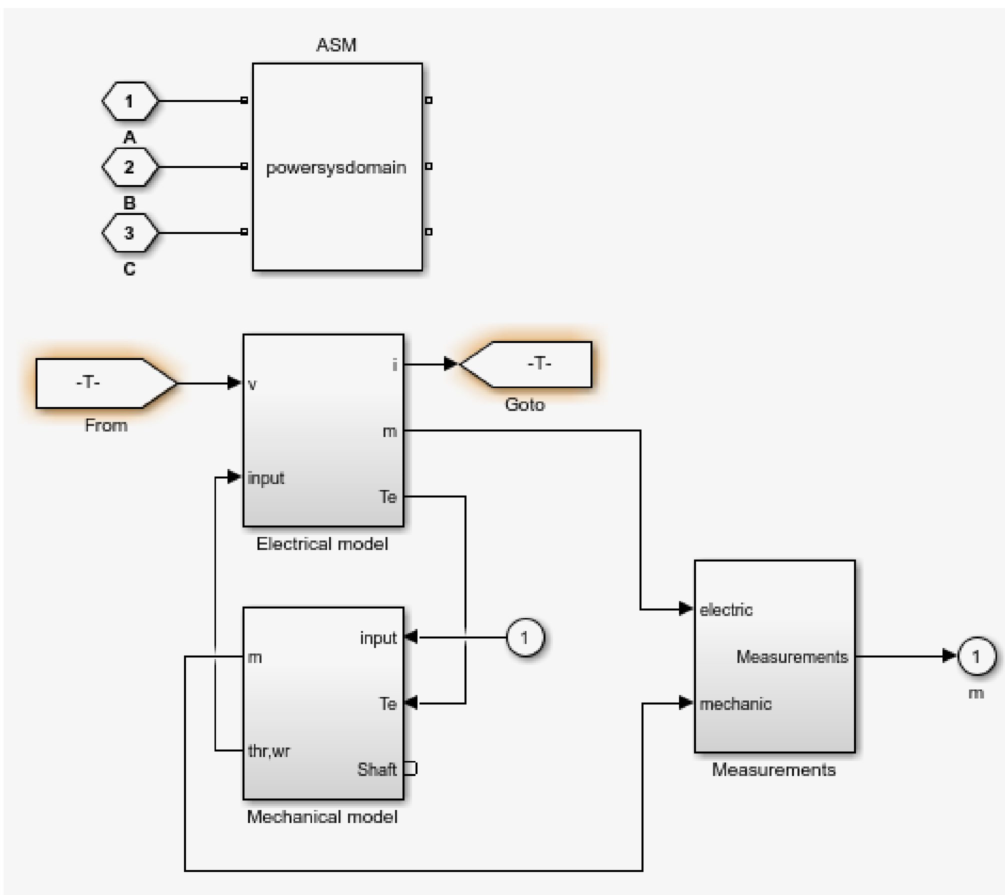

Figure.4.5: Asynchronous machine block in simulink

The outputs of the induction motor are electromagnetic torque, T_e (N.m) and rotor speed, ω (rad/s). To calculate the water discharge rate (Q) of the pump, following equations are considered.

Power provided to the pump from motor P (W),

$$P = T_e \times \omega \tag{4.4}$$

The needed hydraulic power of the pump P (W),

$$P = Q\rho gh/3600 \tag{4.5}$$

Where,

Gravity, g = 9.81 m/s^2

Total dynamic head of the liquid, h = 17.15 m

Water density, ρ =1000 kg/m^3

Therefore, from equations (4.4) and (4.5), the water discharge rate,

$$Q = 0.0000214(T_e \times \omega).$$

In the Simulink model, the product of Te and w are multiplied by the gain 0.0000214 to find out the water discharge rate Q (m^3/s).

4.5 Three Phase Breaker

A three-phase breaker is used between the inverter and asynchronous motor for protection purpose. The opening and closing time of the breaker is set as external control. Figure.4.6 shows the breaker block in detail.

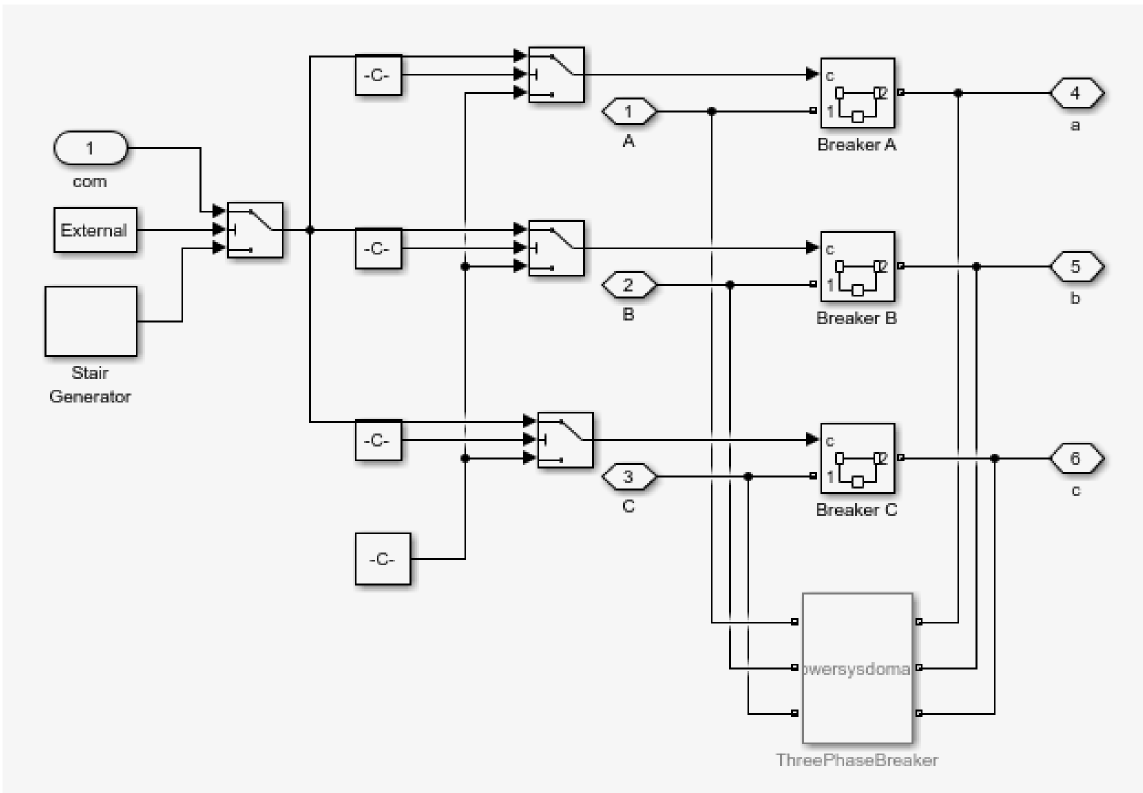

Figure.4.6: Three phase breaker

4.6 Modelling of Battery-Less System

The output voltage of the PV array is 48 V. In the battery-less system, a boost converter is used to increase the voltage level from 48V to 460V to run the induction motor to lift groundwater. A three-level bridge converter is used as an inverter to convert the DC component into AC component. This system consists of a large water tank which can store around 3100 m^3 of water and a limited integrator was used to indicate the tank water level. Following Figure.4.7 demonstrates the dynamic modeling of a battery-less solar irrigation pumping system.

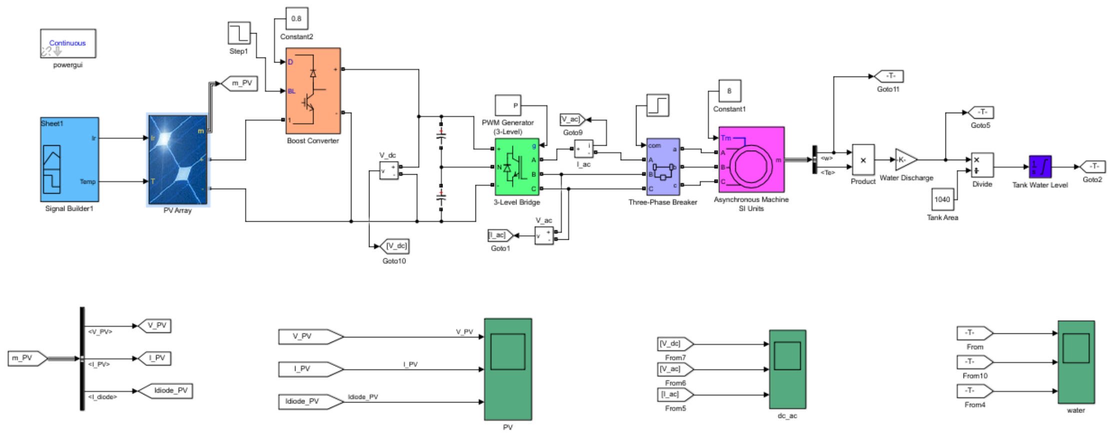

Figure.4.7: Dynamic modeling of the battery-less system in Simulink

4.6.1 Boost Converter

The converter is modeled using a switching-function model directly controlled by the duty cycle signal (0< D <1). This technique yields the fastest simulation. No PWM generator is required here.

In the Simulink model, the duty cycle is selected as 0.8 and all firing pulses are blocked by applying a signal value of 1 at the BL input.

4.6.2 Inverter

A built-in three-level bridge block is used for DC to AC conversion. The number of bridge arms is three and the power electronic device used is IGBT/Diodes. Each arm consists of four switching devices along with their antiparallel diodes and two neutral clamping diodes as shown in the Figure.4.8 below.

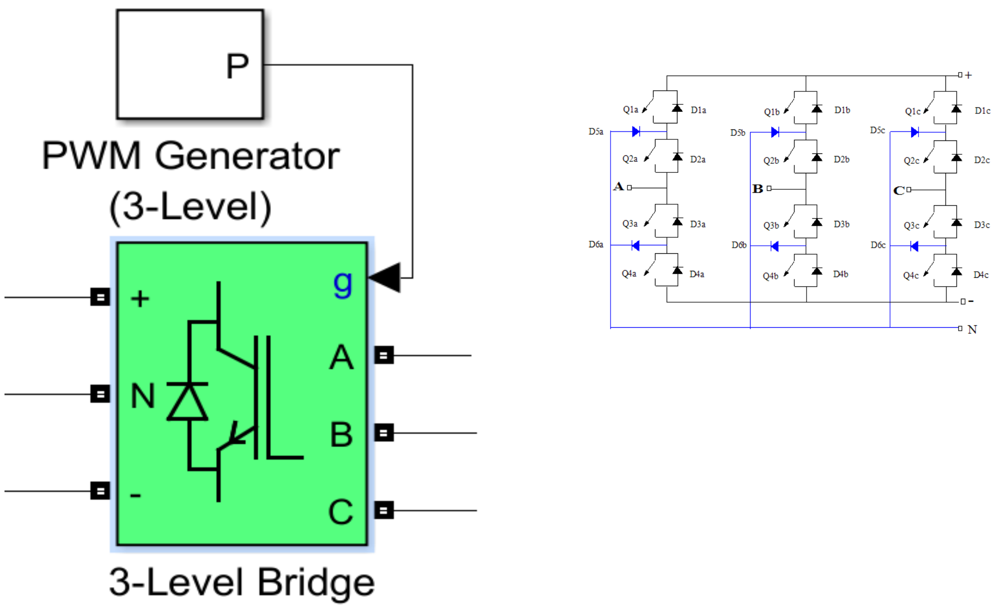

Figure.4.8: Three level bridge inverter

4.6.3 Tank Water Level Measurement

The output value of the tank water discharge is divided by the tank area to find out the tank water level. Then this value is used as the input to a limited integrator the get the exact water level of the tank. The height of the tank is decided as the upper limit of the integrator.

4.7 Simulation Result Analysis of the Battery-Less System

PV module voltage and current at maximum power point are 35.8V and 8.68A accordingly. As the selected panel is 72 cell panel and two number of panels connected in series per string, the bus voltage should be 48V. A total number of strings is decided as 62. Figure.4.9 shows the PV voltage, PV current and diode current. V_PV denotes the PV voltage and the steady state value is around 85 V, which is expected. I_PV and Idiode_PV represent the PV current and diode current accordingly. PV current becomes around 25 A and the diode current fluctuates between 400A to 600 A.

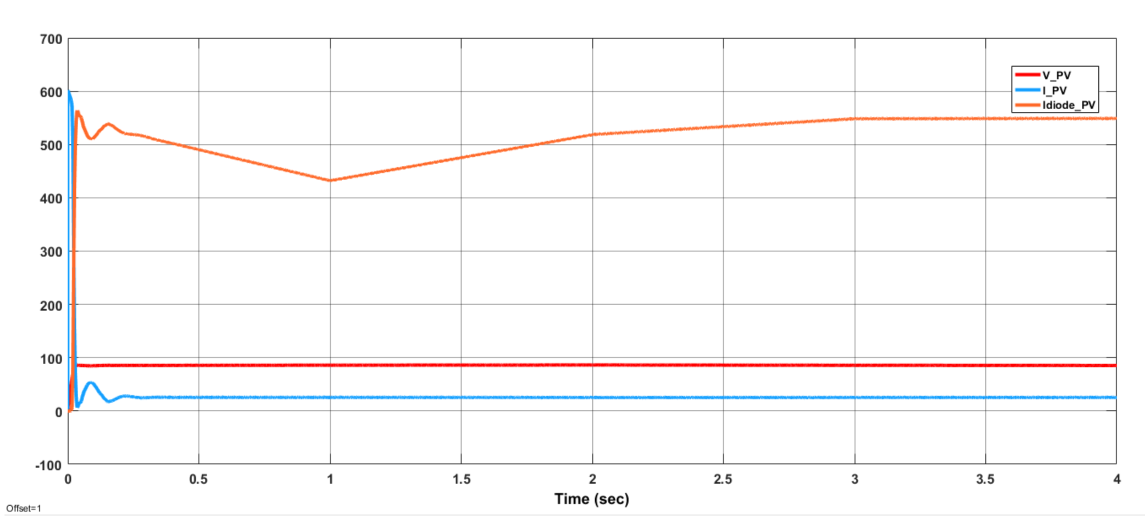

Figure.4.9: PV properties of the battery-less system

Boost converter increases the PV voltage level up to 460V. V_dc denotes the boosted-up dc voltage in Figure.4.10. Then the inverter converts this DC unit into AC unit to run the motor. I_ac and V_ac indicate the converted ac current and voltage accordingly.

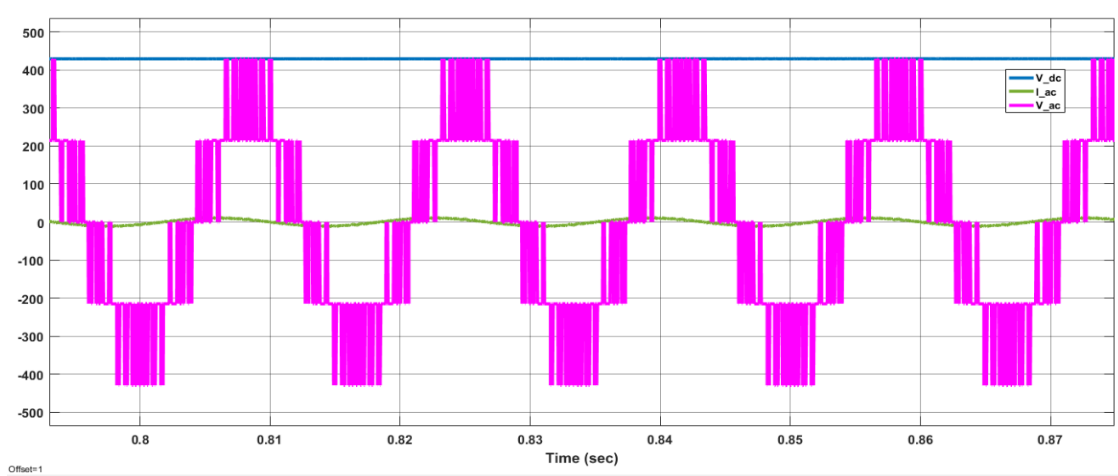

Figure.4.10: AC and DC voltage and current of the battery-less system

Figure.4.11 demonstrates the rotor speed, w (rad/sec). The motor is running at full load and the rotor speed becomes 187 rad/s or 1785.72 r.p.m which was expected. Water discharge and tank water level overlaps in this figure. Figure.4.12 gives a clear view of water discharge and tank water level.

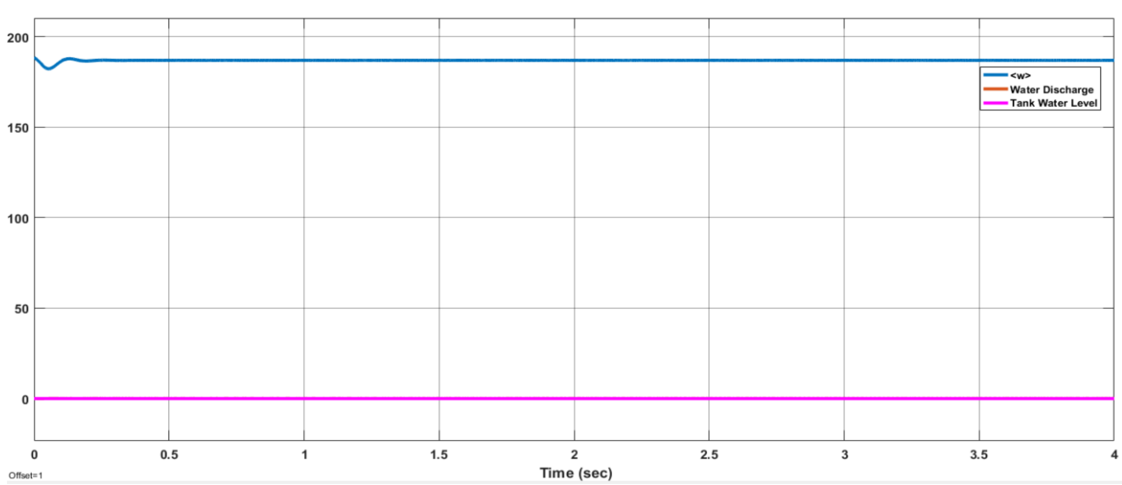

Figure.4.11: Rotor speed of the battery-less system

Figure.4.12 shows the water discharge (m^3/s) and tank water level (m). The average water discharge during five seconds of simulation was 0.045 m^3/s or 162 m^3/h. If the system runs for eight hours, the induction motor will be able to lift 1296 m^3 water per day, which is close to the estimated value. During the first five seconds, the water level in the large water tank (40 m×26 m×3 m) reached 1.74×10^{-4} m. After eight hours of operation, the tank water level would reach at least 1m and volume of lifter water per day would be 1040 m^3.

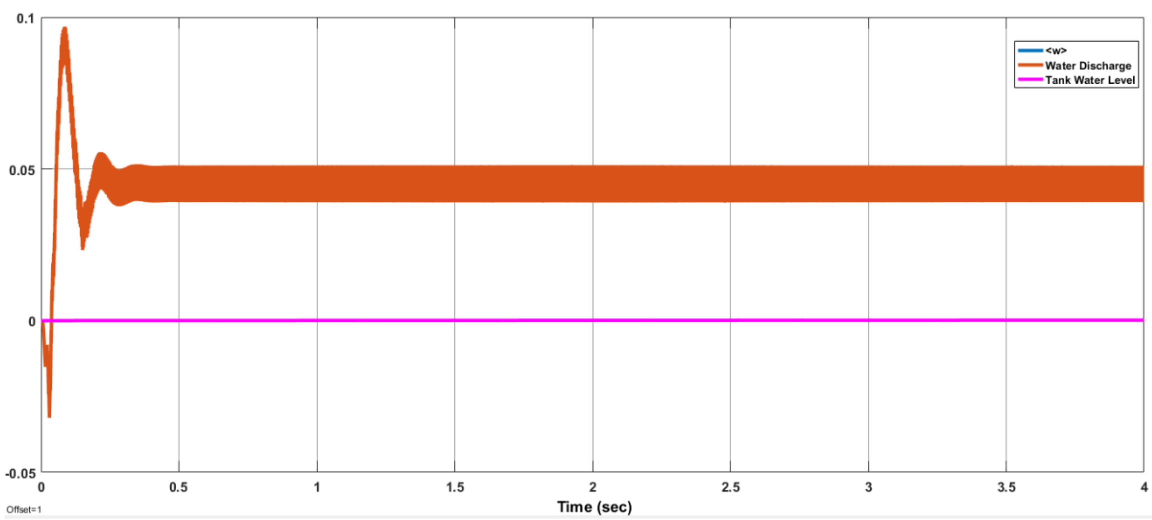

Figure.4.12: Water discharge and tank water level of battery-less system

4.8 Modelling of Battery Based System

Figure.4.13 shows the dynamic model of a battery based solar irrigation pumping system. An MPPT is used here to operate the system at the maximum power point. A two-level bridge converts the DC component into AC component. A three-phase transformer is used instead of a boost converter to increase the voltage level to run the motor. A large battery bank of capacity 3000 Ahr stores energy for further use. In this system, the same water tank (as in battery-less system) is kept to measure the volume of extracted water. The water tank is not included in the battery-based system.

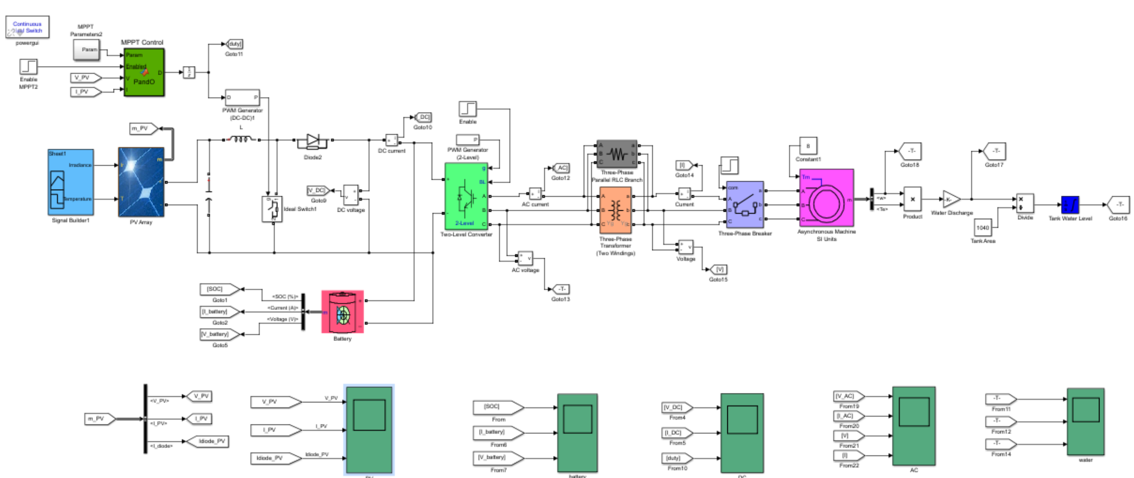

Figure.4.13: Dynamic modeling of the battery-based system in Simulink

4.8.1 Modelling of Battery Based System

The most crucial part of an MPPT is the control algorithm. This algorithm adjusts the duty ratio to find out the maximum power point. There are various methods to get the MPPT i.e. hill climbing method, Perturbation, and Observation, Incremental Conductance, fuzzy logic, neural network, temperature based etc. Perturbation and Observation (P & O) method is the most used in MPPT circuits because of its simplicity. Panel terminal voltage is perturbed and compared with previous power point. The main problem with this method is oscillation occurs around maximum power point because perturbation is applied continuously. It also causes power loss because the perturbation continues even if the algorithm reaches maximum power point. This method is unstable while atmospheric conditions change rapidly. P&O method is described in following Figure.3.14. The MATLAB program is provided in Appendix B.

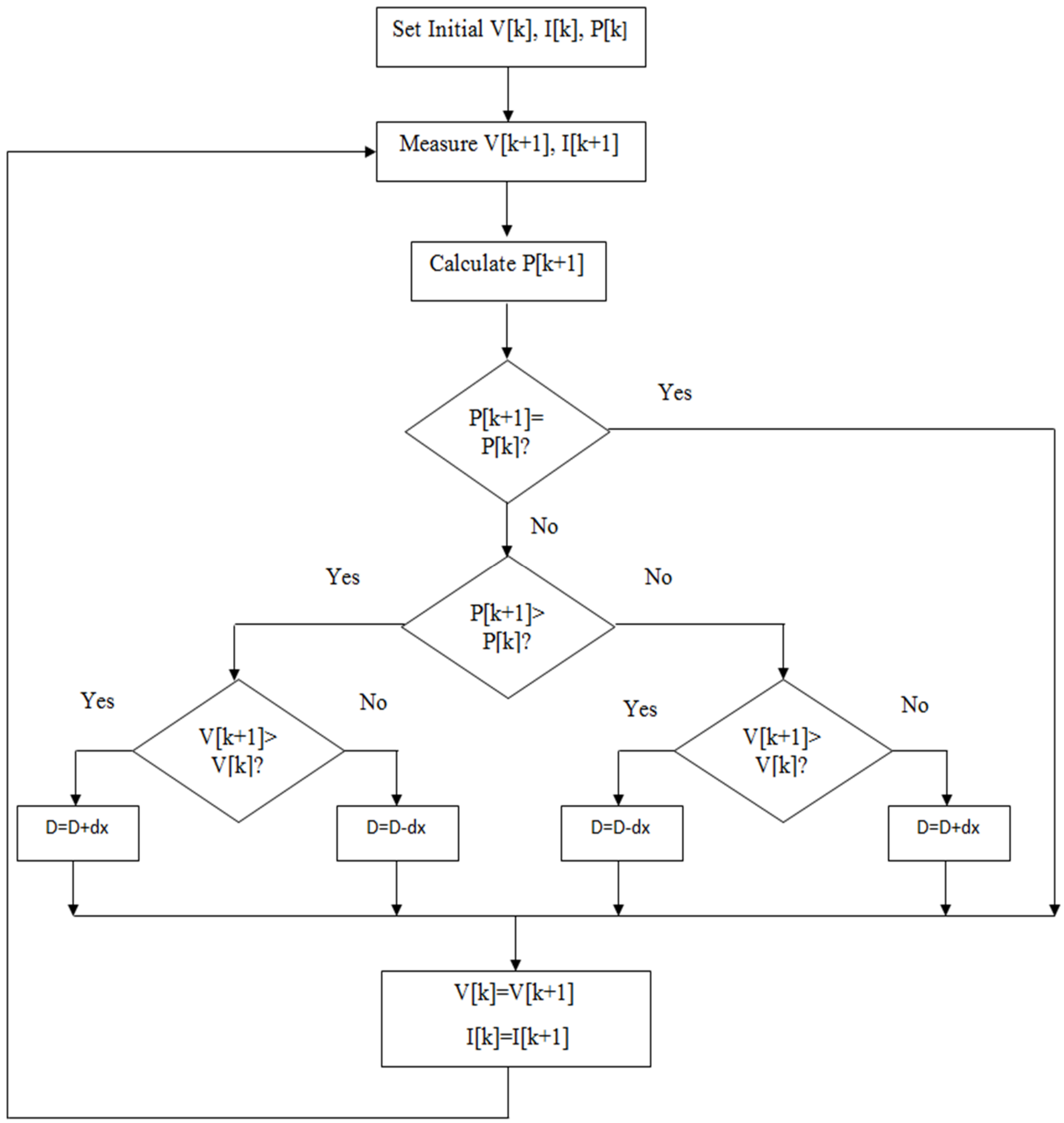

Figure.4.14: Flow chart of P & O method

The parameters for Perturbation and Observation method is given Table.4.1.

Table.4.1: Parameters for perturbation and observation Method

Parameters	Values
Initial value for D output	0.5
Upper limit for D	0.6
Lower limit for D	0.45
Increment value used to increase or decrease	3e-4

4.8.2 Battery Storage

A lead-acid battery bank is used as energy storage whose rated capacity is 3000 Ah. Its nominal voltage is decided as 48 V because it is being fed by 48 V bus. The initial state of charge is selected as 60%. The advantage of a lead-acid battery is there is no temperature effect on it. Figure4.15 shows the battery model.

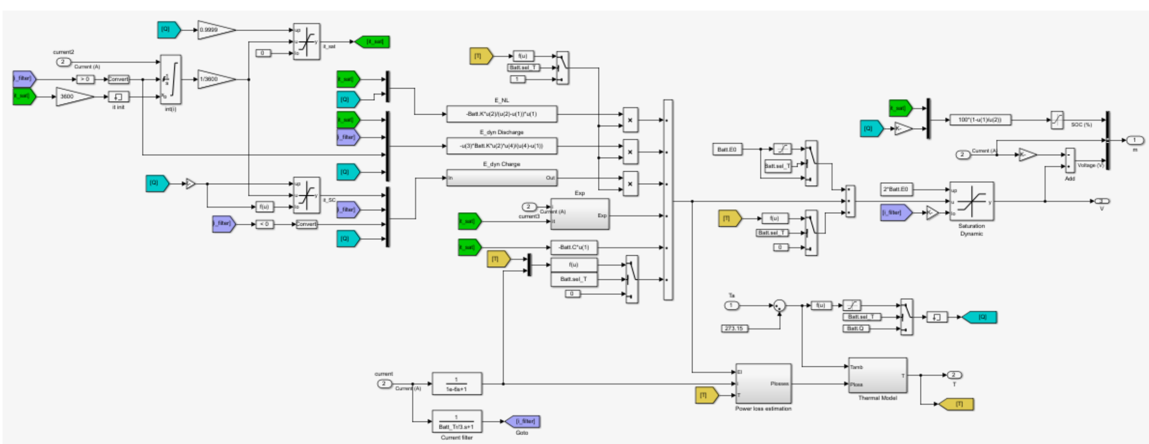

Figure.4.15: Model of battery storage

4.8.3 Inverter

A built-in two-level bridge block is used for DC to AC conversion. The converter is modeled with IGBT/diode pairs controlled by firing pulses produced by a PWM generator. The converter is controlled by a vectorized gating signal. The gating signal contains six firing pulses. The first two pulses control the Q1 and Q2 switching devices (phase A of the converter), pulses three and four control the Q3 and Q4 switching devices (phase B of the converter), and the last two pulses control the Q5 and Q6 switching devices (phase C of the converter). All firing pulses are blocked by applying a signal value of 1 at the BL input. The two-level bridge inverter is shown in Figure.4.16.

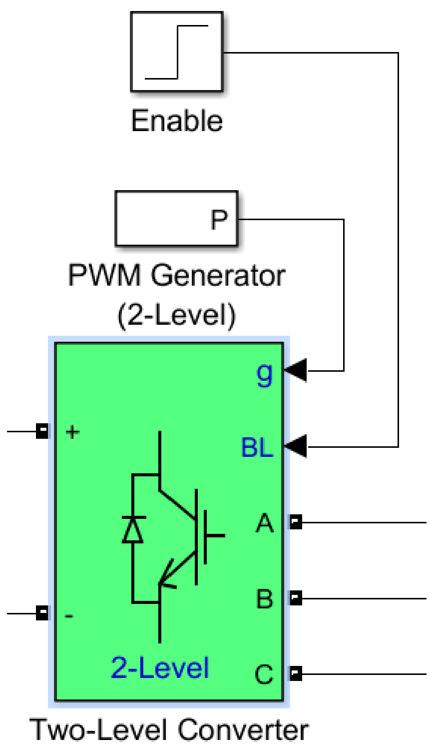

Figure.4.16: Two-level bridge inverter

4.8.4 Transformer

A three-phase step-up transformer is used to increase the voltage level from 48 V to 460 V to run the motor pump set. Here a three-phase transformer (two winding) block is used in Simulink modeling. This block implements a three-phase transformer using three single-phase transformers. The primary and secondary windings are connected in Grounded Y - Grounded Y connection. Figure.4.17 shows the transformer and Table 3.2 provides the transformer parameters.

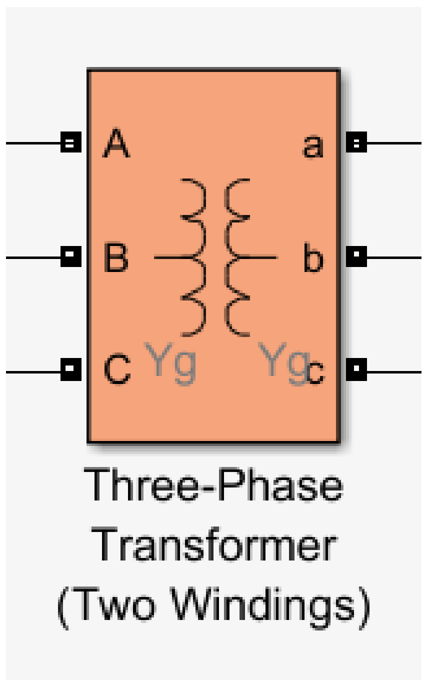

Figure.4.17: Transformer

Table 4.2: Transformer parameters

Parameters		**Values**
Nominal power (VA)		15e3
Nominal frequency (Hz)		60
Primary winding parameters	Ph-Ph R.M.S. voltage (Vrms)	19.59
	winding resistance (Ohn)	0
	winding inductance (H)	0
Secondary Winding Parameters	Ph-Ph R.M.S. voltage (Vrms)	187.77
	winding resistance (Ohn)	500
	winding inductance (H)	500
Magnetization resistance (Ohm)		inf
Magnetization Inductance (H)		inf

4.9 Simulation Results Analysis of the Battery Based System

The number of strings in PV module remain same for the battery-based system, else a small transformer and an MPPT used here instead of a boost voltage. Figure.4.18 shows the diode current, PV voltage, and PV current.

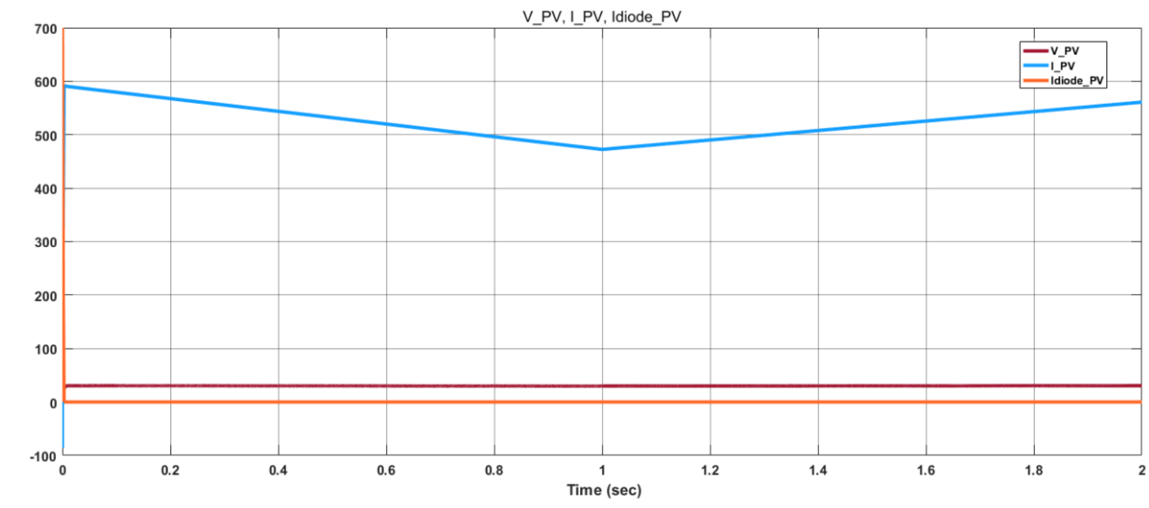

Figure.4.18: PV module components of the battery-based system

The following Figure.4.19 shows DC voltage, DC current and duty cycle of the MPPT tracker. The voltage is 48 V as expected. The value duty cycle is 0.45.

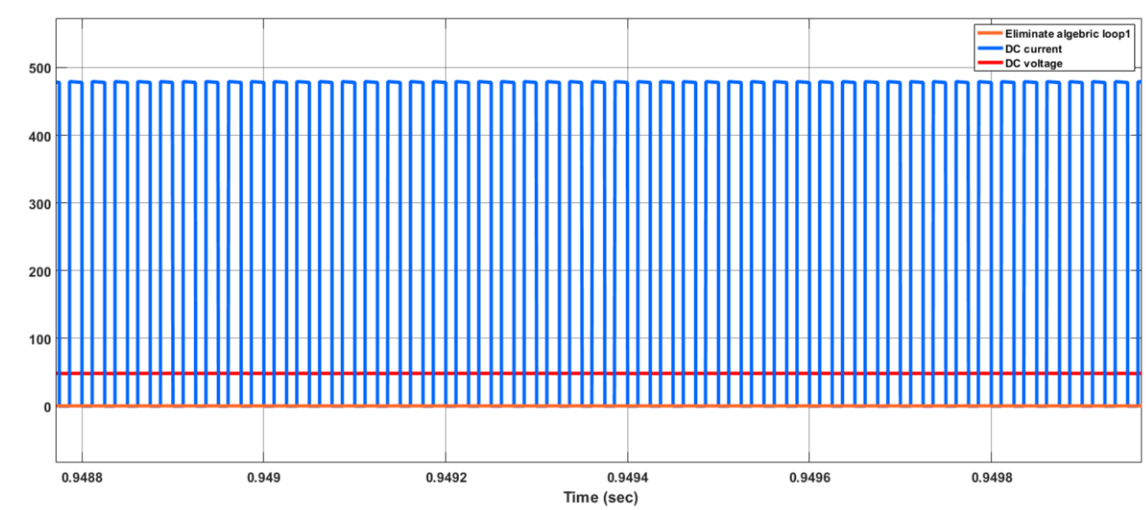

Figure.4.19: DC components of the battery-based system

The battery voltage, current, and state of charge are demonstrated in Figure.4.20. Battery state of charge remains at 60% (initial state of charge was decided as 60%) as the model was run for only two seconds. As the battery was discharging, the direction of current was negative. Battery voltage was same as nominal voltage (48V).

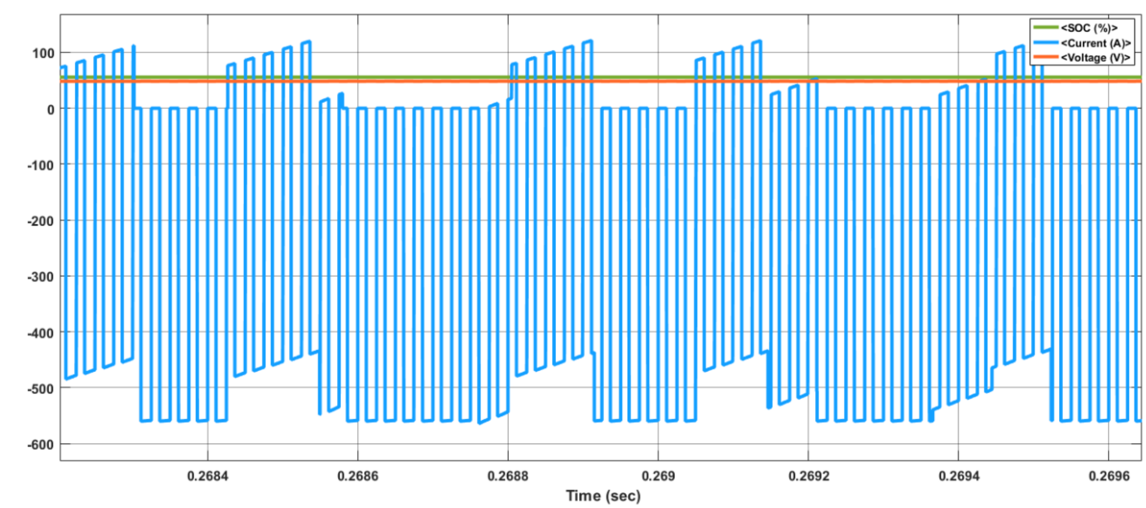

Figure.4.20: Battery storage of the battery-based system

The inverted AC voltage and current is denoted by AC voltage and AC current in Figure.4.21 which are primary side voltage and current of the transformer. The transformer secondary current and voltage are denoted by Current and Voltage accordingly. The following figure shows that the secondary line voltage and line current are 460 V and 15 A accordingly which match the expectation.

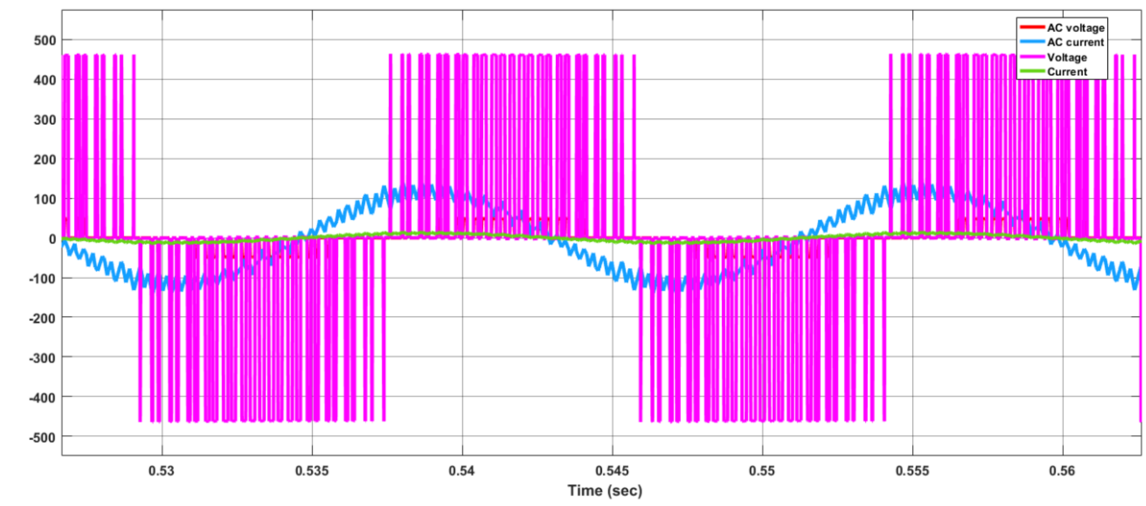

Figure.4.21: Transformer inputs and outputs of the battery-based system

The rotor speed of induction motor is 186 rad/s or 1776.17 r.p.m, like the battery less system shown in Figure.4.22. After one second the rotor speed decreases sharply because the atmospheric condition is changing rapidly, and the system consists of P&O method for maximum power point tracking. Water discharge and tank water level overlaps in this figure. Figure.4.23 gives a clear view of water discharge and tank water level.

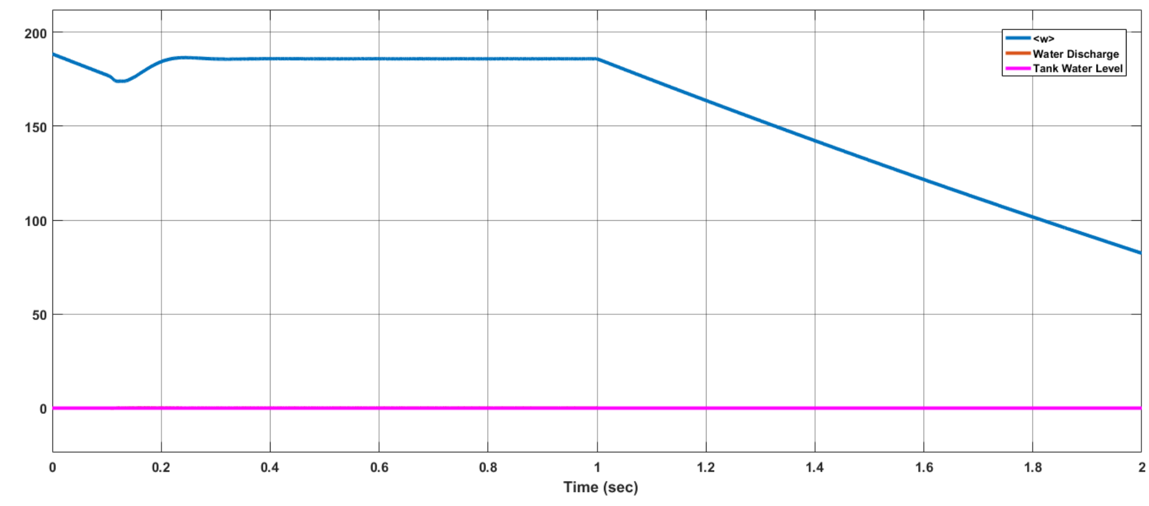

Figure.4.22: Rotor speed of the battery-based system

Figure.4.23 demonstrates the water discharge (m^3/s) and tank water level (m). Water discharge is also same as the battery-less system, 0.05 m^3/s or 180 m^3/h. In case of a battery-based system, the water tank size was kept similar (40 m×26 m×3 m) to measure the volume of the total amount of lifted water. During the first two seconds of simulation, the tank water level reached at 4.24×10^{-5} m. After eight hours of operation, the tank water level would reach at least 0.61m and volume of lifted water per day would be 634.4 m^3. The excess energy would be stored as an electrical form in battery storage.

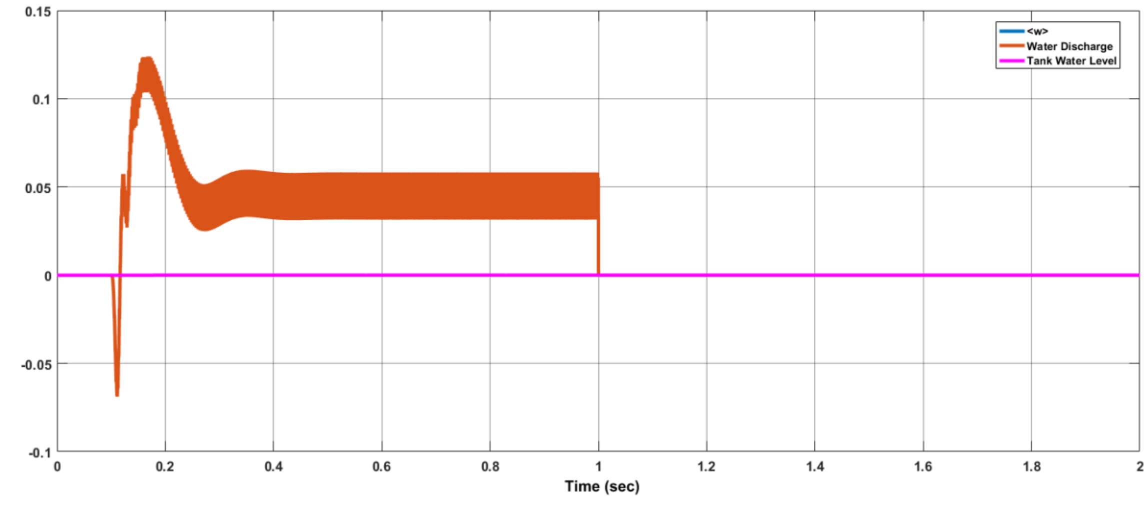

Figure.4.23: Water discharge and tank water level of battery-based system

4.10 Solar Irrigation Pumping System with Both Energy Storage

The author tries to find out the most feasible solution combining both storage systems. For this purpose, the battery storage from the battery-based system is reduced from 3000 Ah to 1400 Ah. A small water tank (22 m×10 m×3 m) is also added to store 660 m^3 of water. The advantage of this system is that the user has both energy storage in electrical form and stored water in a water tank for later use. If any fault occurs in the system, the user can handle the emergency with back-up stored water. Figure.4.24 presents the Simulink modeling of the proposed system.

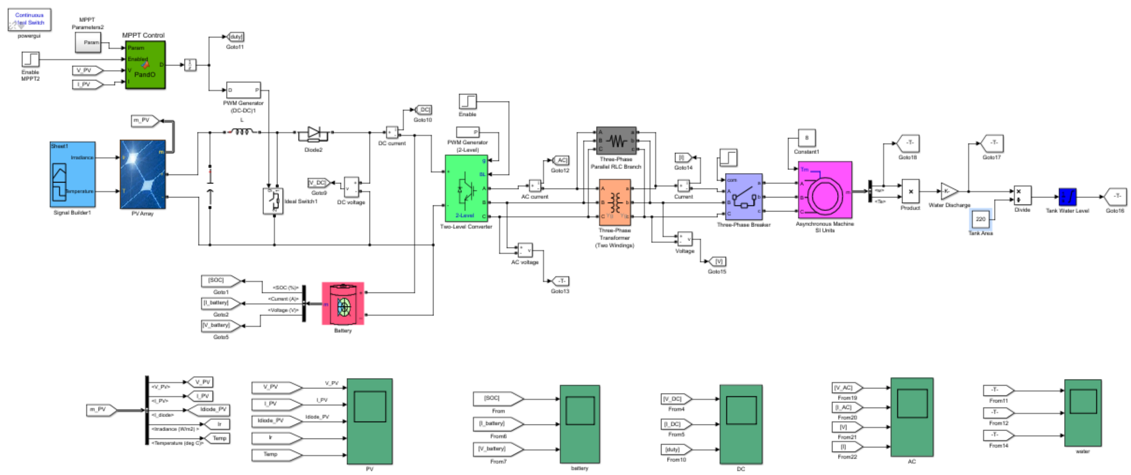

Figure.4.24: Dynamic modeling of the proposed system in Simulink

4.11 Simulation Result Analysis of the Proposed System

The simulation results almost match with the battery-based system. Figure.4.25 shows the diode current, PV voltage and current are similar to the battery-based system.

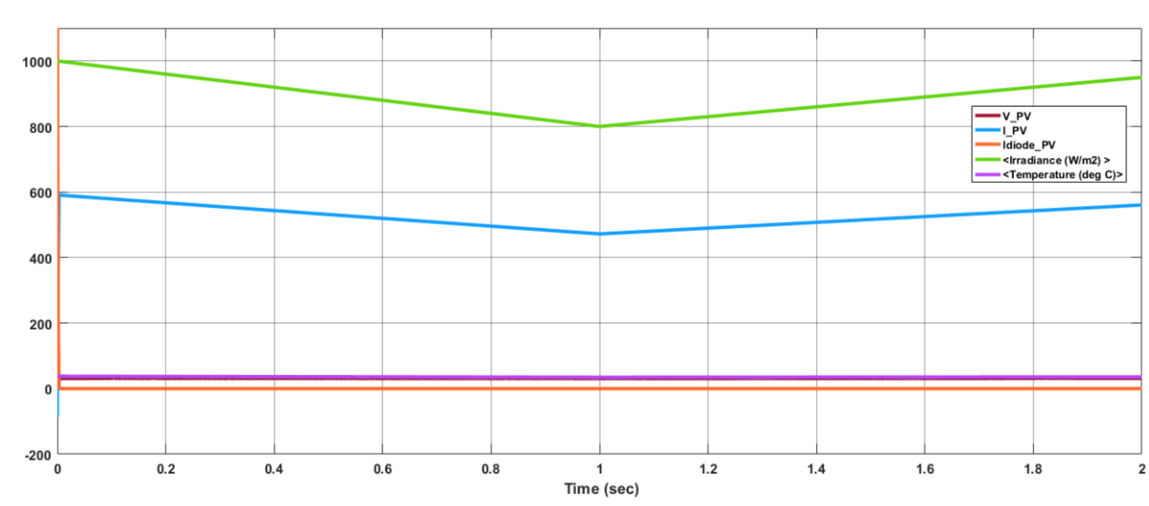

Figure.4.25: PV module components of the proposed system

The following Figure.4.26 shows DC voltage, DC current and duty cycle of the MPPT tracker which are also similar to the battery-based system.

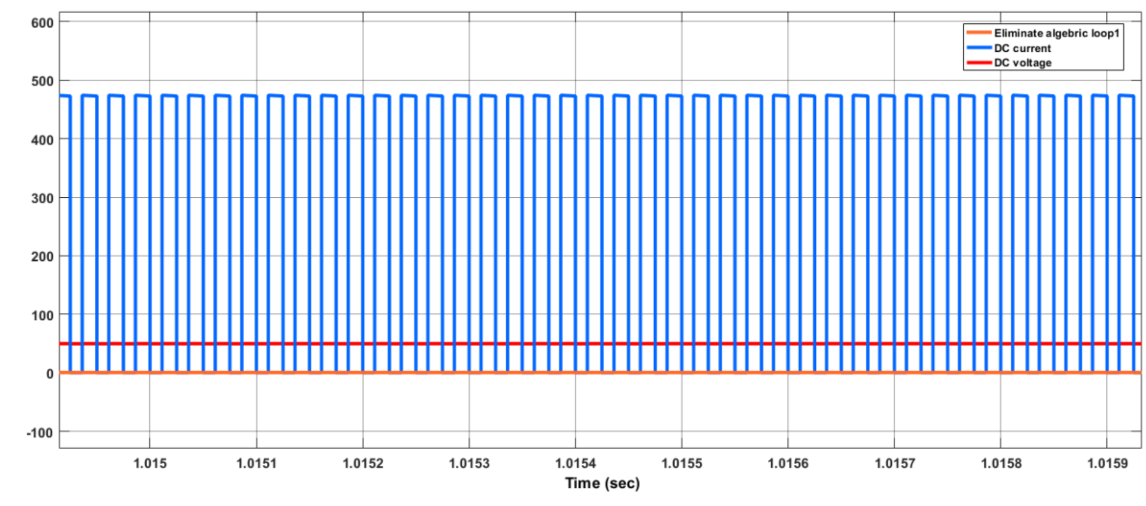

Figure.4.26: DC components of the proposed system

The battery voltage, current, and state of charge are demonstrated in Figure.4.27. Battery state of charge remains at 80% (initial state of charge was decided as 80%) as the model was run for only two seconds. As the battery was discharging, the direction of current was negative. Battery voltage was same as nominal voltage (48 V). The parameters of battery storage are also satisfactory.

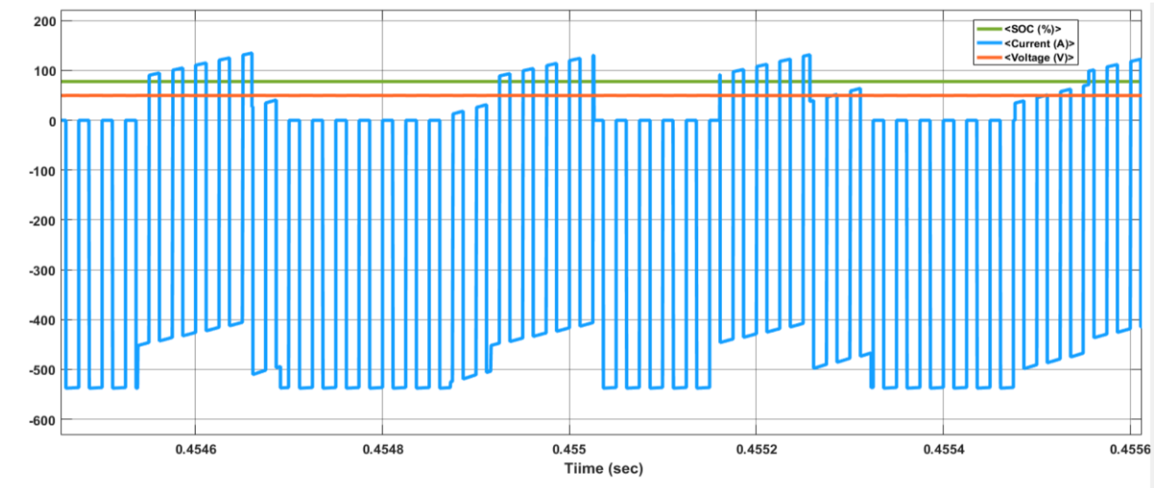

Figure.4.27: Battery storage of the proposed system

The primary and secondary side voltage and current of the transformer are also similar to the battery-based system. The primary voltage (AC voltage), primary current (AC current), secondary voltage (Voltage) and secondary current (Current) are showed in Figure.4.28.

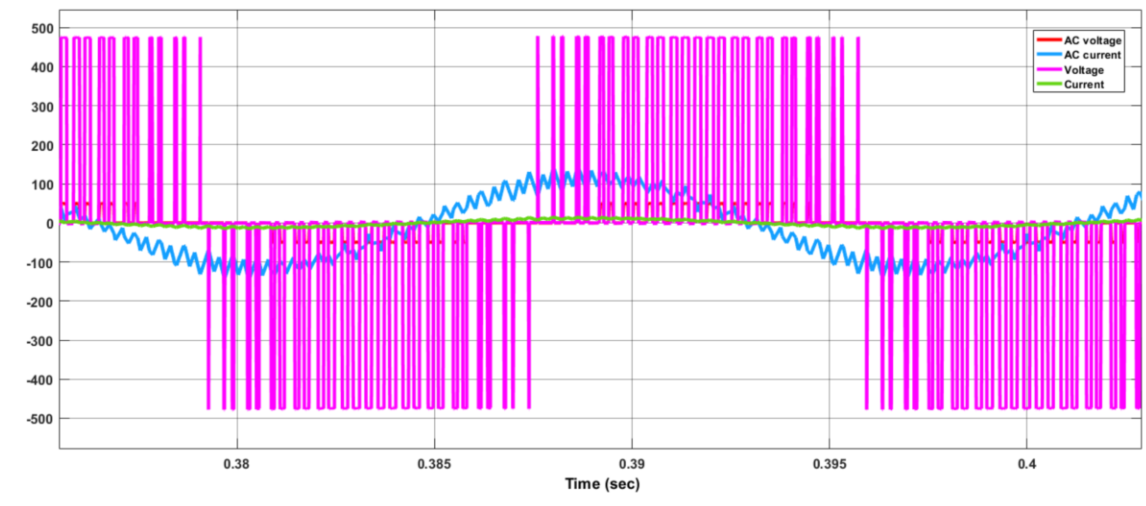

Figure.4.28: Transformer inputs and outputs of the proposed system

The rotor speed of induction motor is 186 rad/s or 1776.17 r.p.m, like both the battery less and battery-based system shown in Figure.4.29. After one second the rotor speed decreases sharply as a battery-based system.

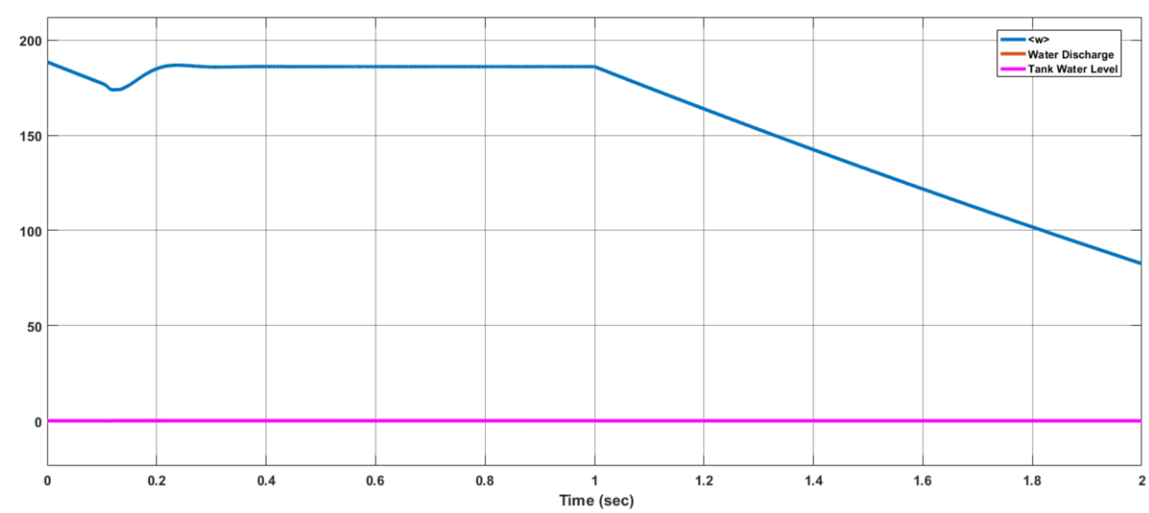

Figure.4.29: Rotor speed of the proposed system

Water discharge and tank water level overlaps in this figure. Figure.4.30 gives a clear view of water discharge and tank water level.

Figure.4.30 demonstrates the water discharge (m^3/s) and tank water level (m). Water discharge is also same as both battery-less and battery-based system, 0.05 m^3/s or 180 m^3/h. In the proposed system, the water tank size (22 m×10 m×3 m) is reduced to store 660 m^3 of water. During the first two seconds of simulation, the tank water level reached at 2.00826×10^{-4} m. After eight hours of operation, the tank would be full, and the water level would reach at 2.89 m. The volume of lifted water per day would be 635.8 m^3. The excess energy would be stored as electrical form in battery storage.

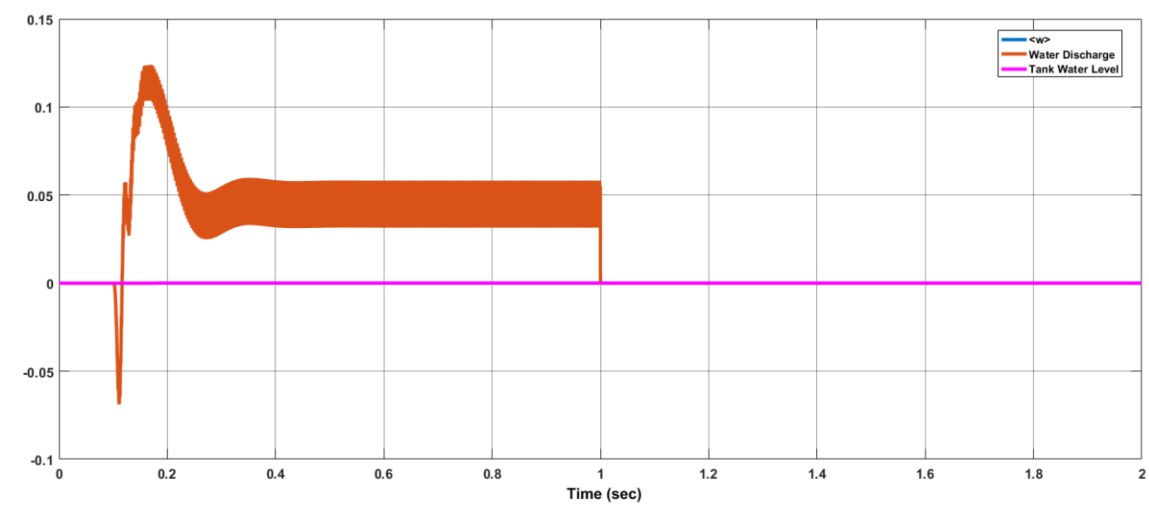

Figure.4.30: Water discharge and tank water level of the proposed system

4.12 Summary

This chapter represents the dynamic modeling and simulation of solar irrigation pumping system. Three different alternatives: (i) battery-less system, (ii) battery-based system, and (iii) combined storage systems are analyzed and discussed. Dynamic behavior of the system components is also observed carefully. The simulation analysis concludes that the rotor speed and the water discharge rate of the combined storage system are similar to the battery less and battery-based system. At the end of the day, i.e., after eight hours of operation, the stored water remains same for the battery based and combined storage system. The control strategy of the solar irrigation pumping system and the economic analysis would be discussed in next chapters.

CHAPTER 5

SENSITIVITY AND EFFECTIVENESS ANALYSIS

5.1 Sensitivity Analysis

Sensitivity analysis is the key to economic analysis. Sensitivity analysis of solar irrigation pumping system was carried out during HOMER optimization with 10% variation in load (119 kW/d, 107 kWh/d and 131 kWh/d) and irradiance (4.52 kWh/m^2/d, 4.07 kWh/m^2/d and 4.99 kWh/m^2/d).

5.1.1 Sensitivity Analysis Based on NPC

Figure.5.1 demonstrates how the total NPC (Net Present Cost) fluctuates with the variation of irradiance and load. For lowest and highest load demand, the total NPC decreases linearly with the increase of irradiance. In case of 119 kWh/d load demand, the NPC falls sharply as irradiance goes higher.

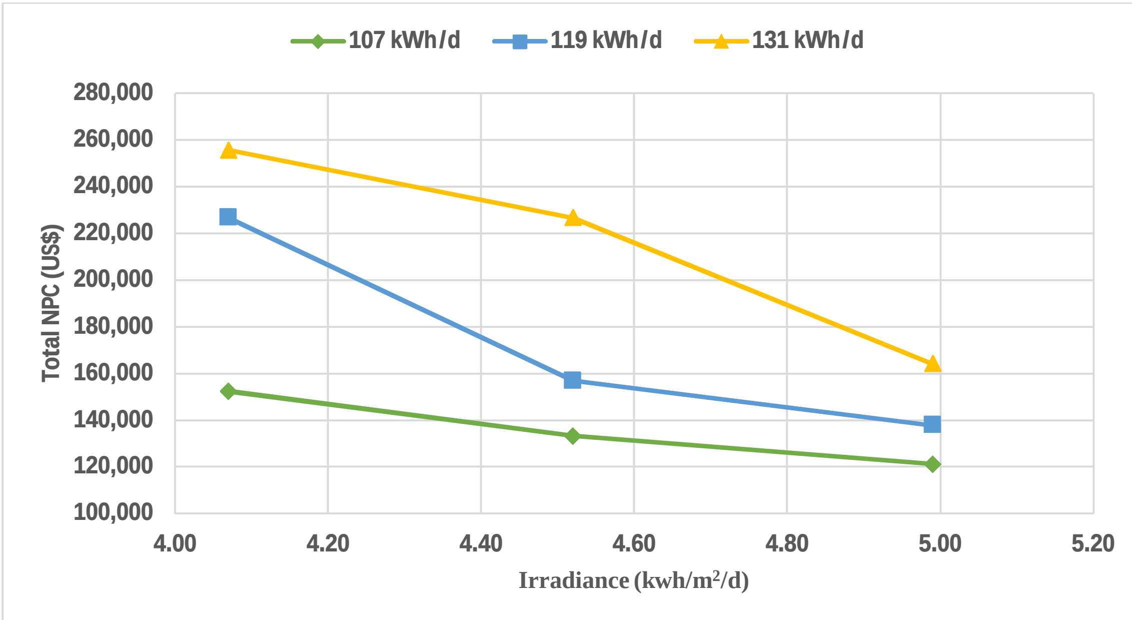

Figure.5.1: Sensitivity analysis based on NPC

5.1.2 Sensitivity Analysis Based on COE

However, the cost of energy (COE) are similar for any voltage demand at highest irradiance level as in Figure.5.2. For lowest irradiance level, the COE is same for 119 kWh/d and 131 kWh/d. The COE of lowest and average load demand become similar when the solar PV modules get average irradiance.

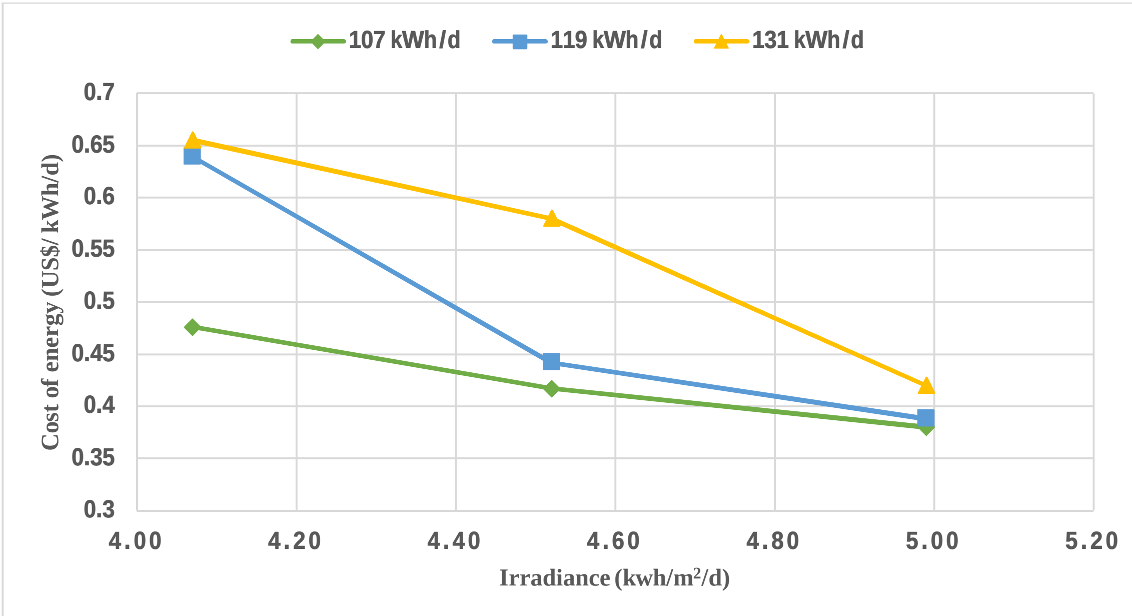

Figure.5.2: Sensitivity analysis based on COE

5.1.3 Sensitivity Analysis Based on Operating Cost

Figure.5.3 shows the similar relationship like Figure.5.1. Operating cost is almost similar for lowest and average load demand at average irradiance. For average load demand, there is a hike in operational cost at lowest irradiance, but it is not true for 107 kWh/d load demand.

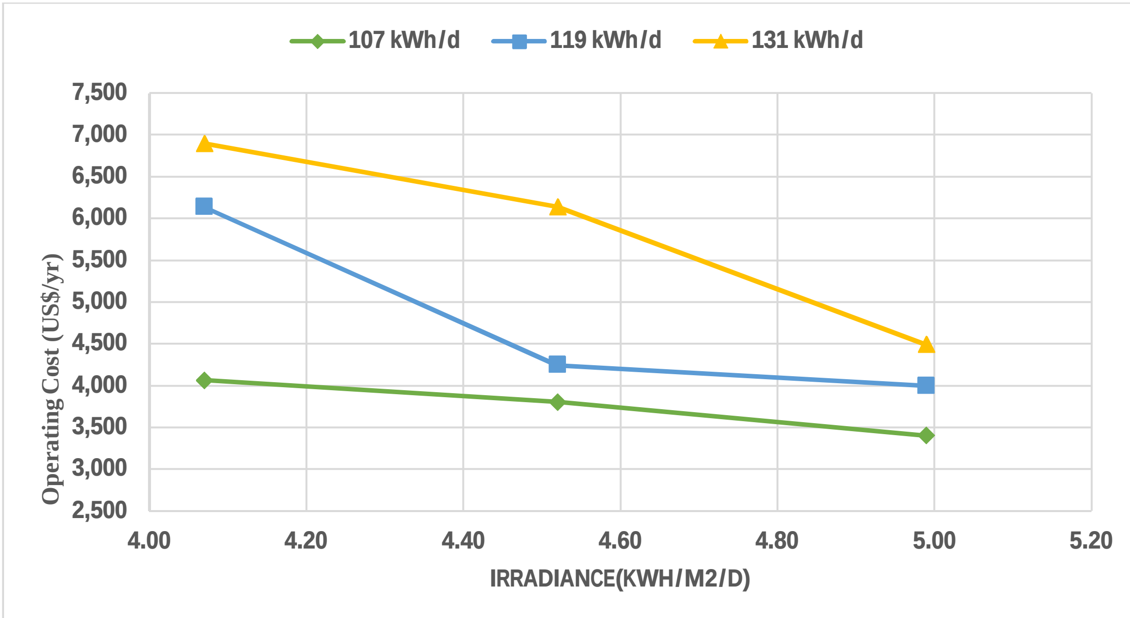

Figure.5.3: Sensitivity analysis based on Operating Cost

5.2 Effectiveness Analysis

Effectiveness analysis is done to get the most feasible solution which is affordable for the farmers in developing or underdeveloped countries. For this purpose, cost breakdown of each alternative is done. Some comparisons are discussed here in the chapter.

5.2.1 Cost Breakdown of Battery-Based System

The battery-based solar irrigation pumping system consists of the solar photovoltaic array, inverter, battery storage and other system components. Figure.5.4 and Figure.5.5 demonstrate the cost breakdown of a battery-based system for one-year of period and twenty-five years of period accordingly.

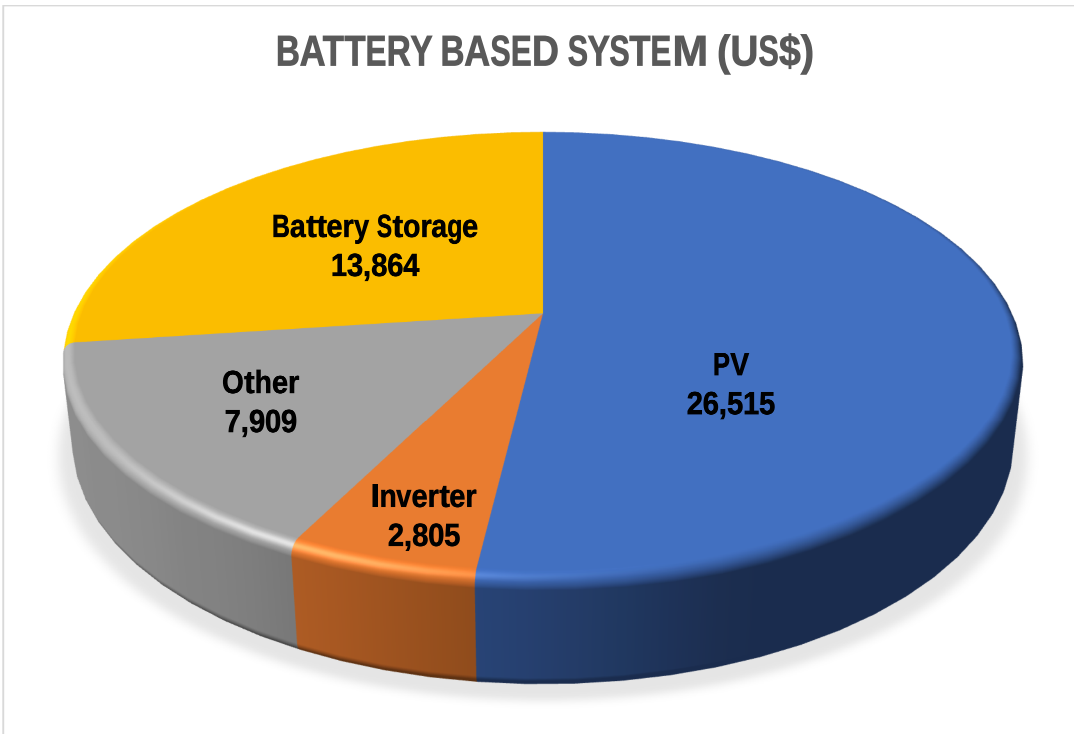

Figure.5.4: Cost breakdown of battery-based system for one year of period

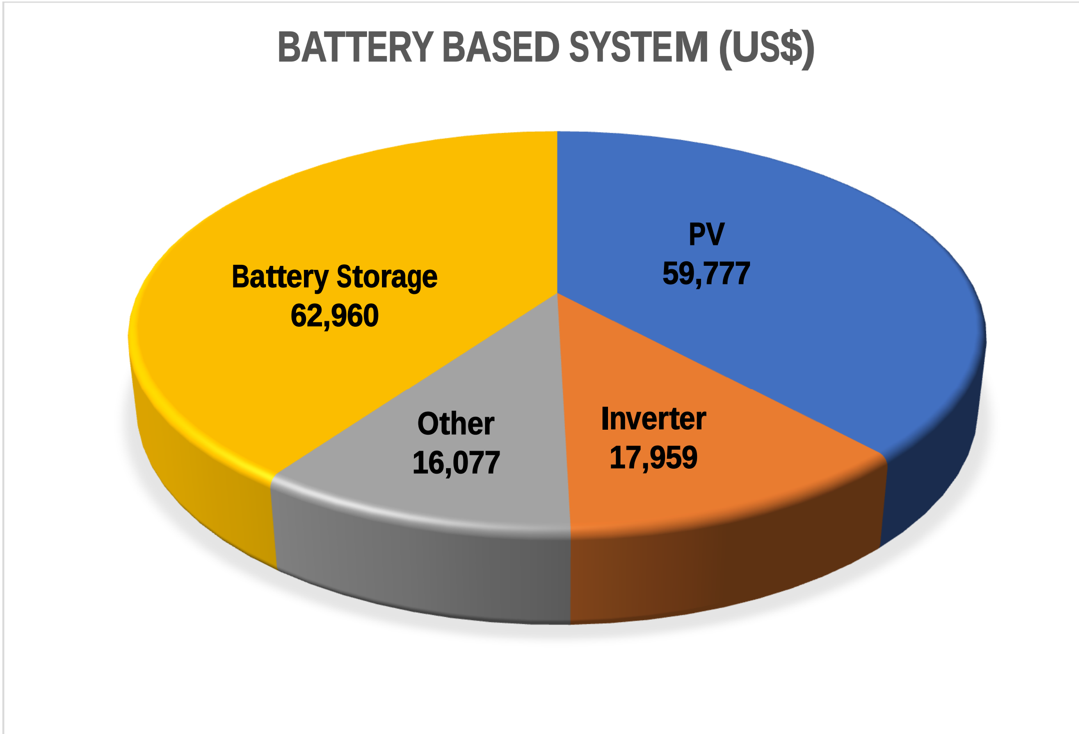

Figure.5.5: Cost breakdown of battery-based system for twenty-five years of the period

HOMER optimization was done for one year and twenty-five years separately. Above figures show that battery cost increases five times and inverter cost increases six times whereas PV cost increases only twice for twenty-five years of the period. This comparison implies that the battery and the inverter costs are the most influential factors for total system cost. One major reason behind this may be the longer life of PV module.

In the battery-based system, the battery needs to be replaced in every four years. Now a day's, maintenance-free AGM (Absorbent Glass Mat) sealed batteries are available in the market. Operation and maintenance cost could be minimized by using them.

5.2.2 Cost Breakdown of Battery-Less System

The battery-less solar irrigation pumping system consists of a large water tank instead of battery storage system to store water for further use. Figure.5.6 and Figure.5.7 describe the cost breakdown of a battery-less system for one-year of the period and twenty-five years of period accordingly.

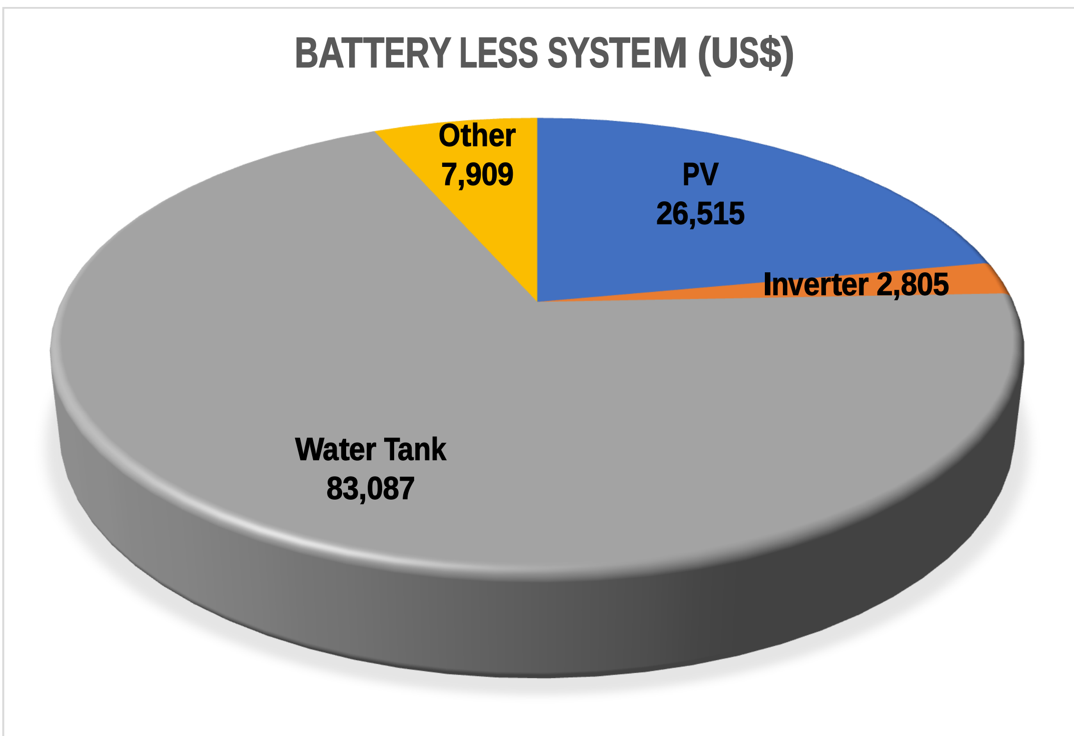

Figure.5.6: Cost breakdown of battery-less system for one year of period

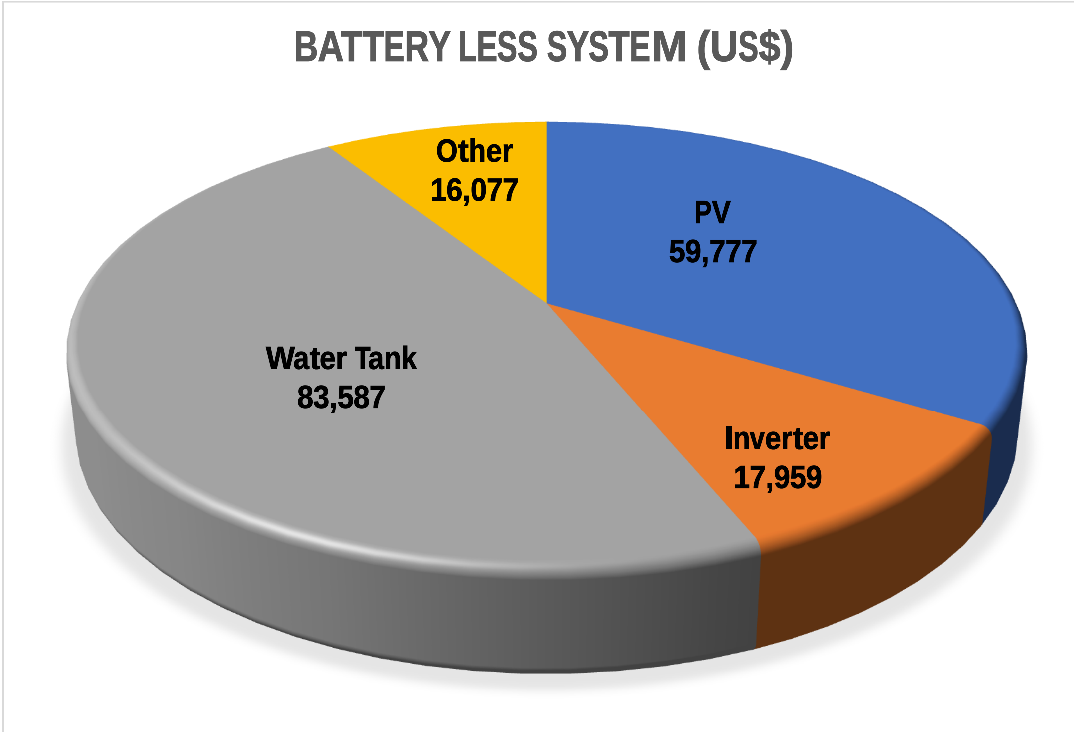

Figure.5.7: Cost breakdown of battery-less system for twenty-five years of the period

HOMER optimization results provide the costs of PV, inverter, and others, except the cost of the water tank. The cost of water tank was calculated manually using the method presented in chapter two. For one year of period or twenty-five years of the period, the cost of water tank remains same and the maintenance cost is almost negligible and no replacement cost is needed for the battery-less system. The increment rate of inverter and PV costs remain same as the battery-based system. Short term project plan is not feasible for battery-less solar irrigation pumping system.

5.2.3 Cost Breakdown of the Proposed System

The proposed solar water pumping system for irrigation consists of both storage system; battery storage and water tank storage. In the proposed system, solar PV array, inverter, and other components are same as a battery-based system. The proposed battery bank (1400A hr) is smaller than the battery bank (3000 Ahr) of the battery-based system. On the other hand, the water storage tank is also smaller (22 m×10 m×3 m) than the large tank in battery-less system (40 m×26 m×3 m). Figure.5.8 and Figure.5.9 show the cost breakdown of the proposed system for one-year of the period and twenty-five years of period accordingly.

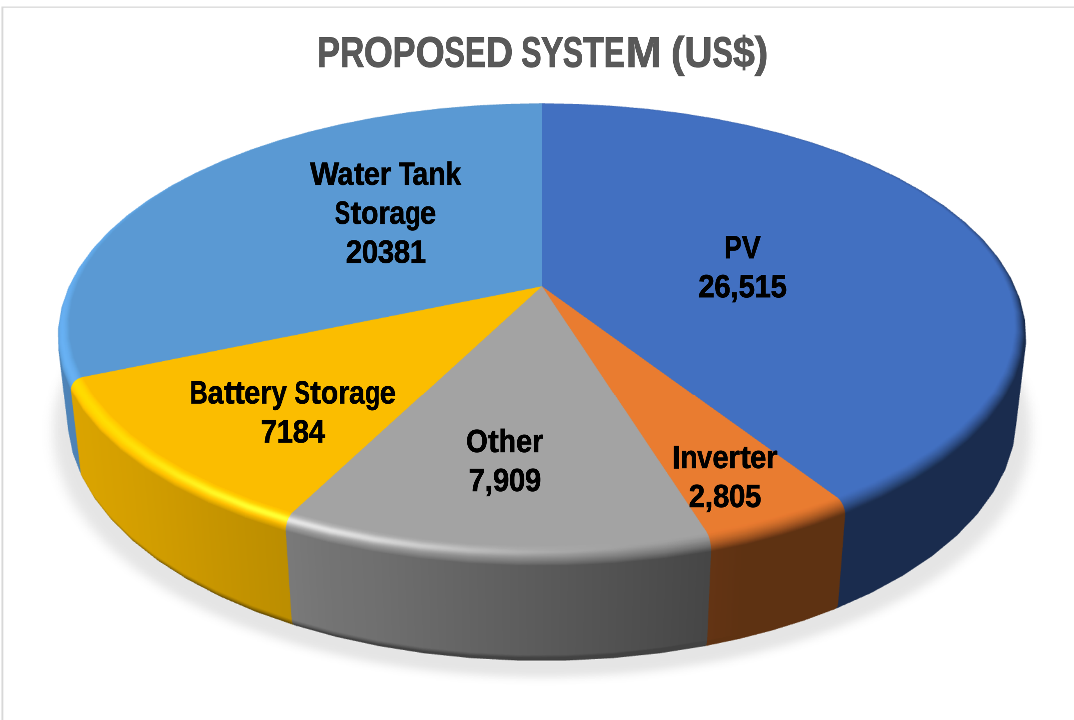

Figure.5.8: Cost breakdown of the proposed system for one year of the period

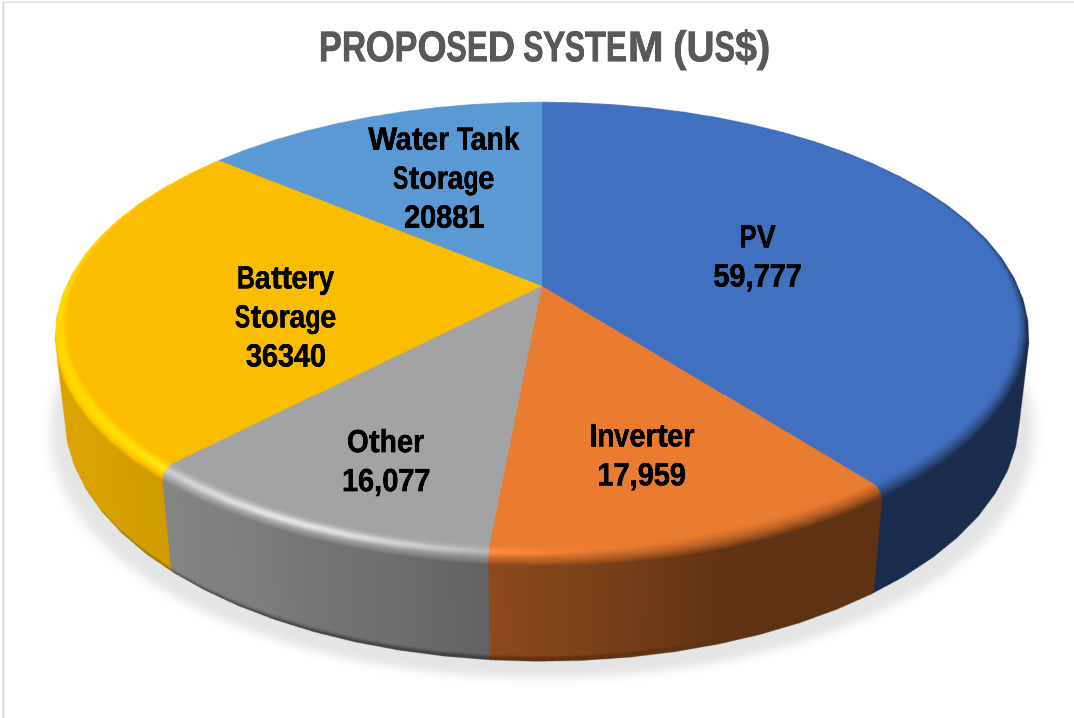

Figure.5.9: Cost breakdown of the proposed system for twenty-five year of the period

Cost for water storage tank remains same for both cases whereas the battery storage cost increases five times. The replacement cost for battery storage is higher whereas, there is no replacement cost for water storage. The cost of storage tank plays a significant role here.

5.3 Comparison Between Alternatives

This thesis represented three alternatives: (i) battery based, (ii) battery-less, and (iii) proposed system comprised of both battery and water tank storage. The conventional way to run an irrigation system in off-grid areas is diesel engine system in developing or underdeveloped countries. The comparison between the above-mentioned alternatives and the conventional system are discussed here.

5.3.1 Conventional Diesel Engine System

HOMER optimization is done for the diesel engine system for the same load. The economic cost breakdown is given in Table 5.1 for twenty-five years of the operational period.

Table 5.1: Economic cost breakdown

Component	Capital (US$)	Replacement (US$)	O&M (US$)	Fuel ($)	Salvage (US$)	Total ($)
Generator	25,000	58,204	94,377	204,759	-506	381,833
Other	7,000	0	6,464	0	0	13,464
System	32,000	58,204	100,841	204,759	-506	395,298

Total net present cost (NPC) of the system was calculated by Homer is $395,297. The levelized cost of energy (COE) is $1.408/kWh and the total operating cost is $56,202/yr.

The diesel generator produces 43,436 kWh energy per year where the AC primary load demand is 43,435 kWh/y. As a result, there is no unmet electric load and the excess electricity is also negligible (0.583kWh/y).

The hours of operation of a diesel generator is 2,920 h/y and the operational life is 2.05 years. The capacity factor is 19.8% and means electrical output is 14.9 kW.

The main disadvantage of the diesel operated engine is that it causes pollution to the environment. Table 5.2 gives an overview about the emission of diesel operated system.

Table 5.2: Emission

Pollutant	**Emission (kg/yr)**
Carbon dioxide	104,267
Carbon monoxide	257
Unburned hydrocarbons	28.5
Particulate matter	19.4
Sulfur dioxide	209
Nitrogen oxides	2,297

5.3.2 Comparing Alternatives for 1 Year Period and 25 Years of Period

Figure.5.10 shows the total cost at the very beginning of the project (first year) while Figure.5.11 illustrates the total cost of the project for twenty-five years of the operational period. The total cost of the diesel engine system is lowest for the one-year operational period, but it is worst solution for longer period.

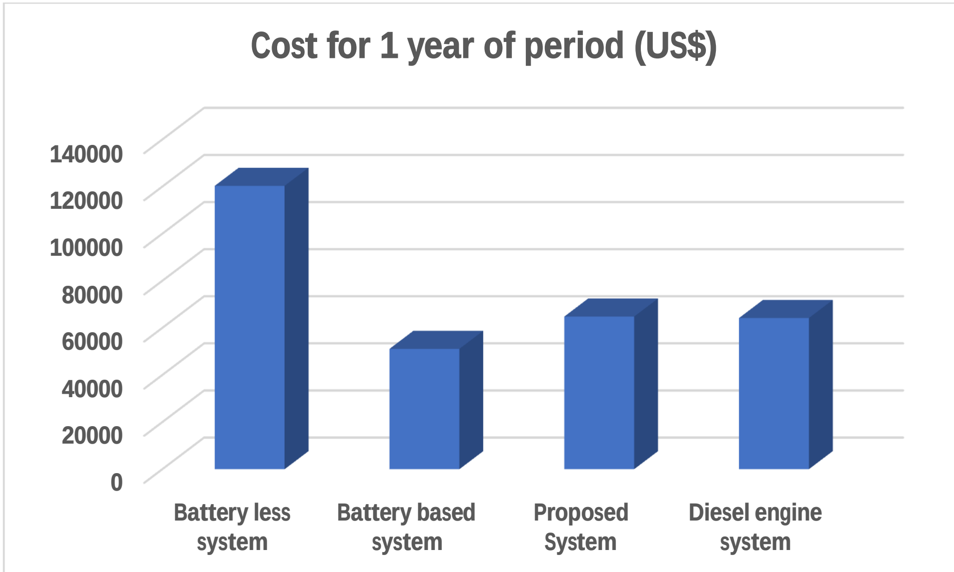

Figure.5.10: System cost for a one-year period

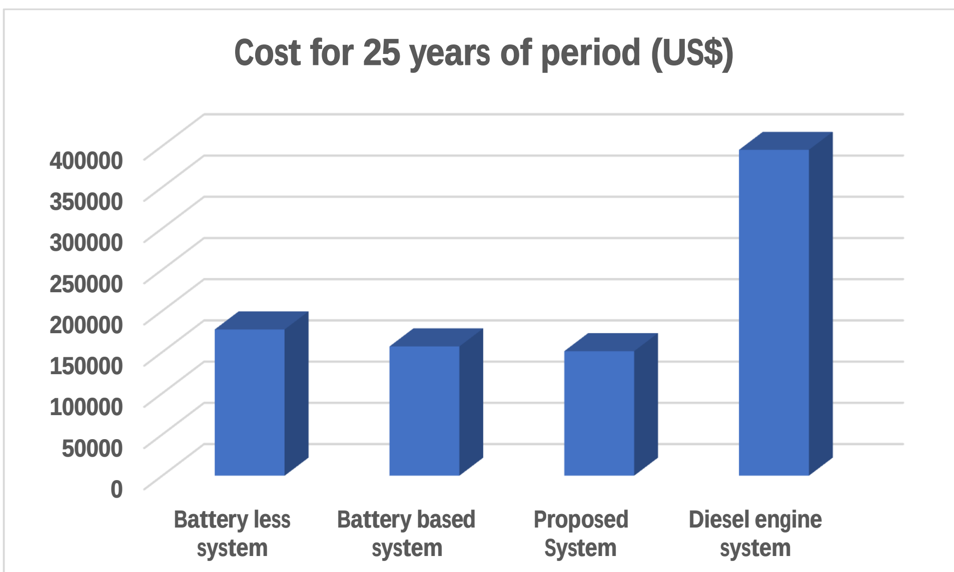

Figure.5.11: System cost for twenty-five years period

Although the cost difference between the battery-less and battery-based system is higher on the first year of the project, the difference decreases strongly for 25 years of the period because there is no replacement cost for the water tank. The replacement cost of battery storage needs to be considered. Combination of both consists of a smaller water tank; half of the tank size used in the battery-less system and a battery storage of 1400 Ah. The total cost of this combination lies between the cost of the battery-less and battery-based system at the very beginning, but it becomes the cheapest solution for 25 years of the period. Combination of both storage system is the reasonable solution because it can store energy in electrical form and store some water for any emergency.

5.2 Summary

Sensitivity analysis shows the variation of total NPC, COE and operating cost with the variation of ±10% load and irradiance. For lowest load demand, costs (NPC, COE and operational cost) and irradiance have a negative relationship. Total NPC, COE and operating costs show hike at lowest irradiance in case of average load demand. All costs are always higher for highest load demand. The effectiveness of the alternative systems was compared from the economic point of view. All categories were simulated in HOMER to obtain the most feasible solution among all group. Present market price (US$) of each component of each group were selected separately as the system elements are different from each other.

CHAPTER 6

DESIGN OF INSTRUMENTATION AND CONTROL SYSTEM

6.1 Automated System

This chapter presents a low cost automated solar water pumping system for irrigation in developing countries. The programmed sensor module detects the temperature, humidity, soil moisture level and sends the information to ESP32 microcontroller. A water level sensor also observes the water level and sends the data to the microcontroller unit. Based on the information and boundary conditions, the microcontroller decides either to start or to stop the pump motor. This paper also describes how to decide soil moisture limits for a particular type of soil. The ESP32 microcontroller also sends results to the web server so that the user can see that. The user can operate the irrigation system far from the field by a simple click on a cellphone. A manual ON/OFF system is also incorporated into the proposed design. A simple and quite low-cost modern ESP32 controlled irrigation system is presented here which is affordable for farmers in developing countries. The proposed system can improve the traditional irrigation system by lowering its cost and has features compatible with current technology.

6.2 Design Strategy

The main objective of this chapter is to design and demonstrate a controlled solar water pumping system for irrigation in Bangladesh. A solar irrigation pumping system consists of solar PV array, inverter, motor-pump set, and storage system. Chapter 3 derived the feasible solutions for both storage system; energy storage in batteries and water storage in a large tank. This chapter will proceed with the second alternative. The proposed system can be explained through Figure.6.1.

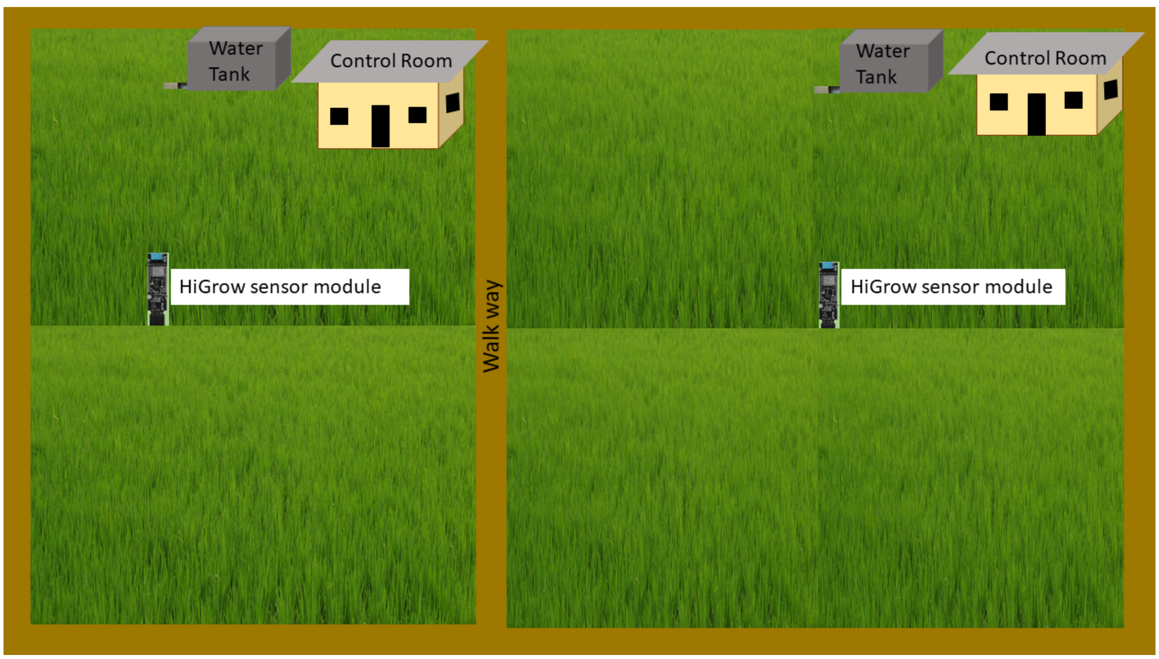

Figure.6.1: Proposed system

If a HiGrow sensor module is installed in the field after uploading the control code, it will detect the field parameters, i.e. temperature, humidity, soil moisture, and send the information to the web server. A water level sensor will also check the water level in the tank and send details to the web server. The water pump motor operates automatically according to the sensor data. The user can also operate the motor by clicking the on/off button created on web page which is easily accessible through any cellphone. There is also a manual switch to control the motor run time. The user does not need to visit the fields to check whether the crops need irrigation or not. He can also control the whole irrigation system by sitting at home or if he is away from the field.

6.3 ESP32 and HiGrow Sensor Module

Water pumping system can be controlled using programmable logic circuits (PLC) and microcontrollers. Such arrangements cost 1000's of dollars and suffer from maintenance issues in developing and underdeveloped countries.

ESP32 was introduced by Espressif System which is a successor to the ESP8266 microcontroller [38]. It is a low cost, low power system on a chip microcontroller with integrated Wi-Fi, dual mode Bluetooth capabilities and power saving features which made it more versatile. ESP32 is compatible with mobile devices and IoT (Internet of Things) applications. It turned out as a reliable option in an industrial environment because of the wide operating temperature range. This microcontroller can act as a complete standalone system or can be operated as a slave device to a host microcontroller.

The HiGrow sensor module is a temperature, humidity and soil moisture, sensor shown in Figure.6.2. It can communicate with cloud application to upload sensor data so that the user can check field condition through any internet browser. It can also be connected to the web server which is responsible for returning a web page to the client when the client is connected to it through HTTP (Hypertext Transfer Protocol). For the temperature and humidity, a sensor module DHT11 is attached with the HiGrow plant monitor. The ESP32 is connected to DHT11 to read temperature and humidity values which are routed to pin 22.

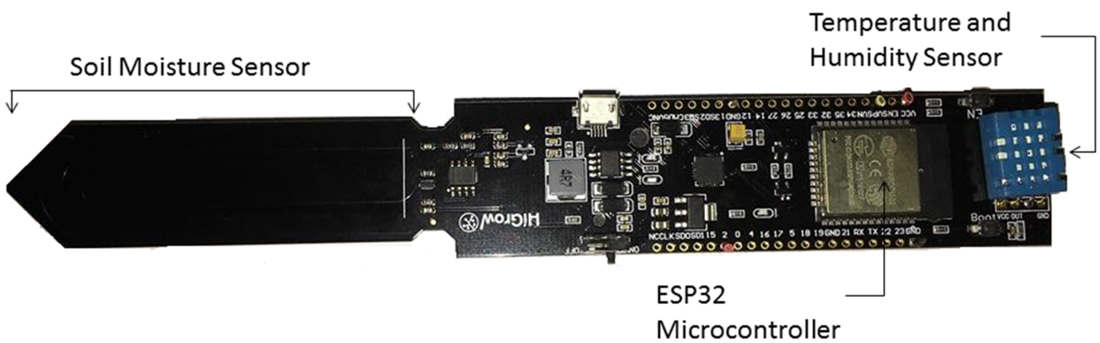

Figure.6.2 HiGrow sensor module

The pointed edge of the HiGrwo module is moisture sensor which monitors the soil moisture level. This moisture sensor is the capacitive type. The capacitor is electrically connected with two small resistors. As the water almost touches the sensor, the dielectric constant of the material between the capacitor plates changes which forces the timer to run at a different frequency. There is an RC oscillator on the output of the timer which effectively generates a relatively stable analog voltage. The generated analog voltage is routed to pin 32. ESP32 comes with an ESP-Wroom-32 microcontroller. According to

Espressif System, The ESP-Wroom-32 is a powerful microcontroller module with generic Wi-Fi and Bluetooth Low Energy (BLE) which has a wide variety of applications. An LG 3000 mAh 18650 battery could make ESP32 run 17 hours or more.

6.4 Proposed Control System

The proposed control system is based on the ESP32 microcontroller device. Figure.6.3 gives an idea about the experimental set-up of the system. 38.4 kWp solar array produces necessary DC energy and a 20.7 kW solar inverter converts this variable DC output into utility frequency AC. This AC power is used to run motor pump set for groundwater extraction. Then the lifted water is stored in a large water tank to irrigate the field. An ESP32 microcontroller is used to control the motor operation based on the field conditions. The ESP32 can be programmed using Arduino software, freely available at www.arduino.cc. The ESP32 control code is commonly referred as sketch. The HiGrow plant monitor senses the temperature, humidity, soil moisture and sends the data to ESP32. The tank water level sensor is connected to ESP32 and sends information about water tank. The output of the microcontroller is connected to a normally open (NO) type relay to control the motor pump operation. The microcontroller controls the motor operation by sending trip signals to the relay.

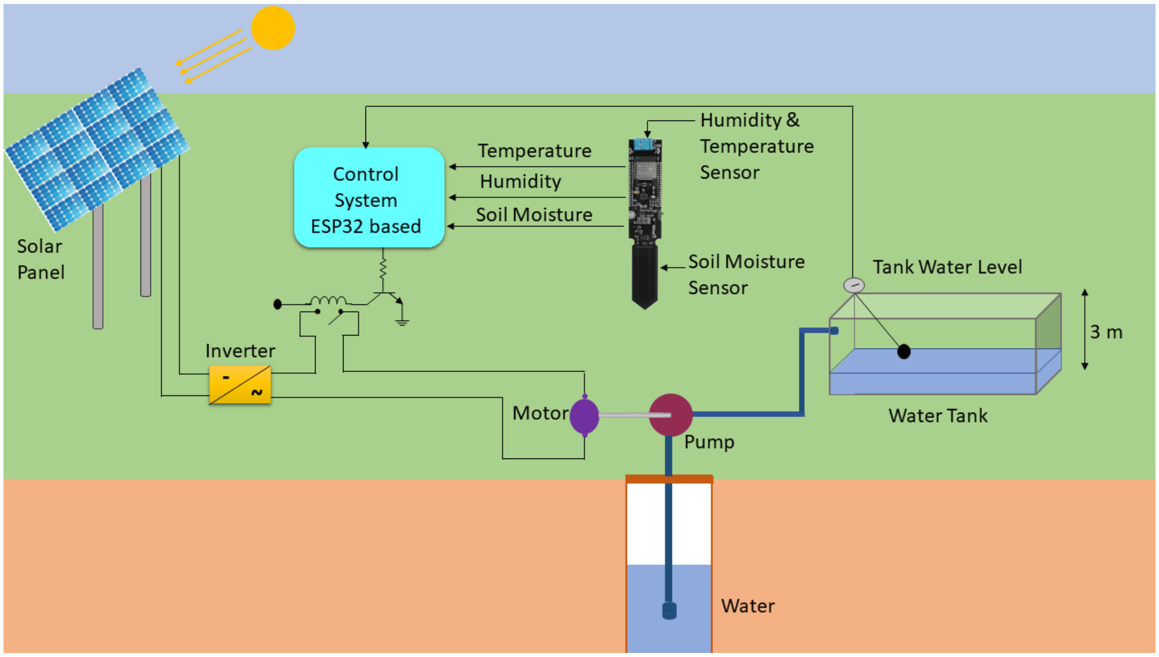

Figure.6.3 Proposed control system

Here in this thesis, a 10KΩ potentiometer is represented as the tank water level sensor. The potentiometer reading is mapped into the tank water level in the scale from 0 m to 3 m as the height of the tank was decided as 3 m. Figure.6.4 describes this mapping in a better way.

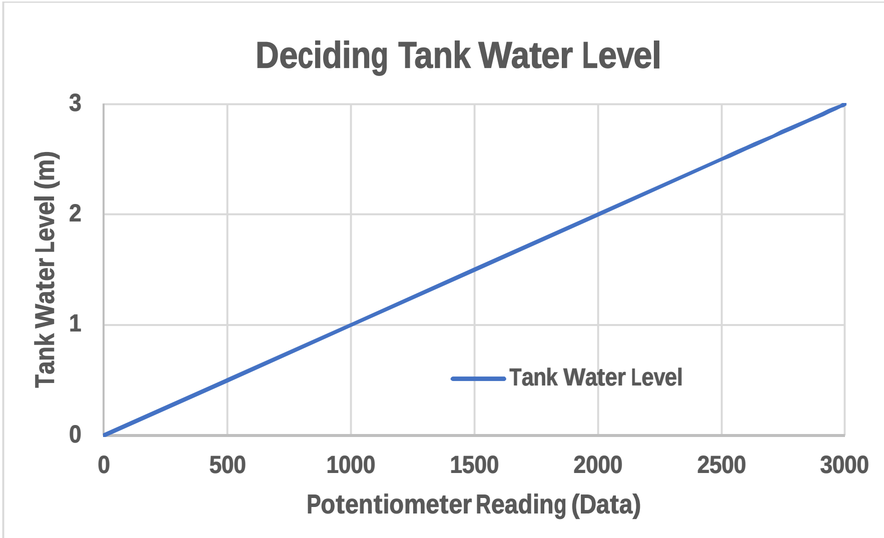

Figure.6.4: Mapping potentiometer reading into tank water level

The capacitive soil moisture sensor in HiGrow sensor module gives the output voltage (mV) reading from the low pass filter. To decide the moisture level limits, the various percentage of water was added to a particular type of soil and the output voltage of soil moisture sensor was tested. This experiment was done with 300 g engineered soil (potting mix) which had 36.2% moisture content initially. Then water was added to the soil up to 549.6% to make it slurry and the output voltages were recorded accordingly. Moisture contents (%) were calculated from equation 6.1.

$$\theta = (W_w/W_s) \times 100\% \qquad \text{(eq. 6.1)}$$

Where, θ = moisture content,

W_w = mass of the water (g)

W_s = mass of the soil (g)

The output voltage in the air is 3383 mV and in the clear water 1700 mV. Figure.6.5 shows the mapping of output voltage for various soil moisture.

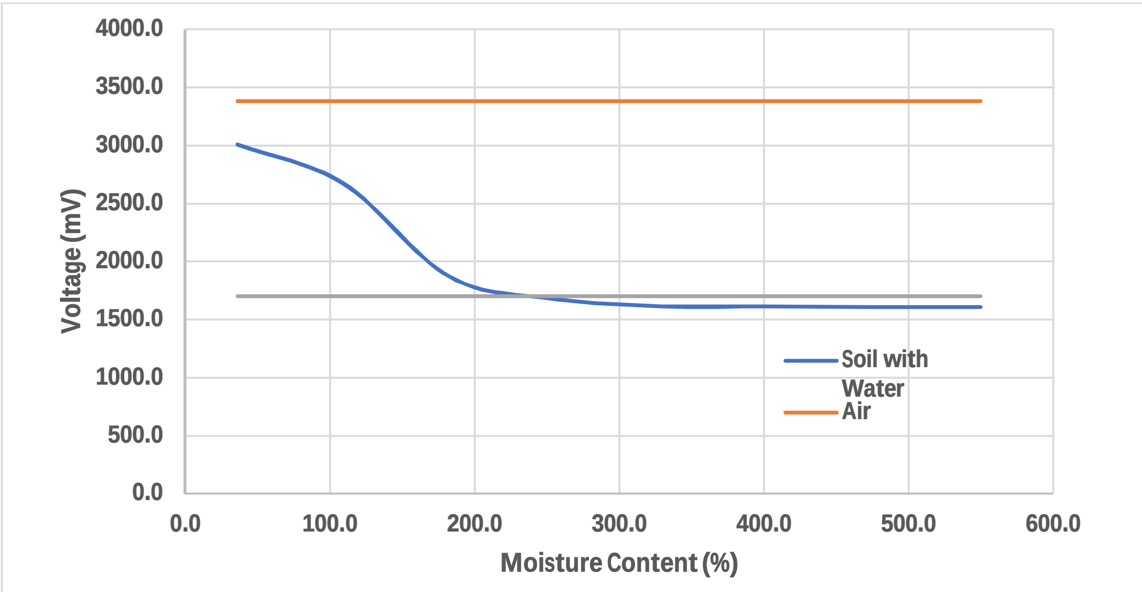

Figure.6.5: Deciding moisture content limit

When more than 200% water was added to the soil, the output voltage of the slurry and clear water became consistent. From the output voltage, the user can know about the soil moisture content. While programming the ESP32 using Arduino 1.8.5 software, the boundary limits for tank water level and soil moisture content were decided from Figure.6.4 and Figure.6.5.

Based on the temperature, humidity, soil moisture content and tank water level, the microcontroller takes the decision whether to run the motor or not. The microcontroller continuously checks the soil moisture, temperature, humidity and tank water level accordingly. If the soil moisture content becomes less than the expected value, ESP32 checks the temperature and humidity. If the temperature becomes greater than the preferred value and humidity less than the selected value, the microcontroller finally checks the tank water level. If the tank water level becomes less than the chosen value, the ESP32 sends the trip signal to the relay to run the water pump motor. After running for two hours, the motor will stop working automatically. This time period two hours was decided randomly. If any of the above conditions become false before completing the runtime, the ESP32 will send the signal to disconnect the circuit. As a result, the motor will stop working as soon as possible. The motor will remain in idle mode until all the conditions become true. In this paper, a built-in LED of the HiGrow module represents the motor state. The built-in LED is connected to pin 13. The control block diagram is presented in the following Figure.6.6. The ESP32 microcontroller also sends the sensor data to a web server. There are two buttons created on the web server page. By clicking on those buttons, the user will also be able to control the motor. The whole Arduino sketch is provided in Appendix C. There is also a manual on/off switch to control the motor.

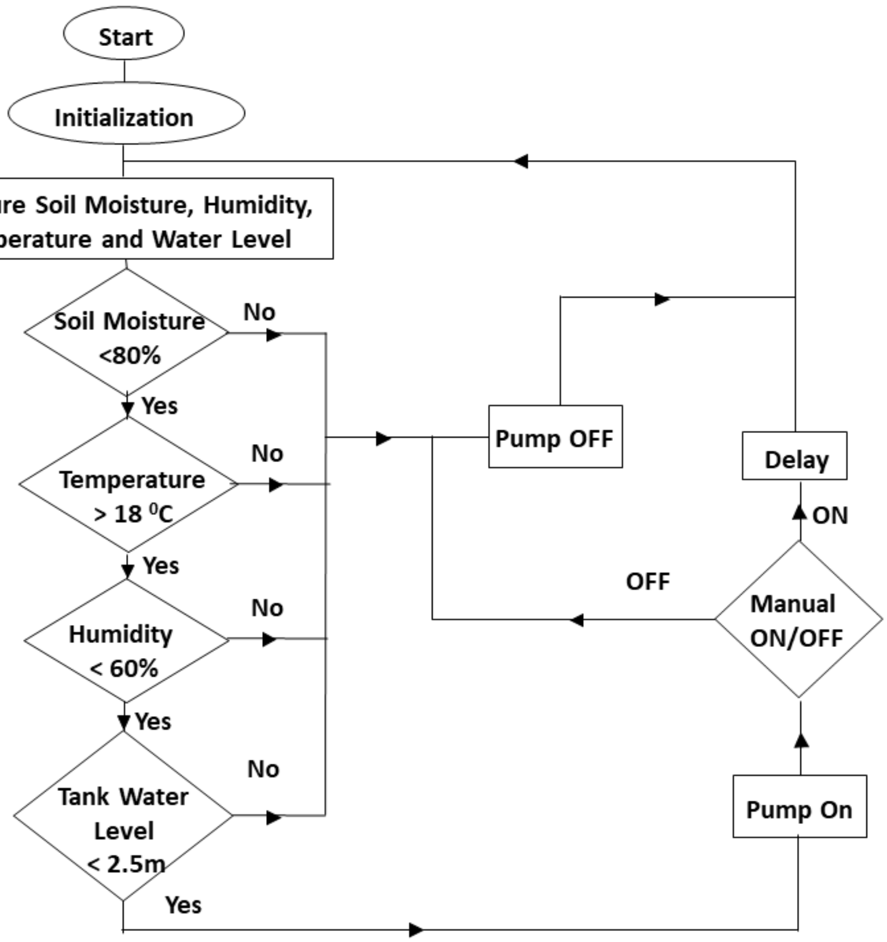

Figure.6.6: Flow chart

6.5 Experimental Results

After uploading the Arduino sketch, the soil moisture sensor of HiGrow sensor module was inserted into the dry soil. The module was powered from a USB port connected to a laptop. Figure.6.7 shows the testing of proposed control design. A webserver running on ESP32 can be accessed from any web browser on a cell phone or on a computer. IP address of the web server was printed on the serial monitor screen. This IP address navigates to the web server through any web browser. The user can check the status through cell phones also.

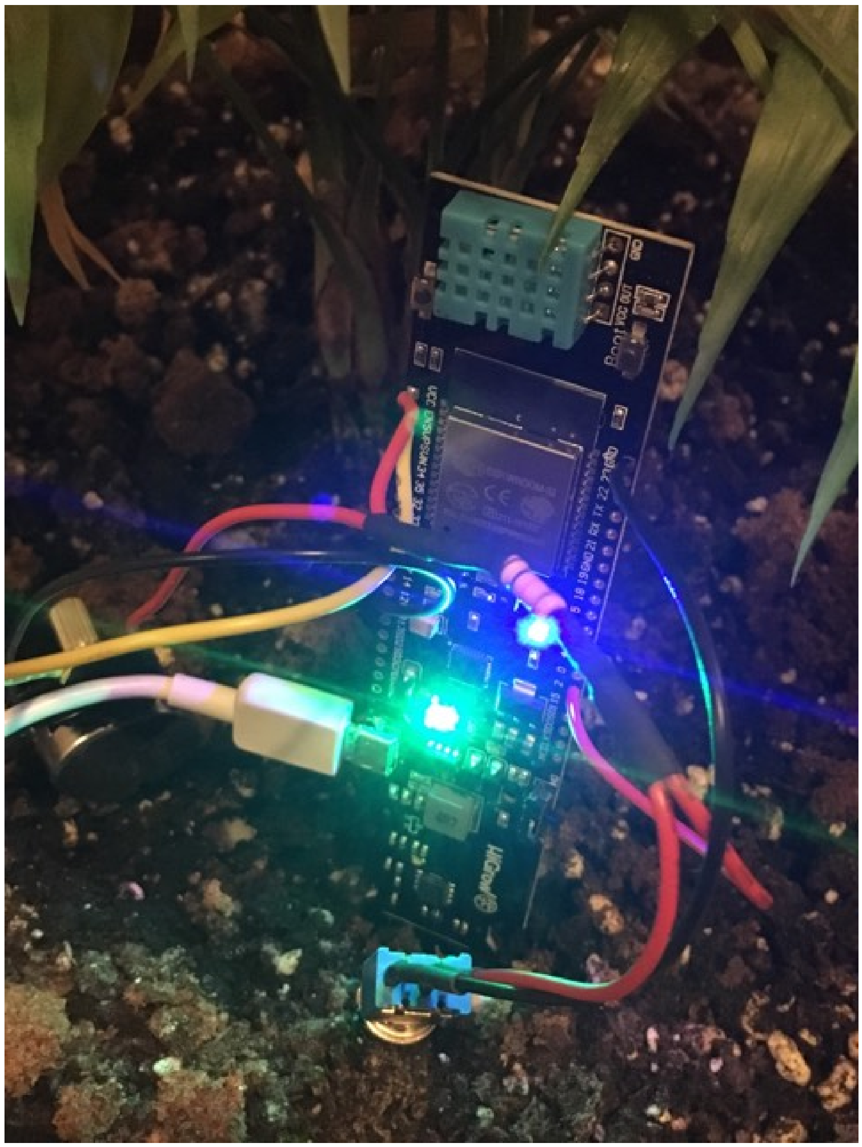

Figure.6.7: Testing

Figure.6.8 shows the web server page when the soil is dry. After adding some water to the soil, Figure.6.9 shows that the reading has changed in web server page. By clicking the ON button, the motor can be turned on and the motor can be turned off by clicking the OFF button. The following web server pages show temperature (both Celsius and Fahrenheit scale), humidity (%), soil moisture content (%) and tank water level (m) for both ON and OFF conditions.

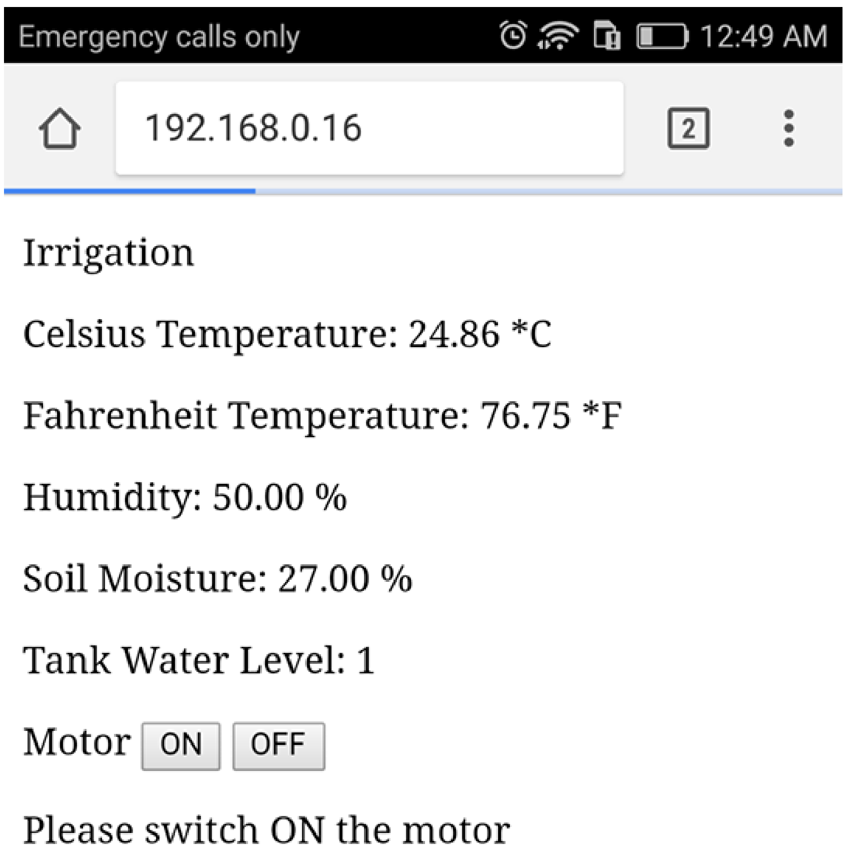

Figure.6.8: Dry soil

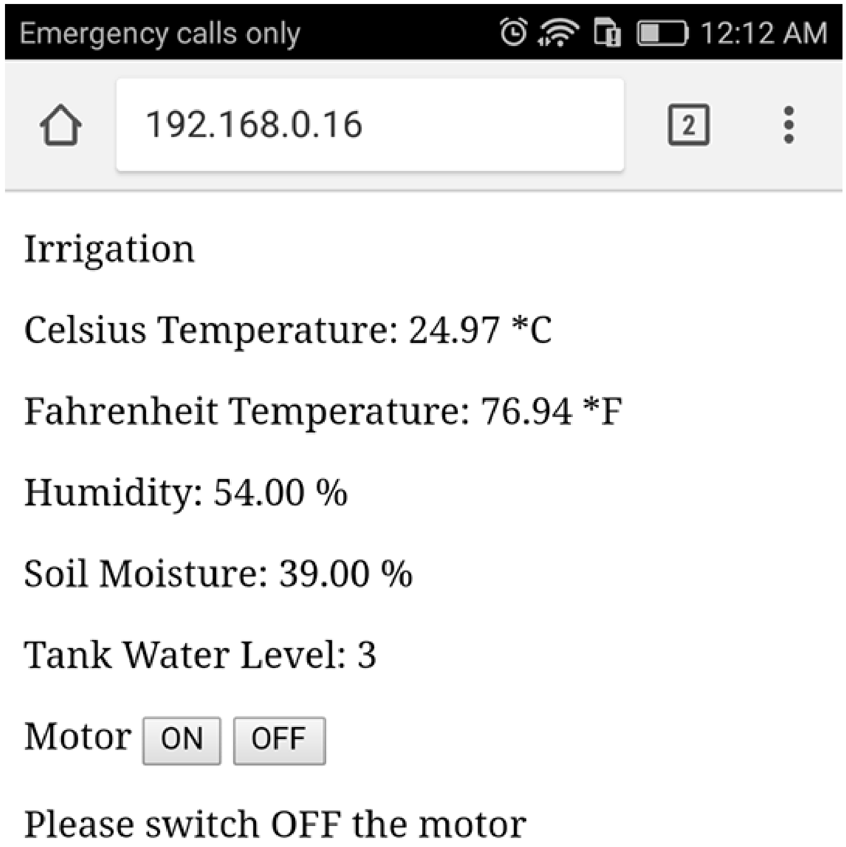

Figure.6.9: Wet soil

6.6 Summary

Selected ESP32 microcontroller and sensor module cost about US$10 that is extremely lower than the cost of PLC used in most of the water pumping systems. The cost of commercial water pumping system controller is more than US$1000. The proposed system is an extremely low cost automatic solar irrigation pumping system that could be used in developing countries.

CHAPTER 7

CONCLUSIONS AND RECOMMENDATIONS FOR FUTURE WORK

7.1 Summary of Conclusions

This research presented an optimal solution for an automated solar irrigation pumping system which is affordable for the marginal farmers in developing countries. For this purpose, daily load data and solar GHI data were collected from an established solar irrigation pumping site in Bangladesh. Sizing estimation was done for the battery-based system in HOMER which was also validated using hand calculation. Water tank equivalent battery storage was also calculated for the battery-less system.

Based on HOMER optimization, dynamic modeling of both alternatives: (i) battery-less system, and (ii) battery-based system was done in MATLAB Simulink to observe the dynamic behavior. The simulation was done for a very short time; 5 seconds for the battery-less system and 2 seconds for the battery-based system since a longer duration needed many days of computer time. The rotor speed was 187 rad/s (1785.72 r.p.m) for the battery-less system and 186 rad/s (1776.17 r.p.m) for a battery-based system which matched with the expected results. The water discharge rate for the battery-less system was 0.04 5m^3/s or 162 m^3/h. After eight hours of operation, the stored water fills only one-third volume (1040 m^3) of the large water tank. On the other hand, the water discharge rate for the battery-based system was 0.05 m^3/s or 180 m^3/h. As the battery is also charging at the same time, after eight hours of operation, the volume of lifts water would be 634.4 m^3. These results encouraged to go for another alternative; a combination of both energy storage system. The proposed model includes a smaller battery bank and a smaller water tank. The dynamic simulation results implied that after eight hours of operation, the battery will be fully charged, and the tank would be full.

An economic analysis based on Total cost was done for all alternatives; battery-less system, battery-based system, a combination of both and diesel engine system. The analysis was done for two different time periods; the first year of installation (one year) and twenty-five years of the operational period. For the longer operational period, the diesel operated engine is the costliest solution and the combined storage system is the most economical solution. Feasibility analysis from the economic point of view helped to find out the reasonable solution among four alternatives. Sensitivity analysis shows the variation of total NPC, COE and operating cost with the variation of ±10% load and irradiance. For lowest load demand, costs (NPC, COE and operational cost) and irradiance have a negative relationship. Total NPC, COE and operating costs show hike at lowest irradiance in case of average load demand. All costs are always higher for highest load demand.

The proposed control system is beneficial for a low cost automated solar irrigation pumping system which is a modest solution for farmers in developing countries. Most of the time the farmers check the soil moisture content by visiting the field and estimation. The recommended system is more convenient because it is not necessary for the users to visit the field each time to take the decision whether to run the motor or not. This system is time-saving and ensures lowest water wastage.

The HiGrow sensor module has capacitive soil moisture sensor which is different from most of the resistive sensors available in the market because resistance sensors are easy to corrode. This module is quite user-friendly and easy to install. HiGrow sensor module electronic part is not water resistant. A water tight enclosure or epoxy coat will be needed to use such sensor in field

While deciding the moisture content limit through output voltage, only one type of engineered soil (potting mix) was considered. Moreover, the soil had mineral contents. So, this calculated soil moisture limit would not be applicable for all kinds of soil or crops. Soil moisture limit would vary from soil to soil, crop to crop. As an example, the soil needs to be fully saturated before harvesting period for the cultivation of *Boro* (mostly irrigated and high yielding rice in Bangladesh). It is highly recommended to test the soil moisture limits before installing this system. The boundary condition for temperature and humidity also vary from place to place.

Renewable energy system offers an alternative way for sustainable development of a country. This research indicates that the solar water pumping system can be integrated to irrigation systems in Bangladesh as it is a feasible solution for a longer period. For twenty-five years of the life cycle, solar PV system will cost half of the diesel engine operated system. The proposed automated solar water pumping system for irrigation is the economically feasible solution to meet the irrigation challenges faced during the dry season.

7.2 Future Work

Sizing, dynamic modeling, and control of an automated solar irrigation pumping system is briefly described in this research paper. The automatic control strategy was done for a small land area. Control strategy for larger field area with multiple scattered IP67 standard sensor is recommended. The sensor battery can be charged with a small solar panel for continuous operation.

Graphical user interface developed in the work is basic. It may be useful to have a better user interface in the local language and with more features. A data download option could also be added. Dynamic simulation for this work was done only for few seconds mainly due to the computer and slow computing issue. Use of some faster computer or a simple model for a long duration simulation is recommended. This work could be used for an implementation in some location in Bangladesh.

REFERENCES

[1] Bangladesh Bureau of Statistics (BBS), “Yearbook of Agricultural Statistics”, 2015.

[2] Shahidul I Khan, Md. Quamrul Islam, Md. Mizanur R. Sarkar, “Design and analysis of a low cost solar water pump for irrigation in Bangladesh” Bangladesh Journals Online Vol 43, NO 2, 2013.

[3] Bangladesh Agricultural Development Corporation (BADC), Shech Bhavan, Dhaka, “Summary of irrigation equipment used, area irrigated and benefited farmers:2010–2011”, 2012.

[4] Biswas, H., Hossain, H., “Solar Pump: a possible solution of irrigation and electric power crisis of Bangladesh”, Int J Comput Appl 62(16), 1–5, 2013.

[5] M.a. Hossain, M. S. Hassan, M.a. Mottalib, M. Hossain, “Feasibility of solar pump for sustainable irrigation in Bangladesh”, Int J Energy Environ Eng. 6:147-155, 2015.

[6] M. Abu-Aligah, “Design of Photovoltaic Water Pumping System and Compare it with Diesel Powered Pump”, Jordan Journal of Mechanical and Industrial Engineering, Vol 5, No. 3, pp.273-280, 2011.

[7] M. Arrouf, S. Ghabrour, “Modelling and simulation of a pumping system fed by photovoltaic generator within the Matlab/Simulink programming environment”, Science Direct. Desalination 209 (2007) 23-30, 2007.

[8] C. Gopal, M. Mohanraj, P. Chandramohon, P. Chandrasekar, “Renewable energy source water pumping systems-A literature review”, Renewable and Sustainable Energy Reviews 25 (2013) 351-370, 2013

[9] Infrastructure Development Company Limited (IDCOL), Bangladesh.

[10] Ibrahim Kholil, “Investing in renewable energy: a snapshot of Bangladesh Bank’s refinancing scheme”, Beta Future Start up, July, 2013.

[11] Grameen Shakti, Grameen Bank Bhaban(9th Floor), Mirpur-2, Dhaka-1216, Bangladesh.

[12] Wagdy R, Nour MA, “Optimum design of a photovoltaic powered pumping system”, Journal of Power Sources 50: l–9, 1994.

[13] Argaw N, “Optimization of photovoltaic water pumps coupled with an interfacing pulse width modulated dc/ac inverter power conditioning devices”, IEEE First WCPEC, Hawaii, December 5–9, 1994.

[14] Loxsom F, Veroj PD, “Estimating the performance of a photovoltaic water pumping system”, Sol Energy, Vol. 52, No. 2, pp. 215–9, 1994.

[15] Katan RE, Agelidis VG, Nayar CV, “Performance analysis of a solar water pumping system”, In: Proceedings of the1996 IEEE international conference on power electronics, drives, and energy systems for industrial growth (PEDES); p.81–7, 1996.

[16] Mohammed Mozammel Hoque, “Photovoltaic water pumping system for irrigation”, 4th International Conference on Mechanical Engineering, Dhaka, Bangladesh, 2001.

[17] Pande PC, Singh AK, Ansari S, Vyas SK, Dave BK, "Design development and testing of a solar PV pump based drip system for orchards", Renewable Energy, 28(2003) 385–96, 2003

[18] Cuadros F, Rodrıguez FL, Marcos A, Coello J, "A procedure to size solar- powered irrigation (photo irrigation) schemes", Sol Energy, 76:465–73, 2004

[19] Zvonimir G, Margeta J, "A model for optimal sizing of photovoltaic irrigation water pumping systems", Sol Energy, 81: 904–16, 2007

[20] N. Forero, J. Herna´ndez, G. Gordillo, Development of a monitoring system for a PV solar plant, Energy Conversion and Management 47 (2006) 2329–2336, 2006

[21] I. Odeh, Y.G. Yohanis, B. Norton, Influence of pumping head, insolation and PV array size on PV water pumping system performance, science direct, Solar Energy 80 (2006) 51–64, 2006

[22] Hamidat, Benyoucef, "Mathematic models of photovoltaic motor-pump systems", Science Direct, Renewable Energy 33 (2008) 933–42,2008

[23] Kala Meah, Sadrul Ula, Steven Barrett, Solar photovoltaic water pumping—opportunities and challenges, Renewable and Sustainable Energy Reviews 12 (2008) 1162–1175, 2008

[24] Yahia Bakelli, Amar Hadj Arab, Boubekeur Azoui, Optimal sizing of photovoltaic pumping system with water tank storage using LPSP concept, Elsevier, science direct, Solar Energy 85 (2011) 288–294, 2011

[25] Mokeddem A, Midoun A, Kadri D, Said H, Iftikhar RA, “Performance of a directly-coupled PV water pumping system” Energy Conversation Management, 52(2011) 3089–95, 2011

[26] Gad HE, “Performance prediction of a proposed photovoltaic water pumping system at South Sinai, Egypt climate conditions”, In: Proceedings of the thirteenth international water technology conference. Hurghada, Egypt, p.739–52, 2009.

[27] Taufik, Akihiro Oi, Makbul Anwari and Mohammad Taufik, Modeling and Simulation of Photovoltaic Water Pumping System, 2009, Third Asia International Conference on Modelling & Simulation, 978-0-7695-3648-4/09, DOI 10.1109/AMS.2009.85, 2009

[28] S. G. Malla, C. N. Bhende, S. Mishra, “Photovoltaic based Water Pumping System”, IEEE, 2011.

[29] Yunseop Kim, Robert G. Evans, William M. Iversen, Remote Sensing and Control of an Irrigation System Using a Distributed Wireless Sensor Network, IEEE TRANSACTIONS ON INSTRUMENTATION AND MEASUREMENT, VOL. 57, NO. 7, JULY 2008

[30] Mahir Dursun and Semih Ozden, A wireless application of drip irrigation automation supported by soil moisture sensors, Scientific Research and Essays Vol. 6(7), pp. 1573-1582, DOI: 10.5897/SRE10.949, ISSN 1992-2248 ©2011 Academic Journals. 2011

[31] L. Prisilla, P. Simon Vasantha Rooban, Dr. L. Arockiam A Novel Method for Water Irrigation System for paddy fields using ANN, International Journal of Computer Science and Network (IJCSN) Volume 1, Issue 2, ISSN 2277-5420, 2012

[32] Jia Uddin, S.M. Taslim Reza, Qader Newaz, Jamal Uddin, Touhidul Islam, Jong-Myon Kim, Automated Irrigation System Using Solar Power,7th International Conference on Electrical and Computer Engineering, 978-1-4673-1436-7/12, IEEE, 2012

[33] Wei Li, The Design of Remote Intelligent Irrigation System based on Web Servers, Applied Mechanics and Materials Vols. 416-417 (2013) pp 806-810 doi:10.4028/www.scientific.net/AMM.416-417.806, 2013

[34] Pavithra D. S. , M. S. Srinath, GSM based Automatic Irrigation Control System for Efficient Use of Resources and Crop Planning by Using an Android Mobile, IOSR Journal of Mechanical and Civil Engineering (IOSR-JMCE, Volume 11, Issue 4 Ver. I, PP 49-55, 2014

[35] S. Harishankar, R Satish Kumar, U. Vingesh and T Viveknath, “Solar powered smart irrigation system”, Advance in Electronic and Electric Engineering, Vol. 4, No. 4, pp. 341-346, 2014

[36] Mr. Muzammil Hussain, Mr. S. P. Gawate, Dr. P. S. Prasad, Ms. P. A. Kamble, Smart Irrigation System with Three Level Access Mechanisms, International Conference on Computation of Power, Energy, Information and Communication, 978-1-4673-6524-6/15/, 2015

[37] MS. Snehal R. Metkar, Prof A. R. Mundhada, Economics of R.C.C. Water tank Resting Over Firm Ground vis-a-vis Pre-stressed Concrete Water Tank Resting over Firm Ground.

[38] Essential MATLAB for Engineers and Scientists, Fifth Edition, by Brian H. Hahn and Daniel T. Valentine, Academic Press © 2013 Citation (book)

[39] Introduction to Simulink with Engineering Applications, Third Edition by Steven T. Karris Orchard Publications © 2011 (678 pages) Citation ISBN:9781934404218 (book)

[40] Mathworks, website: https://www.mathworks.com/help/simulink/index.html

[41] ESP32 Technical Reference Manual, Version 2.8, Espressif system, #101, Block2, 690 Bibo Road, Zhangjiang High-Tech Park, Pudong, Shanghai, China 201203, 2018.

LIST OF PUBLICATIONS

[1] Shatadru Biswas, M. Tariq Iqbal, "Sizing and dynamic modeling of solar water pumping system for irrigation in Bangladesh" 2016 Newfoundland Electrical and Computer Engineering Conference, St. John's, Canada, NL, 2016

[2] Shatadru Biswas, M. Tariq Iqbal, "Dynamic modeling of solar water pumping system with energy storage" 2017 Newfoundland Electrical and Computer Engineering Conference, St. John's, Canada, NL, 2017

[3] Shatadru Biswas, M. Tariq Iqbal, "Dynamic modeling of solar water pumping system with energy storage" Hindawi Journal of Solar Energy. Volume 2018, Article ID 8471715, 2018

[4] Shatadru Biswas, M. Tariq Iqbal, "Solar water pumping system control using a low cost ESP32 microcontroller", 31 Canadian Conference on Electrical and Computer Engineering, Quebec City, Quebec, Canada, 2018

APPENDICES

Appendix A

```
%PV Model
clc;
clear all;
K = 1.3806e-23; % Boltzmann Constant
q = 1.0622e-19; % charge of electrol
Iscn = 9.56;    % Short Circuit Current
Vocn = 45.42;   % Open Circuit Voltage
Kv = -0.41361;  % Temperature coefficient of Voc
Ki = 0.089895;  % Temperature coefficient of Isc
Ns = 72;        % Number of cells in a module
T = 34+273;     % Operating Temperature
Tn = 46+273;    % Nominal Temperature
Gn = 1000;      % Nominal Irradiance
a = 1.1011;     %Diode Idality Factor
Eg = 1.12;      % Band Gap of silocon at Ambient Temperature
G = 900;        % Actual Irradiance
Rs = 0.44015;   % Series Resistance
Rsh = 85.7392;  % Shunt Resistance

Vtn = Ns*(K*Tn/q);
Ion = Iscn/((exp(Vocn/(a*Vtn)))-1);
Io = Ion*((T/Tn)^3)*exp(((q*Eg/(a*K))*((1/Tn)-(1/T))));
Ipvn = Iscn;
Ipv = (Ipvn + Ki*(T-Tn))*(G/Gn);
Vt = Ns*(K*T/q);
I = zeros(454,1);
i = 1;
I(1,1) = 0;

for V = 45.42:-0.1:0
   I_part = Io*(exp((V+(I(i,1)*Rs))/(Vt*a))-1) + ((V+(Rs*I(i,1)))/Rsh) ;
   I(i+1) = Ipv-I_part;
   V1(i) = V;
   P(i) = V*I(i);
   i=i+1;
end
V1(i) = V1 (i-1);
P(i) = P(i-1);
V1 = transpose(V1);
plot(V1,I);
plot(V1,P);
```

Appendix B

```
function D  = PandO(Param, Enabled, V, I)

% MPPT controller based on the Perturb & Observe algorithm.

% D output = Duty cycle of the boost converter (value between 0 and 1)
%
% Enabled input = 1 to enable the MPPT controller
% V input = PV array terminal voltage (V)
% I input = PV array current (A)
%
% Param input:
Dinit = Param(1);  %Initial value for D output
Dmax = Param(2);   %Maximum value for D
Dmin = Param(3);   %Minimum value for D
deltaD = Param(4); %Increment value used to increase/decrease the duty cycle D
% ( increasing D = decreasing Vref )
%

persistent Vold Pold Dold;

dataType = 'double';

if isempty(Vold)
   Vold=0;
   Pold=0;
   Dold=Dinit;
end
P= V*I;
dV= V - Vold;
dP= P - Pold;

if dP ~= 0 & Enabled ~=0
   if dP < 0
      if dV < 0
         D = Dold - deltaD;
      else
         D = Dold + deltaD;
      end
   else
      if dV < 0
         D = Dold + deltaD;
      else
         D = Dold - deltaD;
      end
   end
else D=Dold;
end

if D >= Dmax | D<= Dmin
```

```
    D=Dold;
end

Dold=D;
Vold=V;
Pold=P;
```

Appendix C

```
//Control Code
#include <WiFi.h>
#include "DHT.h"

#define DHTTYPE DHT11   // DHT 11
#define ANALOG_PIN_0 36  //water level sensor

const char* ssid     = "Biswas";
const char* password = "Othoi1234";

WiFiServer server(80);

const int DHTPin = 22;
const int soilMoisturePin = 32;
const int wateringTime = 200000;
const float soilMoistureThreshold = 50;
const float tempThreshold = 20;
const float humidityThreshold = 70;
const float tankupperlimit = 3;
const float tanklowerlimit = 2.5;
float waterLevel = 0;

// Initialize DHT sensor.
DHT dht(DHTPin, DHTTYPE);
```

```
static char celsiusTemp [8];
static char fahrenheitTemp [8];
static char humidityTemp [8];
float soilMoisture = 0;
bool watering = false;
char linebuf[80];
int charcount=0;

void setup() {

  // initialize the DHT sensor
  dht.begin();

  //Initialize serial and wait for port to open:
  Serial.begin(115200);
  pinMode(soilMoisturePin, INPUT);
  pinMode(ANALOG_PIN_0, INPUT);
  pinMode(DHTPin, INPUT);
  pinMode(LED_BUILTIN, OUTPUT);

  while(!Serial) {
    ; // wait for serial port to connect.
  }

  // We start by connecting to a WiFi network
  Serial.println();
  Serial.print("Connecting to ");
```

```
  Serial.println(ssid);

  WiFi.begin(ssid, password);

  // attempt to connect to Wifi network:
  while(WiFi.status() != WL_CONNECTED) {
    // Connect to WPA/WPA2 network. Change this line if using open or WEP network:
    delay(500);
    Serial.print(".");
  }
  Serial.println("");
  Serial.println("WiFi connected");
  Serial.println("IP address: ");
  Serial.println(WiFi.localIP());

server.begin();

}

void loop() {
  //listen for incoming clients
  WiFiClient client = server.available();
  if (client) {
    Serial.println("New client");
    String currentLine = ""; // make a String to hold incoming data from the client
    memset(linebuf,0,sizeof(linebuf));
    charcount=0;
```

```
  // an http request ends with a blank line
  boolean currentLineIsBlank = true;

  while (client.connected()) {
   if (client.available()) {
    char c = client.read();
    Serial.write(c);
    //read char by char HTTP request
    linebuf[charcount]=c;
    if (charcount<sizeof(linebuf)-1) charcount++;
    // if you've gotten to the end of the line (received a newline character) and the line is blank, the http request has ended, so you can send a reply
    if (c == '\n' && currentLineIsBlank) {
     // Sensor readings may also be up to 2 seconds 'old' (its a very slow sensor)
     waterLevel= analogRead(ANALOG_PIN_0);
     waterLevel = map(waterLevel, 0, 4095, 0, 3);
     soilMoisture = analogRead(soilMoisturePin);
     soilMoisture = map(soilMoisture,4000,1572,0,100);
     float h = dht.readHumidity();
     // Read temperature as Celsius (the default)
     float t = dht.readTemperature();
     // Read temperature as Fahrenheit (isFahrenheit = true)
     float f = dht.readTemperature(true);
     // Check if any reads failed and exit early (to try again).
     if (isnan(h) || isnan(t) || isnan(f)) {
      Serial.println("Failed to read from DHT sensor!");
```

```
    strcpy(celsiusTemp,"Failed");
    strcpy(fahrenheitTemp, "Failed");
    strcpy(humidityTemp, "Failed");
  }
  else{
    // Computes temperature values in Celsius + Fahrenheit and Humidity
    float hic = dht.computeHeatIndex(t, h, false);
    dtostrf(hic, 6, 2, celsiusTemp);
    float hif = dht.computeHeatIndex(f, h);
    dtostrf(hif, 6, 2, fahrenheitTemp);
    dtostrf(h, 6, 2, humidityTemp);

}



if (currentLine.length() == 0) {
// send a standard http response header
client.println("HTTP/1.1 200 OK");
client.println("Content-Type: text/html");
client.println("Connection: close");  // the connection will be closed after
completion of the response
client.println();
client.println("<!DOCTYPE HTML><html><head><meta name=\"viewport\"
content=\"width=device-width, initial-scale=1\">");
client.println("<meta http-equiv=\"refresh\" content=\"30\"></head>");
client.println("<body><div style=\"font-size: 5 rem;\"><p>Irrigation</p><p>");
```

```
        client.println("Celsius Temperature: ");
        client.println(celsiusTemp);
        client.println("*C</p><p>");
        client.println("Fahrenheit Temperature: ");
        client.println(fahrenheitTemp);
        client.println("*F</p></div><p>");
        client.println("Humidity: ");
        client.println(humidityTemp);
        client.println("%</p><p>");
        client.println("Soil Moisture: ");
        client.println(soilMoisture);
        client.println("%</p></div>");
        client.println("Tank Water Level: ");
        client.println(waterLevel);
        client.println("</p></div>");

        if (soilMoisture < soilMoistureThreshold){
        if (atoi(celsiusTemp) > tempThreshold && atoi(humidityTemp) <
humidityThreshold){

          if(waterLevel<=tanklowerlimit){
            Serial.println("Please switch ON the motor");
            client.println("Please switch ON the motor");
            client.println("</p></div>");

           }else {
           Serial.println("Please switch OFF the motor");
```

```
            client.println("Please switch OFF the motor");
            client.println("</p></div>");
            }

        }else {
        Serial.println("Please switch OFF the motor");
        client.println("Please switch OFF the motor");
        client.println("</p></div>");
 }

  }else {
  Serial.println("Please switch OFF the motor");
  client.println("Please switch OFF the motor");
  client.println("</p></div>");
  }
  client.println("</body></html>");
  client.println("<p>Motor <a href=\"on\"><button>ON</button></a> <a
href=\"off\"><button>OFF</button></a></p>");
  break;
        }else {    // if you got a newline, then clear currentLine:
          currentLine = "";
         }

        if (soilMoisture < soilMoistureThreshold){
        if (atoi(celsiusTemp) > tempThreshold && atoi(humidityTemp) <
humidityThreshold){
```

```
            if(waterLevel<=tanklowerlimit){
              digitalWrite(LED_BUILTIN, HIGH);
              Serial.println("Motor status : Motor is ON");


              delay(wateringTime);
              digitalWrite(LED_BUILTIN, LOW);
              Serial.println("Motor status : Motor is OFF");
             }else {
             digitalWrite(LED_BUILTIN, LOW);
             Serial.println("Motor status : Motor is OFF");
             }

        }else {
        digitalWrite(LED_BUILTIN, LOW);
        Serial.println("Motor status : Motor is OFF");
        }

  }else {
  digitalWrite(LED_BUILTIN, LOW);
  Serial.println("Motor status : Motor is OFF");
 }
        }
        if (c == '\n') {
          currentLineIsBlank = true;
         if (strstr(linebuf,"GET /on") > 0){
           Serial.println("Motor is ON");
           client.println("Motor is ON");
```

```
          digitalWrite(LED_BUILTIN, HIGH);
        }
        else if (strstr(linebuf,"GET /off") > 0){
          Serial.println("Motor is OFF");
          client.println("Motor is OFF");
          digitalWrite(LED_BUILTIN, LOW);
        }
        currentLineIsBlank = true;
        memset(linebuf,0,sizeof(linebuf));
        charcount=0;
      } else if (c != '\r') {
        // you've gotten a character on the current line
        currentLineIsBlank = false;
      }

      }
    }

    // give the web browser time to receive the data
    delay(1);



    // close the connection:
    client.stop();

  }
}
```